



Publicly Accessible Penn Dissertations

---


2016

# Identification Of Novel Molecular-Genetic Pathways Regulating The Development Of Subpallial Derivatives

David Tischfield

University of Pennsylvania, [tischfield@gmail.com](mailto:tischfield@gmail.com)

Follow this and additional works at: <https://repository.upenn.edu/edissertations>

 Part of the [Genetics Commons](#), [Molecular Biology Commons](#), and the [Neuroscience and Neurobiology Commons](#)

---

## Recommended Citation

Tischfield, David, "Identification Of Novel Molecular-Genetic Pathways Regulating The Development Of Subpallial Derivatives" (2016). *Publicly Accessible Penn Dissertations*. 2611.  
<https://repository.upenn.edu/edissertations/2611>

This paper is posted at ScholarlyCommons. <https://repository.upenn.edu/edissertations/2611>  
For more information, please contact [repository@pobox.upenn.edu](mailto:repository@pobox.upenn.edu).

---

# Identification Of Novel Molecular-Genetic Pathways Regulating The Development Of Subpallial Derivatives

## **Abstract**

The embryonic subpallium produces many different neuronal cell types present throughout the adult telencephalon, including striatal medium spiny neurons (MSN) and cortical interneurons. Dysfunction of either cell type leads to neurological and psychiatric disorders including schizophrenia, epilepsy, and Tourette's syndrome. Thus, understanding the molecular pathways that regulate their development and function has important implications for understanding disease pathogenesis. This work describes novel methods and genetic factors that expand our ability to characterize the development and function of two major subpallial derivatives: cortical interneurons and striatal MSN. The first part of this thesis characterizes a novel enrichment method for producing parvalbumin-expressing (PV) interneurons from mouse embryonic stem cells. This method, which uses an atypical protein kinase C inhibitor to enhance intermediate neurogenesis, results in a markedly increased ratio of PV+ to somatostatin-expressing interneurons. The findings suggest that the mode of neurogenesis influences cortical interneuron fate determination. Moreover, PV+ interneurons can now be generated in large numbers to study their development, screen for factors that affect their physiology, and used in therapeutic applications. The second part of this thesis examines the function of two putative transcription factors, *Zswim5* and *Zswim6*, in the regulation of striatal development. We show that these genes are expressed in subpallial precursors, and in the case of *Zswim6*, expressed in the adult striatum. Next, through the generation of *Zswim5* and *Zswim6* knockout mice, we provide a detailed anatomical, molecular, and behavioral characterization of the resulting phenotypes. Our findings reveal that loss of *Zswim6* causes a reduction in striatal volume and morphological changes in MSN. Additionally, these structural changes are associated with alterations in motor behaviors including hyperactivity, impaired rotarod performance, and hyperresponsiveness to amphetamine. These results demonstrate that *Zswim6* is indispensable for normal brain development and support findings in human genome-wide association studies that implicate *Zswim6* with schizophrenia. Collectively, this dissertation provides novel insights into telencephalic development through the development of in vitro stem cell systems and in vivo disease mouse models that further our ability to test and understand neurological diseases.

## **Degree Type**

Dissertation

## **Degree Name**

Doctor of Philosophy (PhD)

## **Graduate Group**

Neuroscience

## **First Advisor**

Stewart A. Anderson

## **Keywords**

Brain, Development, Interneurons, *Zswim6*

---

**Subject Categories**

Genetics | Molecular Biology | Neuroscience and Neurobiology

IDENTIFICATION OF NOVEL MOLECULAR-GENETIC PATHWAYS  
REGULATING THE DEVELOPMENT OF SUBPALLIAL DERIVATIVES

David Tischfield

A DISSERTATION

in

Neuroscience

Presented to the Faculties of the University of Pennsylvania

in

Partial Fulfillment of the Requirements for the

Degree of Doctor of Philosophy

2016

Supervisor of Dissertation

Graduate Group Chairperson

---

Stewart A. Anderson, MD.  
Associate Professor of Psychiatry

---

Joshua Gold, Ph.D.  
Professor of Neuroscience

*Dissertation Committee*

Douglas J. Epstein, Ph.D.  
Professor of Genetics

Wenqin Luo, M.D. Ph.D.  
Assistant Professor of Neuroscience

Marc Fuccillo, M.D., Ph.D.  
Assistant Professor of Neuroscience

IDENTIFICATION OF NOVEL MOLECULAR-GENETIC PATHWAYS REGULATING THE  
DEVELOPMENT OF SUBPALLIAL DERIVATIVES

COPYRIGHT

2016

David James Tischfield

This work is licensed under the  
Creative Commons Attribution-  
NonCommercial-ShareAlike 3.0  
License

To view a copy of this license, visit

<http://creativecommons.org/licenses/by-nc-sa/2.0/>

*This dissertation is dedicated to my brothers, Max and Sam – the two best friends and scientific compadres a guy could ask for.*

## ACKNOWLEDGEMENTS

This work was funded by R01 MH066912-01 and F30 MH105045-02. This research was also made possible in part due to Florin Tuluc and Eric Reidel at the Children's Hospital of Philadelphia FACS core facility. I would also like to thank members of the Anderson lab, both past and present for helpful discussions and technical assistance. I would especially like to thank my mentor, Stewart Anderson, for allowing me to work so independently on almost anything I thought worthwhile, which allowed me to grow considerably as an experimentalist and critical thinker. To all the members of my thesis committee who helped me along the way. I'd also like to thank Jennifer Tyson, who was both a scientific mentor and close friend to me throughout my PhD. Also Erik Deboer and Sean Ryan, whose presence in lab made everything that much better. Shane Fitzgerald, for being a rock solid laboratory technician, hard worker, and all around good person. Ivor Asztalos, whose aptitude for statistics saved me. To the love of my life, Jillian and her cat Monster, who patiently stood by me during all of the ups and downs that a PhD entails. And lastly, to my family, but not just for the typical reasons. Thank you to my father Jay, who literally helped me get the resources and equipment that I needed at times to do my research. Thank you to my brothers, Max and Sam, both of whom helped me numerous times throughout my PhD to analyze data, think about my projects, and provide moral support. To my extremely talented sister-in-law Victoria Abaira, who was always willing to help me with my research in any way possible. To my mother, whose jovial spirit was always welcome. And to all of my friends not listed here who have made the last 6 years a great 6 years. Thank you.

# **ABSTRACT**

## **IDENTIFICATION OF NOVEL MOLECULAR-GENETIC PATHWAYS REGULATING THE DEVELOPMENT OF SUBPALLIAL DERIVATIVES**

David Tischfield

Dr. Stewart Anderson

The embryonic subpallium produces many different neuronal cell types present throughout the adult telencephalon, including striatal medium spiny neurons (MSN) and cortical interneurons. Dysfunction of either cell type leads to neurological and psychiatric disorders including schizophrenia, epilepsy, and Tourette's syndrome. Thus, understanding the molecular pathways that regulate their development and function has important implications for understanding disease pathogenesis. This work describes novel methods and genetic factors that expand our ability to characterize the development and function of two major subpallial derivatives: cortical interneurons and striatal MSN. The first part of this thesis characterizes a novel enrichment method for producing parvalbumin-expressing (PV) interneurons from mouse embryonic stem cells. This method, which uses an atypical protein kinase C inhibitor to enhance intermediate neurogenesis, results in a markedly increased ratio of PV<sup>+</sup> to somatostatin-



expressing interneurons. The findings suggest that the mode of neurogenesis influences cortical interneuron fate determination. Moreover, PV<sup>+</sup> interneurons can now be generated in large numbers to study their development, screen for factors that affect their physiology, and used in therapeutic applications. The second part of this thesis examines the function of two putative transcription factors, Zswim5 and Zswim6, in the regulation of striatal development. We show that these genes are expressed in subpallial precursors, and in the case of Zswim6, expressed in the adult striatum. Next, through the generation of Zswim5 and Zswim6 knockout mice, we provide a detailed anatomical, molecular, and behavioral characterization of the resulting phenotypes. Our findings reveal that loss of Zswim6 causes a reduction in striatal volume and morphological changes in MSN. Additionally, these structural changes are associated with alterations in motor behaviors including hyperactivity, impaired rotarod performance, and hyperresponsiveness to amphetamine. These results demonstrate that Zswim6 is indispensable for normal brain development and support findings in human genome-wide association studies that implicate Zswim6 with schizophrenia. Collectively, this dissertation provides novel insights into telencephalic development through the development of *in vitro* stem cell systems and *in vivo* disease mouse models that further our ability to test and understand neurological diseases.

# TABLE OF CONTENTS

<b>ACKNOWLEDGMENTS</b> .....	<b>iv</b>
<b>ABSTRACT</b> .....	<b>v</b>
<b>TABLE OF CONTENTS</b> .....	<b>vii</b>
<b>LIST OF TABLES</b> .....	<b>x</b>
<b>LIST OF FIGURES</b> .....	<b>xi</b>
<b>CHAPTER 1</b> .....	<b>1</b>
<b>INTRODUCTION: STRUCTURE, FUNCTION, DEVELOPMENT, INTERNEURONS, AND DISEASES OF THE TELENCEPHALON</b>	
<b>1.1 Structure and Function of the Telencephalon</b> .....	<b>1</b>
Structure and Function of the Pallium	
Structure and Function of the Subpallium	
Structure and Function of the Striatum	
<b>1.2 Development of the Telencephalon</b> .....	<b>6</b>
Early Patterning of the Neuraxis	
Early Patterning of the Telencephalon	
<b>1.3 Molecular-Genetic Controls over Subpallial Development</b> .....	<b>10</b>
Origins of Cortical Interneurons	
Interneuron Subgroup Identification	
Genetic Regulation of Interneuron Development	
The MGE Gives Rise to PV and SST Cortical Interneurons	
Spatiotemporal Biases in Fate	
Division Mode and Progenitor Subtype Influence PV and SST Fate	
Genetic Demarcation of the CGE	
Genetic Regulation of LGE and Striatal Development	
<b>1.4 Interneuron Dysfunction in Neurological Disease</b> .....	<b>27</b>
Epilepsy and Seizure Disorders	
Schizophrenia	
Autism	
<b>1.5 Striatal Dysfunction in Neurological Disease</b> .....	<b>34</b>
Overview	
Tic Disorders and Tourette Syndrome	
Obsessive-Compulsive Disorder	
Schizophrenia	
<b>CHAPTER 2</b> .....	<b>40</b>

# ATYPICAL PKC INHIBITION ENHANCES THE GENERATION OF PV CORTICAL INTERNEURONS FROM EMBRYONIC STEM CELLS

<b>2.1 Generating GABAergic Cortical Interneurons from Mouse Embryonic Stem Cells.....</b>	<b>40</b>
Overview	
Generating Interneurons from mESCs	
<b>2.2 Atypical PKC Inhibition Enhances Generation of PV Cortical Interneurons from Embryonic Stem Cells.....</b>	<b>48</b>
Overview	
Introduction	
Results	
Generation of Nkx2.1 expressing interneuron progenitors	
Atypical PKC inhibition increases the fraction of cyclin-D2 expressing Nkx2.1::mCherry progenitors	
Atypical PKC inhibition influences the mode of neurogenesis	
Atypical PKC inhibition enhances PV fate specification	
Discussion	
<b>CHAPTER 3.....</b>	<b>66</b>
<b>FUNCTION OF THE ZINC FINGER SWIM DOMAIN-CONTAINING PROTEINS 5 &amp; 6 IN FOREBRAIN DEVELOPMENT</b>	
<b>3.1 Introduction to Zinc Finger SWIM Domain-Containing Proteins.....</b>	<b>66</b>
Overview	
SWIM domain-containing proteins 4, 5, 6, and 8	
Zswim6 and human disease	
<b>3.2 Generation of Zswim5 and Zswim6 Knockout Mice and Characterization of their role in Interneuron Development.....</b>	<b>83</b>
Generation of Zswim5 knockout mice	
Study of interneuron development in Zswim5 knockout mice	
Generation of Zswim5/Zswim6 double knockout mice	
Study of interneuron development in Zswim5/Zswim6 double knockout mice	
Discussion	
<b>3.3 Loss of the Schizophrenia Associated Gene Zswim6 Alters Striatal Development and Motor-Dependent Behaviors.....</b>	<b>96</b>
Overview	
Introduction	
Results	
Expression of Zswim6 in the developing and adult forebrain	
Generation of a Zswim6 null mouse	
Abnormal neocortical and striatal development in Zswim6 null mice	
Loss of Zswim6 results in behavioral deficits	
Discussion	
<b>CHAPTER 4.....</b>	<b>119</b>

## ONGOING STUDIES AND FUTURE DIRECTIONS

<b>4.1 Overview.....</b>	<b>119</b>
<b>4.2 RNA and Epigenetic Profiling of mESC-Derived Fate Committed Cortical Interneurons.....</b>	<b>120</b>
<b>4.3 Notch Inhibition to Enhance the Generation of SST-subtypes from Embryonic Stem Cells.....</b>	<b>124</b>
<b>4.4 Embryonic Stem Cell-Derived Interneuron Based Therapy for Epilepsy.....</b>	<b>126</b>
<b>4.5 Ongoing Studies and Future Directions for Understanding Zswim6 Function.....</b>	<b>129</b>
<b>CHAPTER 5.....</b>	<b>134</b>

## MATERIALS AND METHODS

<b>5.1 Materials and Methods for mESC Studies.....</b>	<b>134</b>
Mouse embryonic stem cell culture	
Cell sorting	
Cortical transplantation	
Immunohistochemistry	
In vivo fate quantification	
Live imaging analysis	
Cell counting	
<b>5.2 Materials and Methods for Zswim5 and Zswim6 Studies.....</b>	<b>139</b>
Mouse lines	
Tissue preparation for immunohistochemistry	
Immunohistochemistry	
Cell counting	
Volumetric analyses and surface area	
Quantitative PCR (qPCR analysis)	
Golgi-cox staining and neuron reconstruction	
B-galactosidase staining	
Spine density analysis	
Tissue preparation for in situ RNA hybridization	
In situ RNA hybridization	
Brainstem auditory evoked response (BAER) testing	
Rotarod	
Open field	
Elevated zero maze	
Force plate actometer	
Co-immunoprecipitation and western blot	
Nuclear-cytoplasmic fractionation	
<b>REFERENCES.....</b>	<b>152</b>

## LIST OF TABLES

- Table 3.1** Functional gene ontology analysis for genes whose expression correlates with Zswim5 & Zswim6 expression during human brain development
- Table 5.1** List of primers used in this study

## LIST OF FIGURES

- Figure 1.1** Schematic of basal ganglia circuitry.
- Figure 1.2** Early patterning and transcriptional regulation of the telencephalon.
- Figure 1.3** Origins and diversity of neocortical interneurons.
- Figure 2.1** aPKCi increases the proportion of CD2-expressing Nkx2.1 MGE progenitors.
- Figure 2.2** aPKCi increases the proportion of CD2-expressing Nkx2.1 progenitors in two additional mESC lines.
- Figure 2.3** aPKCi does not affect progenitor proliferation.
- Figure 2.4** Live cell imaging enables analysis of cell divisions and shows that aPKCi increases the proportion of Nkx2.1:mCherry daughter cells that undergo a second division.
- Figure 2.5** Strategy to enhance the generation of parvalbumin (PV)-expressing interneurons from a dual Nkx2.1: mCherry-Lhx6:GFP mouse stem cell reporter line.
- Figure 2.6** aPKCi treated cells express Sox6 and GABA.
- Figure 3.1** Gene tree for Zswim4, 5, 6, and 8 gene evolution
- Figure 3.2** Multiple sequence alignment of BC- and Cullin-boxes in ZSWIM4, 5, and 6.
- Figure 3.3** Schematic illustration of putative Zswim-type cullin-RING E3 ubiquitin ligase
- Figure 3.4** Zswim6 co-immunoprecipitates with Brg1, the main ATPase subunit of SWI/SNF chromatin remodeling complex, in HEK293 cells.
- Figure 3.5** Zswim5 predominantly localizes to the nucleus.
- Figure 3.6** Craniofacial phenotype of a Zswim6 human mutation patient, evolutionary comparative analysis, genomic structure, and predicted protein regions.
- Figure 3.7** Targeting strategy and characterization of Zswim5 knockout mouse obtained from the Knockout Mouse Project (KOMP).
- Figure 3.8** Generation of Zswim5 knockout (KO) mice.

- Figure 3.9** Expression of Zswim5 in the developing mouse forebrain.
- Figure 3.10** Analysis of proliferation and molecular specification in the medial ganglionic eminence (MGE) of Zswim5 mutant mice.
- Figure 3.11** Cortical parvalbumin interneuron numbers are normal in Zswim5 knockout mice.
- Figure 3.12** Generation of Zswim6 null mutant mice.
- Figure 3.13** Analysis of striatal and cortical volume and interneuron numbers in Nkx2.1-cre Zswim5/Zswim6 double knockout mice.
- Figure 3.14** Zswim6 expression during striatal development.
- Figure 3.15** Zswim6 expression during human fetal forebrain development.
- Figure 3.16** Decreased early postnatal survival and forebrain size in Zswim6 null mutants.
- Figure 3.17** Zswim6 null mutants have a reduced number of medium spiny neurons.
- Figure 3.18** Dendritic abnormalities in striatal medium spiny neurons of Zswim6 null mutants.
- Figure 3.19** Zswim6 null mutants have decreased dendritic complexity in medial frontal cortex but not somatomotor cortex.
- Figure 3.20** No evidence for reduced proliferation by striatal progenitors in Zswim6 null mutants.
- Figure 3.21** Behavioral defects in Zswim6 null mutants.
- Figure 3.22** Brainstem auditory evoked response testing on Zswim6 knockout mice.
- Figure 4.1** DAPT forces progenitors to exit the cell cycle.

# CHAPTER 1

## Introduction: Structure, Function, Development, Interneurons, and Diseases of the Telencephalon

### **1.1 Structure and Function of the Telencephalon**

The mature mammalian telencephalon contains of hundreds of distinct neuronal subtypes that are generated from a thin sheet of neuroepithelium during early embryonic development. A major challenge in developmental biology is to understand how early patterning events give rise to different progenitor domains, and how these domains subsequently generate a seemingly endless array of neuronal subtypes that eventually coalesce into functional circuitry that refines and modulates itself with experience. While we have made great progress in identifying genes and molecular pathways that control broad aspects of telencephalic development, we are much further from understanding how multiple, more subtle genetic perturbations that act during embryonic and early



postnatal periods result in the manifestation of more common, complex genetic disorders much later in life. In order to do so, we must first understand how the telencephalon develops on a very fine level and incorporate that knowledge into an understanding of how its mature components interact with each other to produce normal brain function. This introduction will attempt to lay the foundation for my dissertation research, which uses multiple, seemingly disparate approaches to gain insight into one of the world's most complicated systems. To this end, I begin broadly and introduce the telencephalon as it exists in all vertebrates, as a structure consisting of two main territories, the pallium and subpallium, which develop from the anterior end of the neural plate during the first trimester of human existence.

### *Structure and Function of the Pallium*

The pallium consists of the cerebral cortex and the subpallium contains the basal ganglia (BG), parts of the amygdala, and septum. The most evolutionarily advanced region of the cerebral cortex is the neocortex, which is responsible for higher order cognitive processes such as sensory perception and control of voluntary movement<sup>2 3</sup>. On a structural level, the neocortex is organized along two main axes: tangentially into specialized areas with distinct function, connectivity, and cytoarchitecture; and radially into six cellular layers, which can be distinguished from one another based on their morphology, cell types, and connectivity<sup>4</sup>. Within the neocortex there are two main classes of neurons: excitatory glutamatergic neurons (~80%, pyramidal and spiny stellate neurons)

and inhibitory GABAergic interneurons (~20%). Glutamate is the major excitatory neurotransmitter and GABA is the main inhibitory neurotransmitter in the mammalian neocortex, and changes in glutamate and GABA metabolism determine cortical excitability<sup>5</sup>. Whereas glutamatergic neurons form long-range excitatory synaptic connections both within the cortex and outside of it, cortical interneurons are locally projecting and have the potential to modulate large numbers of excitatory cells within their vicinity. Both populations are organized into vertically oriented columns and together they serve to regulate cortical excitability<sup>6 5</sup>.

### *Structure and Function of the Subpallium*

The subpallium, or ventral telencephalon, contains the BG, which are a collection of nuclei that include the dorsal striatum (caudate nucleus and putamen), ventral striatum (nucleus accumbens and olfactory tubercle), globus pallidus, ventral pallidum, substantia nigra (SNr), and subthalamic nucleus. While most of these nuclei project exclusively to other nuclei within the BG, many are interconnected with various parts of the brain including the cerebral cortex, thalamus, and brainstem<sup>7</sup>. The main output nuclei of the BG are the globus pallidus internal segment (GPi) and the substantia nigra pars reticulata (SNr). The main input nucleus is the striatum; however the subthalamic nucleus also receives direct input from the cerebral cortex<sup>8</sup>. Each nucleus has its own complex internal anatomical and neurochemical organization and will not be discussed at length. Together, the BG help control a variety of functions including voluntary

movement, procedural learning, habit formation, cognition, and emotion<sup>7</sup>.

### *Structure and Function of the Striatum*

The human striatum is comprised of two functionally similar nuclei, the caudate and the putamen, which are separated by the internal capsule. In mouse, these nuclei are fused in what is commonly referred to as the caudate-putamen. The striatum receives excitatory inputs from many different cortical areas and thalamic nuclei<sup>9,10</sup>. Different cortical areas project to distinct regions of the striatum, forming parallel circuits that process specific functions (**Figure 1.1**).

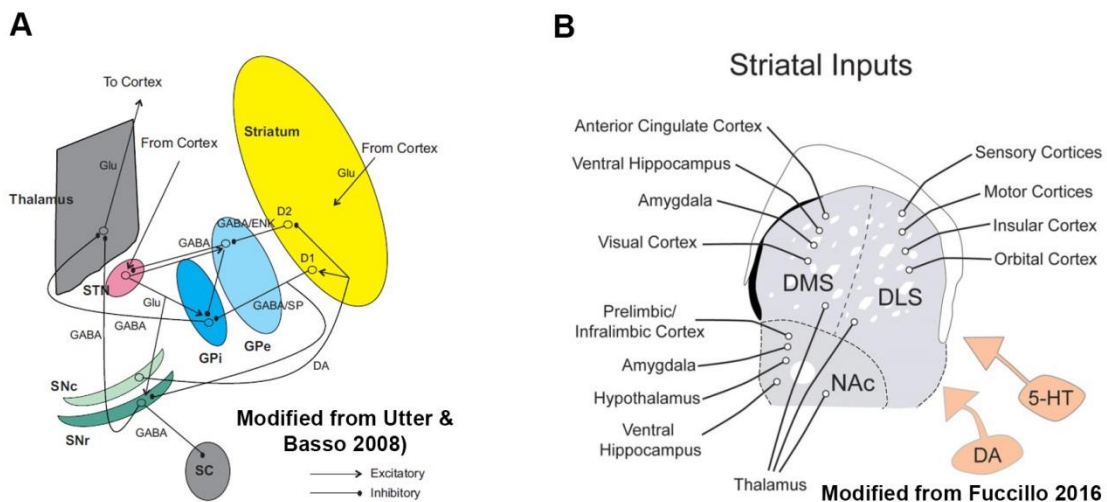


**Figure 1.1. Schematic of basal ganglia circuitry.**

**(A).** BG target structures are shown in gray. Modified from Utter and Basso (2008). **(B).** Summary of the known excitatory inputs to the different striatal subdomains, including the dorsomedial striatum (DMS), dorsolateral striatum (DLS), and nucleus accumbens (NAc). The entire striatum receives innervation from dopaminergic (DA) and serotonergic (5-HT) inputs. Modified from Fuccillo (2016). Abbreviations: GPe, globus pallidus external segment; GPi, globus pallidus internal segment; SC, superior colliculus; SNc, substantia nigra pars compacta; SNr, substantia nigra pars reticulata; STN, subthalamic nucleus; DA, dopamine; D1, dopamine D1 receptor subtype; D2, dopamine D2 receptor subtype; Glu, glutamate; ENK, enkephalin; SP, substance P.

Importantly, the striatum also contains dense innervation from midbrain dopamine neurons, which represents a major site of synaptic plasticity<sup>11</sup>. The striatum is unique in that it completely lacks excitatory neurons. Instead, the striatum contains two main populations of GABAergic neurons: medium spiny projection neurons (MSN) and interneurons, which comprise approximately 95% and 5% of the overall population, respectively<sup>12</sup>. Information flow within the striatum is parceled into two main streams: the direct and indirect pathways, which act in opposing ways to control movement. The direct pathway circuit originates from striatonigral MSN, which receive excitatory glutamatergic input from sensorimotor cortex and thalamus and project to GABAergic neurons in the GPi and SNr. Striatonigral MSN are identified by their high expression of dopamine D1 and muscarinic M4 receptors<sup>12,13</sup>. The indirect pathway circuit originates from striatopallidal MSN, which receive input from the cortex and project to GABAergic neurons in the globus pallidus external segment (GPe). These neurons are identified by their high expression of dopamine D2 and adenosine 2A receptors<sup>12</sup>. Historically, the striatum has also been divided into striatal patch (or striosomal) and matrix compartments, which are defined by their specific neurochemical markers and connectivity<sup>14</sup>. The patch compartment is characterized by areas of dense alpha-opiate receptor binding, low acetylcholinesterase labeling, and projections to dopaminergic cells of the substantia nigra pars compacta and islands in the pars reticulata<sup>15,16</sup>. Matrix neurons are identified by their expression of the calcium-binding protein calbindin

and dense innervation of SST fibers<sup>14-16</sup>. This compartment primarily projects to the substantia nigra pars reticulata<sup>14,15</sup>. In addition, studies using retrograde tracers have also revealed that patch and matrix compartments are differentially targeted by corticostriatal neurons from different cortical layers and by dopaminergic neurons from the ventral tegmental area and substantia nigra<sup>17,18</sup>. Together, these circuits regulate multiple aspects of human behavior, and dysfunction in any number of them may result in a wide spectrum of neurological and psychiatric disease.

## **1.2 Development of the Telencephalon**

### *Early Patterning of the Neuraxis*

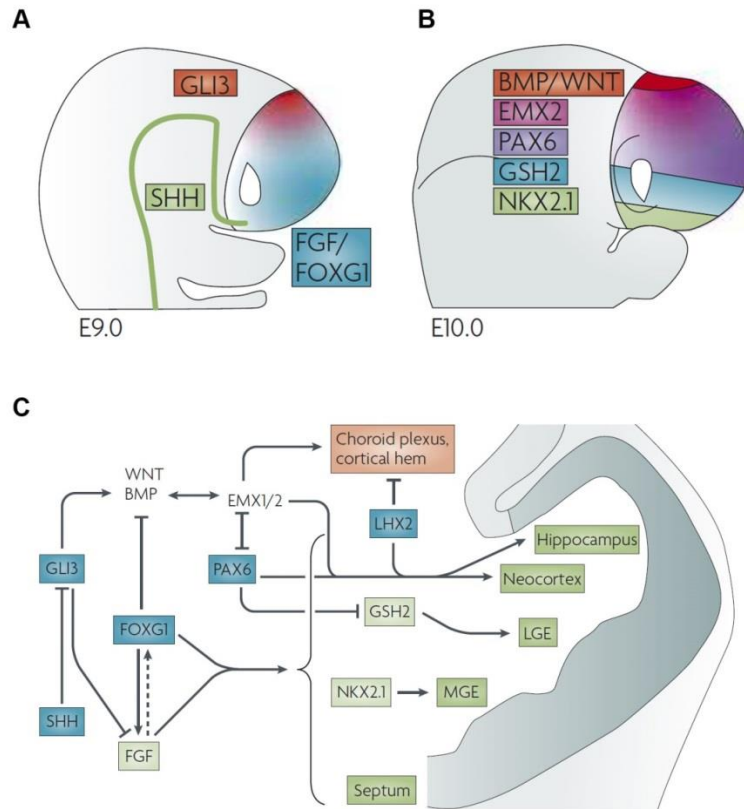
Telencephalic development is regulated by multiple intrinsic genetic programs that are shaped by secreted factors, or morphogens. The process begins with the neural plate, a flat sheet of ectodermal cells (also known as neuroepithelium) that evaginates and fuses dorsally to form the neural tube. Across its full extent, the neural tube contains multipotent neural stem cells that generate both neurons and glia of the central nervous system (CNS). Wnt proteins, fibroblast growth factors (FGFs) and retinoic acid are expressed from the caudal end of the neural plate and function to induce posterior character. Antagonists of these factors, such as cerberus and dickkopf, are secreted from the anterior visceral endoderm and act to stabilize anterior character<sup>19</sup>. Subsequently, three primary vesicles develop in the rostral portion of the neural tube: the prosencephalon (forebrain),

mesencephalon (midbrain) and rhombencephalon (hindbrain). The caudal neural tube remains undifferentiated and eventually gives rise to the spinal cord. The prosencephalon then forms secondary vesicles that give rise to the telencephalon and diencephalon (thalamus and hypothalamus), a process largely controlled by the secreted Wnt antagonist Tlc<sup>20</sup>.

### *Early Patterning of the Telencephalon*

FGFs serve as organizing factors in telencephalic patterning as soon as neuroectoderm first separates from ectoderm<sup>21,22</sup>. Within the anterior neural ridge (ANR), cells begin to express FGF8, which acts as an organizer to pattern the emerging telencephalon<sup>23</sup>. Adjacent to the ANR, the anterior neural plate expresses the transcription factor Foxg1<sup>24</sup>. Foxg1 and FGF8 form a positive feedback loop which promotes the induction and maintenance of telencephalic character<sup>22,25</sup>. Dorsal-ventral (D-V) patterning of the telencephalon is predominantly controlled by the dorsalizing effects of Gli3 and the ventralizing influence of sonic hedgehog (Shh)<sup>26,27</sup>. Sonic hedgehog is expressed from the notochord and serves to restrict genes instructive for dorsal fates. Together with Foxg1, Shh establishes the ventral telencephalon. As the telencephalon continues to grow, Wnt and FGF signaling becomes more specialized, and together with bone morphogenetic proteins (BMPs), these factors specify the dorsal telencephalic domain<sup>28,29</sup>. Downstream of these secreted morphogens, several key transcription factors delineate the different telencephalic subdomains. Within the ventral telencephalon, FGF and Shh signaling activate

the expression of Nkx2.1, a homeodomain (HD) transcription factor that defines the medial ganglionic eminence (MGE)<sup>21,22,30</sup>. As Nkx2.1 upregulates, the homeobox transcription factor Pax6, which is initially expressed throughout the telencephalon, downregulates in the ventral telencephalon and forms a sharp boundary with Nkx2.1 that demarcates the D-V border. Slightly later in development, the Pax6- and Nkx2.1-expressing regions become separated by a domain of Gsx2 expression, which specifies the lateral ganglionic eminence (LGE). The MGE will eventually give rise to interneurons in many forebrain areas, including the cortex. The LGE primarily gives rise to MSN, but a region in the dorsal domain that co-expresses Gsx2 and Pax6, has been shown to give rise to olfactory bulb interneurons (**Figure 1.2**). However briefly, the dorsal cortex is also established by gradients of transcription factors that upregulate in response to signaling molecules and morphogens expressed from localized patterning centers. Of these transcription factors, Pax6, Sp8, Emx2, and COUP-TFI play integral roles in cortical area patterning<sup>31</sup>. A more detailed description of the transcriptional programs regulating subpallial development is provided in the sections to come.



Modified from Hébert and Fishell (2008)

**Figure 1.2. Early patterning and transcriptional regulation of the telencephalon.**

**(A).** Dorsal (top) and ventral (bottom) subdivisions of the mouse telencephalon at E9. Shh is expressed from the ventral domain and antagonizes the dorsalizing effects of Gli3. Foxg1 and FGF are expressed from the anterior plate cells and form a positive feedback loop with Shh to specify ventral character and inhibit BMP/Wnt signaling.

**(B).** By E10, the dorsal-most domain is split into BMP/Wnt expressing regions that are adjacent to countergradients of the transcription factors Emx2 and Pax6. Meanwhile, the ventral domain has been split into overlapping Nkx2.1 and Gsh2/Gsx2-expressing regions.

**(C).** Shown in blue are the factors responsible for broadly establishing the early telencephalic domains and their antagonistic/agonistic actions. Downstream transcription factors, such as Gsh2/Gsx2 and Nkx2.1 then further subdivide the telencephalon. In the dorsal telencephalon, Gli3 promotes the expression of BMP and Wnt proteins, which are required for EMX1/2 expression. EMX1/2, together with Pax6 and Lhx2, further subdivide the dorsal telencephalon. Modified from Hébert and Fishell (2008).



### **1.3 Molecular-Genetic Controls over Subpallial Development**

#### *Overview*

The subpallium is an exemplary case of telencephalic complexity given the diversity of neuronal subtypes that it generates. These neurons go on to form the BG, parts of the amygdala and septum, and as will be discussed in the following sections, an almost endless array of cortical interneurons. However, the scope of the work presented in this dissertation mainly concerns the production of cortical interneurons and striatal derivatives. As such, the first part of this section will outline the origins, classification schemas, and generation of cortical interneurons. The second part of this section will touch upon the genesis of the striatum and the molecular regulation governing the development of its principal cell type, the medium spiny neuron.

#### *Origins of Cortical Interneurons*

Much of what we know about cortical interneuron development comes from studies carried out in rodents, and this work will be the major focus of the following introductory section. Recently however, key papers examining developing human fetal tissue, developing non-human primate tissue, and through the manipulation of human embryonic stem cells, have shown that many of these developmental programs are conserved across species<sup>32,33</sup>. Unsurprisingly, abnormalities in interneuron development can lead to disordered cognition, and as such, interneuronopathies have been implicated in a variety of

neurological diseases including epilepsy, autism and schizophrenia<sup>34 35 36 37 38</sup>.

Unlike glutamatergic projection neurons, which originate in the dorsal telencephalon and migrate radially along glial processes to populate the cortex, interneurons are born in the ventral telencephalon and undergo a long tangential migration up into the cortical plate<sup>39 40 41 42</sup>. Numerous fate mapping studies relying on the use of genetic labeling and transplantation assays have demonstrated that different cortical interneuron subtypes originate from distinct locations within the ventral telencephalon at different developmental stages<sup>43 44-47 48 49</sup>. During embryonic development, the ventral telencephalon can be divided into two main regions: the ganglionic eminences and the preoptic area (PoA)/ anterior entopeduncular (AEP) domains<sup>50</sup>. The ganglionic eminences can be further subdivided into three anatomically distinct domains termed the medial, lateral, and caudal (CGE) ganglionic eminences. The vast majority (~90-95%) of cortical interneurons originate within the MGE, CGE, and AEP/PoA, with a small, somewhat controversial contribution from the LGE<sup>51 52 47</sup>. As is the case for glutamatergic projection neurons, most cortical interneurons are born between embryonic day 11 (E11) and E17.5 in the mouse. Birth dating studies demonstrate that cortical neurons develop radially in an “inside-out” fashion, such that later-born neurons migrate past their predecessors to occupy more superficial layers of the cortex<sup>53</sup>. Interestingly, despite their vastly different origins, recent data suggests that interneurons and projection neurons born at the same time occupy the same cortical layer, suggesting that the migration and

differentiation of these two populations is on some level coordinated<sup>39 54 55 56 57</sup>.

### *Interneuron Subgroup Identification*

The neocortex needs to perform multiple types of neuronal computations in a diverse and flexible fashion. GABAergic inhibitory interneurons largely make this possible by regulating the balance of activity, synaptic integration, synchrony, spike dynamics and oscillations of neuronal ensembles<sup>58</sup>. The ability of interneurons to perform such complex and specific functions depends upon their high degree of cellular diversity. Each interneuron subtype differs from one another in terms of its morphological, neurochemical, and electrophysiological properties<sup>59 60</sup>. Perhaps as a consequence of this heterogeneity, specific interneuron subtypes are differentially implicated in the pathobiology of various neurological and psychiatric disorders<sup>61 62 63 64 59,65,66</sup>.

Roughly 50% of all cortical interneurons originate within the MGE and go on to express the calcium binding protein parvalbumin (PV). PV interneurons can be grouped into two morphological categories, either basket or chandeliers subtypes, and have non-adapting fast-spiking electrophysiological profiles<sup>67-69</sup>. Whereas PV basket interneurons target the cell body and proximal dendrites of their synaptic partners, chandelier cells specifically target the axon initial segment<sup>70 71</sup>. PV expressing basket cells target both pyramidal cells as well as other interneurons and are electrically coupled to other PV cells via gap-junctions<sup>72,73</sup>. This feature enables PV cells to regulate cortical network

synchrony and coordinate oscillations. In particular, PV cells are essential for initiating gamma oscillations, which are involved in higher order cognitive functions and shown to be abnormal in several neuropsychiatric disorders<sup>74</sup>.

The second largest neurochemical category, comprising approximately 20% of all cortical interneurons, expresses the neuropeptide somatostatin (SST). While in the cortex PV and SST interneurons are absolutely non-overlapping, a small population (~6%) of hippocampal interneurons expresses both neurochemical markers<sup>75</sup>. SST expression in neocortex has typically been associated with Martinotti cells, which characteristically target the apical dendrites of pyramidal cells in layer I, where they elaborate vast arborizations that spread horizontally to neighboring columns. SST interneurons display heterogeneous morphologies and have non-fast spiking, accommodating electrophysiological profiles<sup>76 77 68,78-80</sup>. About a third of SST interneurons in frontal, somatosensory, and visual cortex co-label with calretinin (CR) and are morphologically and electrophysiologically distinct from the SST<sup>+</sup>/CR<sup>-</sup> subgroup<sup>81</sup>. Another type of SST-expressing cell, termed the X94 cell after the transgenic mouse from which it was first described, are located in layers IV and V and have axonal projections that profusely innervate layer IV<sup>77</sup>.

The remaining 30% of cortical interneurons that do not express PV or SST express the 5HT3a receptor. This group of cells is especially heterogeneous and remains to be fully characterized, but contains CR, reelin, and vasoactive intestinal peptide (VIP) expressing subtypes<sup>82 83</sup>. VIP interneurons account for

40% of the 5HT3aR population in S1 and are particularly enriched in layers II/III. There appear to be several types of VIP interneurons, including neurons with bipolar, bitufted, and multipolar morphologies that express different markers (e.g. CCK and type 1 cannabinoid receptors) and exhibit diverse electrophysiological properties. CR cells have bipolar or double bouquet morphologies and tend to exhibit rapidly adapting firing patterns, while reelin-expressing neurogliaform cells display late-spiking firing patterns. Lastly, subsets of multipolar interneurons that express neuropeptide-Y (NPY) have rapidly adapting or irregular electrophysiological characteristics<sup>84 85</sup>. Taken together, the MGE produces the bulk of PV and SST-expressing subtypes, while the CGE gives rise to mostly 5HT3aR-expressing cells.

The aforementioned identification scheme is based on decade's worth of morphological, molecular, physiological and developmental data that has often complicated, rather than simplified efforts to classify cortical interneurons. In fact, estimates for the number of cortical interneuron subtypes have ranged from around a dozen to upwards of several hundred<sup>86,87</sup>. To overcome this challenge, some groups have suggested that interneurons exist as an assortment of species that fall along a continuum<sup>86</sup>. More recently, another group has put forth the idea that the large diversity of interneuron classes may in fact originate from only handful of cardinal cell types that develop their unique cellular properties through interactions with other neurons and local cues<sup>88</sup>. From a functional point of view, this enables interneurons that share the same genetic origins to evolve

properties that fit their function. In a sense, interneuron complexity can be taken as a proxy for the complexity of the cerebral cortex and the functions that it performs. Regardless, the question remains of how and when interneuron fate is determined. Interneurons traverse relatively long distances from their place of origin in the subpallium to their ultimate location upon maturation as compared to pyramidal cells, which follow ordered, and relatively simple migration programs<sup>89,90</sup>. Either several different intrinsic complex migration and fate determination programs are hardwired at the time of cell cycle exit or, interneurons maintain some degree of plasticity that allows them to adapt to environmental cues after migration to the cortex<sup>88</sup>.

#### *Genetic Regulation of Interneuron Development*

The initial evidence indicating that cortical interneurons come from the ventral telencephalon came from observations of Dlx1/Dlx2 expression, followed by analysis of the Dlx1/Dlx2 double mutant mice, which have a severe block in interneuron migration that results in a 4-fold reduction in neocortical interneurons<sup>39,91,92</sup>. Thus, the initial stages of interneuron development depend on the proper patterning of the ventral telencephalon. This process is partly controlled through gradients of Shh, which serve to regulate the expression of downstream transcription factors including members of the basic helix-loop-helix and homeodomain (HD) families. Together, these factors serve to pattern the neural tube through their combinatorial transcriptional codes, which define distinct progenitor pools along the D-V axis of the neural tube<sup>93</sup>. Of these, Dlx1,

Dlx2, Gsx1, Gsx2, and Ascl2 (also known as Mash1) are required for the generation of all cortical interneurons<sup>94 95</sup>. Dlx1/Dlx2 and Mash1 are required for the generation of early- and late-born subpallial progenitors, respectively<sup>92,96,97</sup>. Dlx1/Dlx2 also serve to repress oligodendrocyte production in favor of neuronal fates through antagonism of Olig-2 expression<sup>39 98 99</sup>. In contrast to Mash1, which turns off as progenitors exit the cell cycle, Dlx1/Dlx2 stay on and operate at several different stages of GABAergic interneuron maturation ranging from GABAergic identity acquisition to regulating the initiation and termination of migratory behavior. Gsx-1 and -2 have somewhat redundant functions and together promote an LGE regional fate, largely via cross-repression of Gsx2 and Pax6<sup>100 101 102 103</sup>. Together with Nkx2.1, this genetically determined map delineates numerous progenitor pools that give rise to progeny with diverse fate potentials. However, it is becoming increasingly clear that these factors, while instrumental in establishing the basic layout of the ventral telencephalon, by themselves cannot account for the tremendous diversity of neuronal subtypes that are present in the mature forebrain. Therefore, there must be numerous, as of yet uncharacterized transcriptional regulatory factors that act on a combinatorial level with cardinal patterning genes to generate the neuronal constituents of the many forebrain regions.

#### *The MGE Gives Rise to PV and SST Cortical Interneurons*

PV and SST expressing cortical interneurons are the primary cortical interneuron subtypes focused on in this thesis work. They originate in the MGE and comprise

over half of all of neocortical interneurons<sup>83 104</sup>. A number of key transcription factors within the MGE have been identified, and while the list is not complete, the genetic program that instructs the development of PV and SST lineages has begun to emerge. This cascade of gene expression begins around E9 with the transcription factor Nkx2.1, which acts as a master regulator to promote MGE-derived interneuron fates over CGE-derived cell types<sup>47 105</sup>. Within the MGE, Nkx6.2 is expressed dorsally in a region that appears to be partially Nkx2.1 negative and is particularly important for the development of a subset of SST/CR co-expressing cortical interneurons<sup>27,106 107 108</sup>. Nkx2.1 mediates neuronal progenitor identity, regulates neuronal subtype specification, and directs neuronal migration<sup>109</sup>. Nkx2.1 is downregulated in migrating interneuron precursors destined for the cortex, but expression continues postnatally in striatal lineages<sup>110</sup>. The transcription factor Sip1 (also known as Zeb2) has been shown to regulate Nkx2.1 levels either directly or indirectly in post-mitotic cortical interneuron precursors<sup>111,112</sup>. Nkx2.1 is also expressed in the septum, AEP and PoA<sup>105 45 113</sup>. In addition to preventing the MGE domain from acquiring CGE identity, Nkx2.1 directly activates a second transcription factor within the MGE – Lhx6 – which is required for the proper differentiation of both PV- and SST-expressing interneurons<sup>113</sup>. Interestingly, Lhx6 is initially expressed in both GABAergic and cholinergic (ChAT) striatal interneuron precursors<sup>114</sup>. However, as development progresses, Lhx7 and Islet1 upregulate in ChAT-fated cells and cause Lhx6 to turn off, thereby allowing Lhx7 and Islet1 to bind to and activate



cholinergic specific genes<sup>115</sup>. In the absence of Lhx7, cholinergic fated interneurons switch fate and differentiate toward GABAergic interneurons of the striatum<sup>116</sup>. Downstream of Lhx6 are a series of factors including Sox6 and Satb1, which selectively affect both PV- and SST-expressing interneuron differentiation<sup>117 118</sup>. Although Sox6 is required for general PV and SST interneuron subtype differentiation, PV expression appears more dependent than SST on Sox6 function since perturbing Sox6 in mouse prevents cells from expressing PV with no effect on SST expression<sup>119 120</sup>. Together, Nkx2.1 and Lhx6 are required for the normal development of PV and SST subgroups<sup>49 121 122</sup>. Nkx2.1 is expressed in all MGE progenitors and Lhx6 is upregulated at, or shortly before, cell cycle exit<sup>123</sup> and continues to be expressed throughout adulthood<sup>35 107 124</sup>. While many aspects of how these transcription factors function are still being worked out, new tools, including the work presented in these thesis, have been developed to meet this challenge.

### *Spatiotemporal Biases in Fate*

Previous work from our lab, as well as others, has identified a spatial and temporal bias within the MGE for PV versus SST interneuron generation<sup>108</sup>. Transplantation assays of dorsal and ventral MGE at different time points revealed that while a mix of fates are present in both regions, SST precursors are enriched in early dorsal (dMGE) and PV precursors are enriched in late ventral (vMGE) MGE<sup>104</sup>. Shh signaling is required for Nkx2.1 expression and gradations of Shh strength within the MGE have been shown to influence PV versus SST

fates<sup>26,125 126</sup>. Blocking Shh signaling is sufficient to prevent Nkx2.1 protein expression and can cause MGE-derived progeny to adopt a CGE-like CR<sup>+</sup> bipolar fate<sup>126 127</sup>. Higher levels of Shh signaling promotes the generation of SST-expressing interneurons as compared to PV-expressing cells<sup>108</sup>. By exposing vMGE progenitors to exogenous Shh, PV fate can be suppressed in favor of SST fates<sup>127</sup>. In line with these findings, the dMGE has higher levels of Shh signaling as shown by enhanced expression of Gli1 and Gli2, despite Shh being secreted in an overall low to high D-V gradient<sup>108</sup>. Although spatiotemporal biases in the generation of interneuron subtypes exists within the ventral telencephalon, a heterogeneous population of subtypes are generated within the same regions at the same time<sup>107</sup>. This heterogeneity is paralleled by a diversity of progenitor cells that are capable of producing both neuronal and glial cell types, as well as those whose fate potential is more restricted<sup>128</sup>.

#### *Division Mode and Progenitor Subtype Influence PV and SST Fate*

The following section lays the groundwork for much of our rationale to do the work presented in this thesis, and as such, will be covered in considerable detail. Several studies have clearly demonstrated that different modes of division seem to be involved in the production of PV vs SST subgroups. Cyclin D1 and D2 are regulators of cell cycle dynamics that are expressed in largely non-overlapping niches. While both cyclins are expressed throughout the telencephalic germinal zones, cyclin D1 is predominantly expressed in the ventricular zone (VZ) while cyclin D2 is expressed in the subventricular zone (SVZ)<sup>129-131</sup>. The SVZ is mainly

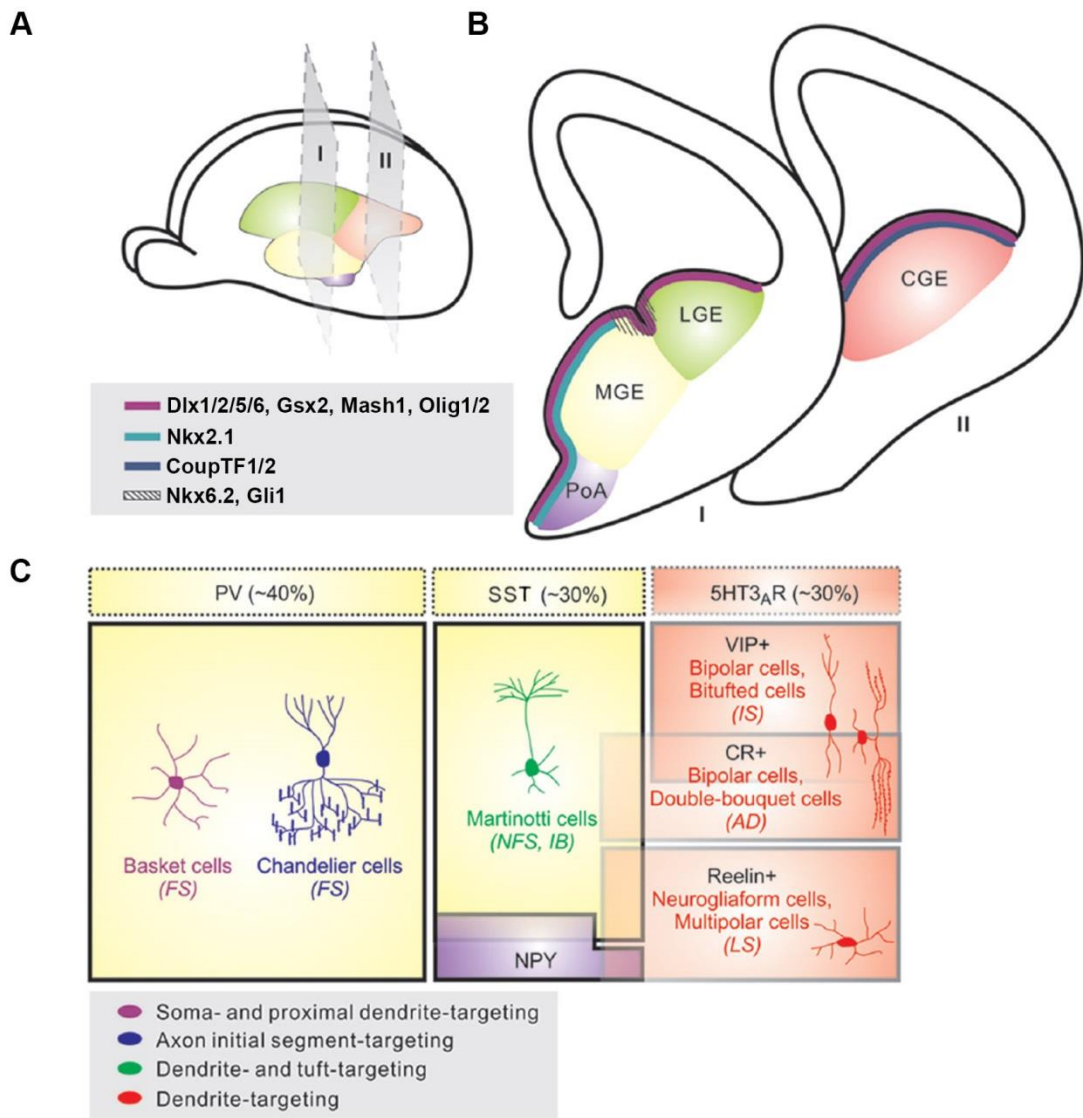
comprised of intermediate progenitors, which arise from divisions of radial glia occurring at the apical surface. Thus, cyclin D2 is both a marker of intermediate progenitors and a regulator of their mitotic behavior<sup>131 132</sup>. Interestingly, cyclin D2-null mice have a specific 30–40% reduction of neocortical PV<sup>+</sup> interneurons, but these mice have a normal complement of SST<sup>+</sup> interneurons<sup>131</sup>. These data suggest that asymmetric divisions occurring at the VZ surface primarily generate SST<sup>+</sup> cells, whereas PV<sup>+</sup> neurons seem to be generated through symmetric neurogenic events yielding intermediate progenitors in the SVZ of the MGE<sup>131</sup>. A recent study from our lab has recently used *in vivo* fate mapping to demonstrate this point<sup>133</sup>. In this study, the authors utilized *in utero* electroporation to conduct *in vivo* fate mapping of cortical interneurons originating from either apical progenitors or intermediate progenitors. In order to fate map apical progenitors, the authors took advantage of the tubulin  $\alpha$ -1 promoter (pT $\alpha$ 1), which labels neocortical progenitors at the apical surface that are known to generate relatively few intermediate progenitors (herein referred to as short neural precursors, or SNPs)<sup>134,135</sup>. Electroporation of pT $\alpha$ 1-GFP into the MGE revealed that SNPs primarily undergo neurogenic divisions, and therefore bypass the intermediate progenitor phase, to produce a ~2:1 ratio of SST<sup>+</sup>:PV<sup>+</sup> interneurons. On the other hand, electroporation with a nestin promoter-enhancer construct, which fate maps all MGE apical progenitors and their progeny, produced a ~2:1 ratio of PV<sup>+</sup>/SST<sup>+</sup> interneurons, consistent with the overall ratio of PV:SST interneurons produced within the MGE. Next the authors tested

whether directing MGE progenitors toward either apical or intermediate neurogenic divisions would bias their fate toward SST and PV-expressing interneurons, respectively. Remarkably, electroporation of a dominant-negative version of the Mastermind-like-1 protein (dnMAML), which blocks Notch signaling and promotes cell cycle exit, greatly reduced the number of cyclin D2 expressing intermediate progenitors and nearly doubled the ratio of SST<sup>+</sup> to PV<sup>+</sup> interneurons produced. The reciprocal experiment, which used overexpression of inscuteable to drive apical progenitors into basal progenitor states, resulted in a 3.5:1 ratio of PV<sup>+</sup> to SST<sup>+</sup> interneurons. Collectively, these results indicate that not only is interneuron fate diversity a function of spatiotemporal localization of progenitors within the MGE, but also of the apical-basal location of neurogenic division.

#### *Genetic Demarcation of the CGE*

Morphologically, the CGE has no clear boundaries and exists as a fusion of the MGE and LGE starting at the coronal level of the mid to caudal thalamus. The CGE produces approximately one-third of all cortical interneurons. These interneurons express 5HT3aR, predominantly display bipolar and bitufted morphologies, and express a number of neurochemical markers including CR, VIP, NPY, and Reelin<sup>39 52 47 48 82</sup>. Relative to the MGE, there are few genetic markers known to be specific to the CGE-derived lineages<sup>88</sup>. However, the orphan nuclear receptor, COUP-TFII, which is expressed in CGE, is involved in the migration and specification of CGE-derived neocortical interneurons<sup>136</sup>. In

addition, the HD protein, Prox1, is known to be expressed in a subset of CGE/LGE- and PoA-derived interneurons during embryonic development and maintained in the mature cortex<sup>137</sup>. Loss of Prox1 impairs the integration of CGE-derived cortical interneuron precursors into superficial layers and differentially regulates the postnatal maturation of reelin, VIP, and VIP/calbindin expressing subtypes<sup>138</sup>. COUP-TFI and Mash1 are also expressed in the CGE<sup>58</sup>. Interestingly, loss of COUP-TFI in SVZ progenitors and post-mitotic precursors leads to a reduction of late-born, CGE-derived VIP and CR expressing cortical interneurons, and a corresponding increase of early-born MGE-derived PV<sup>+</sup> interneurons<sup>139</sup>. This loss is associated with increased expression of cyclin D2 in the dorsal MGE, suggesting that the increase in PV<sup>+</sup> cell number is due to an increase the number of intermediate progenitors. The ventral CGE also expresses Nkx2.1, while the dorsal CGE strongly expresses Gsx2 and ER81, two transcription factors that are required for the proper patterning of the LGE and for the production of olfactory bulb interneurons, respectively<sup>30</sup>. However, while Nkx6.2 and COUP-TFI/II are widely expressed within the CGE, they are not restricted to it<sup>106</sup> (**Figure 1.3**). Ongoing efforts to identify CGE-specific transcriptional programs will likely help determine the molecular mechanisms underlying interneuron specification within this spatial domain.



Modified from Sultan, Brown, and Shi (2013)

**Figure 1.3. Origins and diversity of neocortical interneurons.**

**(A).** Neocortical interneurons are produced by neuronal progenitors in the ventral telencephalon. Most interneurons arise from either the CGE (pink) or MGE (yellow), with a small contribution from the PoA (purple). A small, controversial source may also arise from the LGE (green). **(B).** A number of transcription factors are differentially expressed within the subpallium and specify the LGE, MGE, CGE, and PoA. Whereas *Dlx1/2/5/6*, *Gsh2* (also known as *Gsx2*), *Mash1*, and *Olig1/2* are expressed throughout the subpallial germinal zone, factors such as *Nkx2.1* and *CoupTF1/2* are only expressed in the developing MGE/PoA and CGE, respectively. *Nkx6.2* and *Gli1* are expressed within a narrow region located in between the LGE and MGE. **(C).** Neocortical interneurons are highly diverse and differ from one another on morphological, neurochemical, electrophysiological, and targeting levels. Roughly 40% of neocortical interneurons are fast-spiking (FS) parvalbumin (PV)-expressing interneurons and can be classified into basket or chandelier subtypes. Not all chandelier subtypes, however, express PV. Approximately 30% of cells express somatostatin (SST) and are morphologically heterogeneous. These are typically non-FS. The remaining 30% express the serotonin receptor 5-HT<sub>3</sub>AR and contain vasointestinal peptide (VIP)-expressing and/or calretinin (CR)-expressing cells with bipolar or double-bouquet morphologies and fast adapting firing (AD) patterns, as well as Reelin-expressing, late-spiking (LS), neurogliaform cells. A small population of neocortical interneurons, some of which overlap with SST, express NPY and display irregular or fast AD firing properties. Modified from Sultan, Brown, and Shi (2013).

*Genetic Regulation of LGE and Striatal Development*

The LGE can be subdivided into dorsal and ventral domains<sup>140 141</sup>. The dorsal domain of the LGE (dLGE) expresses *Pax6*, *Ngn2*, *Dbx1*, and *Er81*. This region predominantly gives rise to olfactory bulb interneurons, but may also contribute neurons to the striatum proper and autonomic amygdaloid complex<sup>140 141 142</sup>. Notably, although the dLGE appears to be the primary source of olfactory bulb interneurons, subsets of this population may also be generated within the pallium and septum<sup>143</sup>. The ventral LGE (vLGE) expresses *Gsx2*, *Mash1*, and low levels

of Pax6, and largely produces MSN<sup>140 142 144 145</sup>. As mentioned earlier, Dlx1/Dlx2 and Mash1 are important regulators of LGE development. Loss of Dlx1/Dlx2 results in a severe reduction of later born striatal matrix neurons, while loss of Mash1 causes premature differentiation of VZ progenitors<sup>92,96</sup>. In Gsx2 knockout mice, there is ectopic expression of Ngn2 in the LGE and a subsequent loss of Mash1 and Dlx2<sup>142</sup>. However, even though early development of the LGE appears to be compromised in Gsx2 mutants, as development proceeds, Gsx1 is able to partially compensate for Gsx2 loss of function as evidenced by a molecular reestablishment of the cortical-striatal boundary and slight increase in expression of the striatal-matrix marker calbindin<sup>100,141,146</sup>. Although no phenotype in Gsx1 mice was initially noted, it was recently shown that Gsx1, in part through down regulation of Gsx2, directs progenitors toward a mature neuronal fate<sup>103</sup>.

The nuclear receptor ligand retinoic acid (RA) is another important signaling molecule implicated in the survival, proliferation, specification, and differentiation of many neuronal and progenitor cells types during brain development<sup>101,147-151</sup>. Beginning around E12.5, RA is produced in the LGE SVZ by the enzyme Raldh3, where it regulates striatal neuron differentiation<sup>150,152</sup>. RA plays an important role in initiating the expression of Gad67, an enzyme necessary for GABA synthesis, in striatal precursors<sup>153</sup>. A recent study examining retinoic acid receptor  $\beta$  (Rar $\beta$ ) knockout mice showed that these mice have a specific deficit in the striatonigral output pathway, which primarily consists of dopamine receptor D1



(Drd1)-expressing MSN<sup>154</sup>. The transcription factor Nolz1, which is expressed in late LGE progenitors and differentiating striatal precursors, has been shown to act downstream of Gsx2 to activate the Rar $\beta$  receptor<sup>155</sup>. The development of the striatonigral pathway has also been shown to depend on the transcription factor Islet-1, which is expressed in progenitors and post-mitotic precursors that give rise to the striatonigral pathway<sup>156,157</sup>. Loss of Islet-1 impacts the survival, differentiation, and axonal targeting of striatonigral neurons<sup>156,157</sup>. Importantly, Islet-1 functions to repress striatopallidal genetic programs within striatal precursors in favor of striatonigral ones<sup>157</sup>. As a result, mice that lack Islet-1 are hyperactive and have altered responses to pharmacological reagents that stimulate the dopamine D1 receptor pathway<sup>156</sup>. The early B-Cell Factor 1 (Ebf1) is yet another transcription factor implicated in the development of the striatonigral pathway<sup>158-160</sup>. Ebf1 mutant mice have a reduction in striatal volume due to increased cell death and a reduction in the number of striatonigral matrix neurons with relative sparing of those in the patch compartment<sup>159,160</sup>. Until recently, relatively little was known about factors that specifically regulate striatopallidal pathway development. However, a recent study has shown that the transcription factor Sp9 is essential in this process<sup>161</sup>. Sp9 is expressed downstream of Mash1 in LGE progenitors, maintained in post-mitotic striatopallidal MSNs, and required for their generation, differentiation, and survival<sup>161</sup>. Ctip2 (also known as Bcl11b) is another transcription factor expressed in early post-mitotic MSN that is required for multiple aspects of

striatal development<sup>162</sup>. In Ctip2 knockout mice, MSN do not fully differentiate, as demonstrated by reduced expression of multiple mature MSN markers<sup>162</sup>. MSN also aggregate into disordered clusters, which causes a severe disruption in patch-matrix organization<sup>162</sup>. The forkhead box protein, Foxp1, is a long known marker MSN, though its function in striatal development has not been studied until recently<sup>163</sup>. Using conditional inactivation of Foxp1 in brain, it was shown that Foxp1 causes a severe reduction in striatal volume, most likely through defects in progenitor proliferation<sup>164</sup>. Foxp1 also regulates the morphology of MSN and in Foxp1 heterozygous mice, MSN have significantly increased excitability<sup>164,165</sup>. In sum, retinoic acid, acting in concert with transcriptional regulators including Rar $\beta$ , Islet-1, Ebf1, Ctip2, Nolz1, Sp9, and Foxp1, has been shown to play critical roles in multiple aspects of striatal development.

#### **1.4 Interneuron Dysfunction in Neurological Disease**

##### *Epilepsy and Seizure Disorders*

Proper function of the cerebral cortex requires a precise balance of excitation and inhibition. While pyramidal neurons send information between cortical areas and from the cortex to other areas of the brain, inhibitory tone from cortical GABAergic interneurons shapes that activity through synchronized oscillations<sup>166</sup><sup>167</sup>. These two systems must work in a tightly controlled equilibrium in order to produce normal brain function and cognition. Thus, many important developmental and physiological mechanisms have evolved to maintain this

critical balance. For example, GABAergic interneurons are the principal cellular agents responsible for dampening hyperexcitability in the brain. As such, deficits in GABAergic interneurons are implicated in the pathobiology of various seizure disorders. Studies of animal models involving both genetic and acquired forms of epilepsy support this notion<sup>34</sup>. For example, mutations in the Aristeless-related homeobox gene (ARX) are frequently associated with epileptic encephalopathies that present in infancy and childhood<sup>168 45 169,170 171 172</sup>. ARX mutations are known to cause a number of neurological diseases ranging from disorders of neuronal migration that result in lissencephaly to mild intellectual disability<sup>173,174</sup>. However, despite the wide range of phenotypes that ARX mutation patients present with, all share epilepsy as a major common symptom<sup>172</sup>. In the most severe cases, mutations in ARX cause a syndrome known as X-linked lissencephaly with ambiguous genitalia (XLAG) that is characterized by severe developmental delay and intractable seizures<sup>175</sup>. Post-mortem examination of patients' brains revealed a nearly complete loss of cortical interneurons, which has been replicated in studies of Arx mutant mice<sup>172,176-178</sup>. ARX expression is mainly restricted to GABAergic neurons and loss of ARX has numerous consequences on this population including abnormal migration and neuronal differentiation<sup>179-181</sup>.

Dravet syndrome (DS) is another form of early infantile epileptic encephalopathy that is thought to arise as a consequence of interneuron dysfunction. DS patients typically present within the first year of life with multiple different seizure types

including prolonged convulsive seizures and frequent episodes of status epilepticus that are often treatment resistant<sup>182</sup>. DS is caused by heterozygous mutations in the gene SCN1A, which encodes the type I voltage gated sodium channel NAV1.1. NAV1.1 is a critical determinant of neuronal activity and underlies action potential generation, and has been shown to be particularly important for the function of fast-spiking PV interneurons<sup>183,184 185</sup>. A recent study using induced pluripotent stem cells (iPSCs) derived from DS patients found that inhibitory interneurons differentiated from iPSCs in vitro had pronounced defects in action potential firing, whereas the excitability of glutamatergic neurons derived from the same patient line were indistinguishable from controls<sup>186</sup>. Patients with DS may progress normally early on in life, however they go on to develop cognitive impairments and behavioral disturbances, including hyperactivity and autistic-like traits that sometimes present after seizure onset. Although seizure frequency decreases with age, many patients die from status epilepticus or from sudden unexpected death in epilepsy (SUDEP)<sup>187</sup>. Studies from Scn1a<sup>+/-</sup> mice have shown that GABAergic interneurons have dramatically reduced sodium currents that result in an impaired ability to sustain high frequency action potential firing. This causes an overall decrease in inhibitory tone that enables the activity of excitatory pyramidal neuron ensembles to go unchecked.

The most common treatments for epilepsy are medications that act by potentiating GABA function. These include drugs like barbiturates and benzodiazepines, which bind to GABA<sub>A</sub> or GABA<sub>B</sub> receptors, which collectively

cause dampening of neuronal activity through either the influx of hyperpolarizing chloride ions (GABA<sub>A</sub>) or through more slowly acting metabotropic effects (GABA<sub>B</sub>)<sup>34</sup>. About 20-30% of patients with epilepsy are refractory to all forms of medical therapy and must consider other options. Surgery may be an effective treatment option in some cases, but depends on many factors, including the site of seizure origin. Although not clinically available yet, cell-replacement therapies have also emerged as a promising treatment option for epilepsy<sup>188,189 190</sup>. Interneurons have the remarkable capacity to survive, migrate, and integrate into host cortical circuitry post-transplantation. As such, several groups have published proof-of-principal studies demonstrating its feasibility. For instance, transplantation of interneuron precursors into neonatal neocortex of Kv1.1 mutant mice was shown to significantly reduce the frequency of spontaneous electrographic seizures<sup>191</sup>. Subsequently, multiple studies have gone on to show that interneuron precursor transplantation into neonatal or adult neocortex or hippocampus can ameliorate both the development of seizure activity and the intensity of seizures already established<sup>192-194</sup>.

### *Schizophrenia*

Interneuron dysfunction has been suspected to underlie a variety of neurodevelopmental disorders in humans, including schizophrenia<sup>195</sup>. Post-mortem studies examining the prefrontal cortices of schizophrenic patients have found a 40% reduction in GABAergic synapses<sup>196</sup>. Since then, follow-up studies looking at mRNA expression levels in post-mortem brain samples has shown

significant decreases of numerous interneuron markers including PV, SST, CR, and NPY<sup>197</sup>. Schizophrenia is characterized by three groups of symptoms: 1) positive symptoms, such as hallucinations and delusions, 2) negative symptoms, including flat affect and social withdrawal, and 3) cognitive symptoms, such as deficits in attention and working memory<sup>198,199</sup>. Rather than being due to deficits in interneuron number, GABAergic dysfunction in schizophrenia may arise from more-subtle alterations in inhibitory circuits at the level of specific synapses<sup>200</sup>. Interestingly, some of the deficits observed in individuals with schizophrenia are similar to those observed in patients with bipolar disorder, suggesting that a common underlying disease mechanism may exist across these disorders<sup>201</sup>. Numerous mechanisms may be responsible for the disruption of inhibitory function detected in schizophrenia, all of which converge upon PV<sup>+</sup> interneurons as central features in this disorder. Specifically, PV<sup>+</sup> interneurons have lower levels of GAD67 expression in patient brains, and prefrontal cortex gamma oscillations are impaired in schizophrenic patients both at rest and during working memory tasks<sup>36</sup>. Multiple genes that have been associated with schizophrenia are also involved in PV interneuron development, including ERBB4 and DISC1<sup>202,203 204 205 206</sup>. In mice, conditional deletion of Erbb4 in PV<sup>+</sup> interneurons alone is able to recapitulate many phenotypes associated with schizophrenia including decreased GAD67 mRNA levels, decreased dendritic spine density of cortical pyramidal neurons, alterations in cortical excitation, and a net increase in baseline gamma oscillations<sup>207</sup>. These results, together with studies of human

post-mortem brain tissue, strongly implicate that GABAergic deficits may be specific to PV interneurons and that schizophrenia susceptibility genes play a role in the development of PV interneuron subtypes. However, a growing body of literature continues to suggest that subtle changes in the excitatory-inhibitory balance may be a common theme across a range of neuropsychiatric disorders including Tourette syndrome, autism, and anxiety disorders<sup>167 196 208 209,210</sup>. Given that different subclasses of interneurons contribute to the generation and pacing of distinct forms of neuronal activity via their unique targeting properties, the functional effects of abnormal GABAergic inhibition likely depend on which subtype of interneuron is involved. As such, it is important to gain an understanding of the different genetic programs that contribute to the development of distinct neuronal subtypes, since perturbations to any one of these programs could contribute differentially to the spectrum of neuropsychiatric disease.

### *Autism*

In contrast to schizophrenia, which appears to involve remarkable cellular specificity, autism spectrum disorders (ASDs) such as Rett's syndrome might have a more-generalized disruption of cortical excitation and inhibition<sup>167</sup>. Rett's syndrome is characterized by impaired language skills, cognitive deficits, stereotypic behaviors and respiratory problems<sup>211</sup>. In more than 90% of cases, Rett's syndrome is caused by loss-of-function mutations in the gene MECP2, which binds methylated DNA and functions as a transcriptional repressor<sup>212</sup>.

When MECP2 function is perturbed, inhibitory neurons contain reduced levels of GABA, and this deficiency is thought to underlie the disease phenotype<sup>38</sup>. In fact, loss of MECP2 function solely in mouse forebrain GABAergic neurons is sufficient to recapitulate most of the features of Rett's syndrome, including repetitive behaviors, increased sociability, cognitive deficits, impaired motor coordination, and cortical hyperexcitability<sup>167 38</sup>. MECP2 functionally interacts with BDNF, which plays a key role in the development and maturation of inhibitory circuits<sup>213</sup>. Further evidence linking GABAergic deficits with the pathophysiology of ASD and related disabilities comes from studies linking genes encoding proteins of the neuroligin–neurexin complex with susceptibility to autism or Asperger's syndrome<sup>214,215 216 217</sup>. On the contrary, excessive inhibition within specific neural circuits may also be pathological as is found in Down's syndrome<sup>167</sup>. Down's syndrome, which is caused by trisomy of chromosome 21, is characterized by distinct facial features, intellectual disability, and deficits in cognitive processes that involve hippocampal function<sup>218</sup>. Some of these deficits, such as those that deal with spatial memory, have been replicated in a mouse model of Down's syndrome, and the underlying mechanism seems to involve excessive inhibition in the hippocampal dentate gyrus<sup>219-221</sup>.

In sum, a large body of literature directly implicates GABAergic dysfunction in the pathogenesis of numerous neurological and psychiatric diseases. Since heterogeneity in interneuron function is key in modulating cortical circuit activity, perturbations to particular subtypes has differential contributions to human



disease states. Further characterization of how interneuronopathies play a role in specific disease etiologies is necessary if we wish to develop targeted, effective treatment options. Thus, there is a growing need to understand the genetic programs directing interneuron genesis and function, as well as for the development of new methods to generate interneuron subtypes in vitro.

## **1.5 Striatal Dysfunction in Neurological Disease**

### *Overview*

The BG is a group of highly interconnected subcortical brain structures that are conserved across vertebrate species stemming as far back as anamniotes<sup>222,223</sup>. Its functions are diverse, ranging from control of movement to learning-related motor functions, including habit formation, reinforcement learning, and motor sequence acquisition<sup>224</sup>. A series of recurrent neural loops linking the BG with specific input and output structures enables it to perform its numerous functions<sup>10,11</sup>. The BG receives excitatory synaptic input from different cortical areas, in addition to thalamic nuclei, insula, and amygdala, which diffusely target  $Drd1^+$  and  $Drd2^+$  expressing MSN of the striatum<sup>12</sup>. MSN process these signals and relay output to motor regions of the thalamus either directly through the SNr/GPi or indirectly via the GPe and STN before heading to the SNr/GPi. In turn, the thalamus, with modulation from midbrain nuclei, projects back to neocortical areas that initially targeted the striatum, thereby providing sensory feedback control of ongoing behavior<sup>12,223,224</sup>. Dysfunction in any of these BG nuclei can

result in debilitating disease, and thus understanding the molecular-genetic controls over its development and function has considerable value. The collection of neurological disorders linked to BG dysfunction is vast, and includes Tourette syndrome (TS), autism, obsessive compulsive disorder (OCD), schizophrenia, dystonia, Parkinson's, and Huntington's disease<sup>12,223,224</sup>.

### *Tic Disorders and Tourette Syndrome*

Although tic disorders and TS are considered separate clinical syndromes, they are often comorbid and thought to share similar disease etiology<sup>225</sup>. Tourette syndrome, which affects around 1% of the population, is characterized by sudden, repetitive, involuntary movements or vocalizations that typically begin between 3 and 9 years of age<sup>226</sup>. Tics are generally associated with an urge or sensation that drives the individual to perform the action, but unlike other types of abnormal movements, they can typically be suppressed<sup>224</sup>. The urge to perform them, however, may be so great that in some instances they are termed involuntary. Evidence that the BG, in particular corticostriatal circuits, is involved in TS partly stems from observations of tics in patients with diseases that directly affect the BG, such as Huntington disease<sup>224</sup>. Patients with TS have also been shown to have a consistent reduction in striatal volume<sup>227,228</sup>. In support of a BG pathophysiological basis, drugs that block dopamine or cause dopamine depletion are highly effective at suppressing tics, whereas pro-dopaminergic drugs exacerbate tics<sup>224</sup>. In more severe cases, deep brain stimulation of thalamic nuclei tightly linked to the BG or different BG nuclei themselves has

emerged as an established effective treatment option. Post-mortem evaluation of patients with severe TS has revealed that specific interneuron populations, most notably ChAT<sup>+</sup> and PV<sup>+</sup> interneurons, are reduced in both number and density in the striatum<sup>210,229</sup>. A recent study from Xu and colleagues used targeted ablation of ChAT interneurons in the dorsal striatum to investigate the effects of reduced cholinergic drive on mouse behavior<sup>230</sup>. They found that a 50% reduction of ChAT cells in the dorsolateral striatum produced behavioral manifestations of TS including stereotypic repetitive grooming and abnormal tic-like movements after acute stress or amphetamine treatment<sup>230</sup>. Together, multiple lines of evidence link BG dysfunction to TS and tic disorders.

#### *Obsessive-Compulsive Disorder*

Roughly 30% of patients with TS also meet criteria for OCD, which affects between 2 and 3% of the overall population<sup>231</sup>. OCD is characterized by recurrent intrusive thoughts or images (obsessions) that may be followed by repetitive compulsive behaviors<sup>224</sup>. Importantly, these repeated behaviors do not provide pleasure or reward, but rather relieve anxiety or provide a sense of completion<sup>224</sup>. Like TS, OCD is believed to have a strong genetic component, but to date only a few genetic associations have been identified<sup>232</sup>. Numerous studies, however, point toward the involvement of cortico-striato-thalamocortical circuitry in OCD pathogenesis<sup>233,234</sup>. Like TS, differences in striatal volume have been reported in patients with OCD<sup>235-237</sup> and fMRI studies have shown altered activities in the striatum, orbitofrontal cortex (OFC), and anterior cingulate (ACC) cortex during

resting state and during the expression of symptoms<sup>238,239</sup>. OCD is most commonly treated with selective serotonin-reuptake inhibitors (SSRI) and cognitive behavioral therapy, and studies have shown decreased activity in the striatum and OFC following these treatments<sup>232,240</sup>. Recently, genetic animal models of OCD have been generated that exhibit both corticostriatal dysfunction, as well as a common dysfunction in glutamate signaling<sup>232</sup>. For example, Sapap3 is a postsynaptic scaffolding protein highly enriched in the striatum that has been linked to trichotillomania, a compulsive tendency to pull out ones hair<sup>241</sup>. In mice, Sapap3 loss-of-function causes excessive grooming, increased anxiety, abnormally high spontaneous activity of MSN, and interesting a decrease in the number of PV<sup>+</sup> interneurons in the dorsomedial striatum<sup>241-243</sup>. The finding of decreased PV interneurons supports the notion that a lack of inhibitory drive in striatal microcircuitry could cause MSN hyperexcitability and suggests that imbalances in excitation and inhibition could contribute to OCD pathogenesis. Furthermore, deletion of the gene Slitrk5 in mice induces a number of OCD associated behavioral abnormalities, in addition to reduced striatal volume and decreased MSN dendritic complexity<sup>244</sup>. Together, multiple lines of evidence from clinical and experimental work point to the importance of the striatum and corticostriatal pathways in the pathogenesis of OCD and obsessive compulsive-related disorders.

### *Schizophrenia*

The dopamine hypothesis of schizophrenia attributes the symptoms of

schizophrenia to a dysregulation of dopaminergic signal transduction<sup>245-247</sup>. This hypothesis was based on observations that psychostimulants such as amphetamine were known to exacerbate psychotic symptoms, whereas antipsychotic medications, which primarily work by blocking dopamine receptors or function, are highly efficacious in alleviating these symptoms<sup>247</sup>. In particular, striatal dopamine hyperactivity has been one of the most replicated physiological findings in schizophrenia. For example, several post-mortem studies of schizophrenic patients have reported an increase in subcortical dopamine and dopamine metabolite (e.g. homo-vanillic acid) levels<sup>248</sup>. This is supported by imaging findings showing increased synthesis of dopamine within the striatum of schizophrenic patients<sup>245</sup>. Furthermore, an upregulation of striatal D2 receptors has been observed in post-mortem studies of drug-naïve patients, and this has been replicated in several PET imaging studies showing increased D2 receptor occupancy<sup>249</sup>. Higher dopamine availability, as measured by amphetamine-induced dopamine release, has also been found on PET imaging in schizophrenic patients, supporting the notion that increased stimulation of D2 receptors could be part of the etiology of schizophrenia<sup>250</sup>. Further support comes from genetic studies, which have consistently found associations between variations in genes involved in dopamine signaling, such as *Drd2*, and schizophrenia<sup>246,251</sup>. While multiple lines of evidence support dopaminergic hyperactivity in the striatum (mesostriatal and mesolimbic pathways), this does not appear to generalize to all areas of the brain. MRI and PET imaging suggest

that cortical dopamine hypofunction contributes to the cognitive symptoms in schizophrenia<sup>252</sup>. This raises the question of whether hypodopaminergic function in the cortex and hyperdopaminergic function in the striatum are driven by a common disease process, or whether one drives the other. While reciprocal connectivity between the cortex and striatum makes this determination difficult in humans, animal models have been much more helpful. In both rats and primates, dopamine depletion in the prefrontal cortex leads to an increase in subcortical dopamine turnover and dopamine D2 receptor numbers<sup>253,254</sup>. On the other hand, overexpression of dopamine D2 receptors in the mouse striatum leads to impairment in prefrontal-dependent cognitive tasks that are associated with schizophrenia, decreased prefrontal cortex dopamine turnover, and increased D1 receptor activation in the prefrontal cortex<sup>255-257</sup>. Interestingly, overexpression of the D2 receptor in striatum leads to a decrease in striatal volume that is secondary to changes in MSN morphology<sup>258</sup>. Medication-naïve schizophrenic patients also show decreases in striatal volume as well as alterations in MSN morphology. It has also been shown that children of schizophrenic patients have decreased striatal volume relative to children without a family history of mental illness, suggesting that a reduction in striatal volume might be an early event in the development of the disease or an underlying risk trait<sup>245</sup>. Together, multiple lines of evidence from human clinical and post-mortem studies, as well as animal models support a role for the striatum in the pathogenesis of schizophrenia.

## CHAPTER 2

# Atypical PKC Inhibition Enhances the Generation of PV Cortical Interneurons from Embryonic Stem Cells

### 2.1 Generating GABAergic Cortical Interneurons from Mouse Embryonic Stem Cells

#### *Overview*

Embryonic stem cells (ESCs) are a renewable resource that have the potential to differentiate into almost any cell type within the human body. They can be used to model human development, screen for factors that affect cellular physiology, and used to treat human disease. However, before we can realize their full potential, several significant barriers must be overcome. Perhaps the most difficult challenge is to develop methods that direct the differentiation of stem cells into specific cell types. Moreover, in order to fully utilize their potential, cells derived *in vitro* through the use of ESCs must, to a large extent, be as similar to

their *in vivo* counterparts as possible. This includes the expression of neurochemical markers, morphology, and ultimately, their ability to function equally in the same environment. From the standpoint of understanding and treating neurological and psychiatric diseases, there is much to be gained from being able to generate an endless supply of distinct neuronal subtypes *in vitro*. If we consider interneurons, this is especially challenging given the astonishing diversity of interneuron subtypes that exist. If we are to achieve the promise of interneuron-based therapies for interneuron related diseases, we must be able to produce enriched populations of particular subtypes since interneuron subtypes are differentially affected in various disorders<sup>190,259-262</sup>. To complicate matters, many aspects of interneuron fate are extrinsically determined through interactions with neighboring cells, which are numerous in type and wired together into intricate circuits that are laid down during embryonic and early postnatal development. In order to promote their differentiation, neurons derived *in vitro* are usually replated onto a layer of feeder cells (typically other neurons and/or glia) that support their growth and provide the necessary synaptic inputs to promote their functional maturation. Alternatively, neurons can be transplanted into the regions of neonatal or adult brains where they are normally found. This method is typically superior to feeder layers in terms of promoting a mature fate. In the case of human ESC-derived interneurons, xenographic transplantation usually elicits an immunogenic reaction. Although this problem can be overcome with the use of immunosuppressants or immunodeficient hosts, a more



fundamental barrier is at hand: the protracted maturation of human-ESC derived interneurons<sup>263</sup>. Even several months post-transplantation, human ESC-derived interneurons continue to express immature neuronal markers, suggesting that they are following a prolonged intrinsic maturation program mimicking normal human development<sup>264 265 266 267 263</sup>. Fortunately, the molecular programs that direct cortical interneuron development are largely conserved between mouse and human, including Nkx2.1 and Lhx6 expression patterns<sup>33 32</sup>. By 30 days post-transplant into mouse neonatal neocortex, mESC-derived cortical interneurons display morphological, neurochemical, and electrophysiological signatures characteristic of mature cortical interneurons<sup>268,269</sup>. Hence, mESCs enable the study of interneuron development in a practical time frame and in an accessible system, which is of great translational value. The following chapter describes progress using an atypical protein kinase C inhibitor to enhance the generation of PV<sup>+</sup> interneurons from mESCs.

### *Generating Interneurons from mESCs*

Over the past decade, many groups, including our own, have succeeded in generating cortical interneurons from mESCs<sup>268-273</sup>. This has been achieved largely by recapitulating *in vitro* using growth factors and small molecule inhibitors the sequence of events that induce telencephalic character and ventral patterning endogenously. As will be discussed, neural fate commitment is first achieved through inhibition of mesoendoderm induction pathways, which are otherwise promoted. Following neural induction, the naïve neural progenitors are

then patterned using ventralizing factors such as Shh. Watanabe and colleagues pioneered this field by describing a differentiation protocol to efficiently generate telencephalic precursors from mESCs using a suspension embryoid body (EB) method in serum-free media<sup>271</sup>. Interestingly, they showed that roughly 70% of mESCs undergo neural conversion to Nestin<sup>+</sup> neural progenitors after 8 days in serum-free suspension culture followed by 2 days of adherent culture<sup>271</sup>. This was in contrast to serum-containing media, which for reasons that are not fully understood promotes differentiation into primitive endodermal and mesodermal lineages<sup>274</sup>. With the addition of the Wnt and Nodal antagonists Dkk1 and LeftyA during the first 5 days of culture, they were able to increase this to ~90%, as shown through the use of a Sox1::GFP mESC reporter line, which identifies early neuroectodermal cells<sup>271</sup>. Of these cells, roughly ~35% expressed the telencephalic marker Foxg1<sup>271</sup>. This data suggests that the first 5 days of differentiation are critical for achieving efficient telencephalic induction. Next, the authors showed that by adding the dorsalizing factor Wnt3a and ventralizing factor Shh, they could induce the expression of Pax6 and Nkx2.1, respectively, within the Foxg1 population<sup>271</sup>. Approximately 5–15% of all the cells generated were Foxg1<sup>+</sup>/Nkx2.1<sup>+</sup>, and could be regarded as ventral telencephalic-like and ~5–8% of the cells were Foxg1<sup>-</sup>/Nkx2.1<sup>+</sup>, probably representing a ventral diencephalic hypothalamic precursor<sup>271</sup>. Although this study also reported the generation of a small percentage of GABA<sup>+</sup> neurons after 20 days in culture, they did not characterize which subtype(s) of GABA<sup>+</sup> neurons they represented. Our

group built upon this early work by developing a Lhx6::GFP mESC reporter line, which was used to generate, visualize, and isolate cortical interneuron precursors of an MGE-like lineage<sup>268</sup>. This protocol used the BMP inhibitor noggin from differentiation days (DD) 0 to 5 to initiate neural induction, followed by the addition of FGF2 and IGF1 from DD5-8<sup>268</sup>. The patterning effects of FGF2 and IGF1 were not thoroughly investigated, but are thought to increase neural progenitor proliferation (personal communication). Shh was also added from DD5-12 to promote ventral telencephalic character. The Lhx6::GFP<sup>+</sup> cells were FACS isolated and transplanted into mouse neonatal neocortex to investigate their *in vivo* potential<sup>268</sup>. Analysis of these brains 30 days post-transplantation revealed that Lhx6::GFP<sup>+</sup> cells migrated extensively in the tangential plane away from the injection site<sup>268</sup>. These cells expressed GABA and displayed morphologies consistent with MGE-derived cortical interneurons<sup>268</sup>. Further analysis showed that a majority of these cells expressed mature interneuron markers such as PV, SST, and NPY and had electrophysiological profiles characteristic of their *in vivo* counterparts<sup>268</sup>. However, only 2% of all cells expressed Lhx6::GFP. Moreover, the protocol lacked the ability to specifically bias their fates to one subgroup over the other<sup>268</sup>. Therefore, further protocol optimization was necessary in order to generate higher yields of interneuron precursors, which was subsequently accomplished in a recent publication from our lab. In order to improve the telencephalic induction in our differentiation paradigm, and thereby increase the fraction of cells that could go on to become

Foxg1<sup>+</sup>/Nkx2.1<sup>+</sup> progenitors, we took advantage of the cross-regulatory network of Shh and Wnt signaling that is required for normal MGE development<sup>20,29,275,276</sup>. In this system, Wnts are strongly expressed in the dorsal and caudal domains of the developing CNS, whereas Dkk1, an endogenous WNT inhibitor, is expressed from the anterior visceral endoderm<sup>277</sup>. Together, Dkk1 and Wnt/ $\beta$ -catenin mediate anterior-posterior axis polarization by functioning as repulsive and attractive guidance cues, respectively, during visceral endoderm cell migration<sup>28,252,253</sup>. Therefore, in order to prevent cells from adopting caudal or dorsal fates, we applied the small molecule WNT inhibitor XAV939<sup>278</sup> together with the BMP inhibitor LDN-193189 from differentiation days (DD) 0-5 in our previously published differentiation protocol<sup>268</sup>. Remarkably, this resulted in a 90% conversion of mESCs to a Foxg1 expressing forebrain-like fate by DD12<sup>269</sup>. Additionally, XAV potently induced a ventral telencephalic fate in mESCs differentiated via this paradigm as evidenced by a 20-fold increase in Foxg1 and Nkx2.1 co-expression. To add the capacity of isolating interneuron progenitors to our Lhx6::GFP line, an Nkx2.1 bacterial artificial chromosome in which mCherry expression is driven by the Nkx2.1 promoter was inserted. As expected, nearly all DD12 FACS-isolated Nkx2.1::mCherry-expressing cells go on to express Lhx6::GFP within 24-36 hours, and following transplantation into neonatal neocortex, ~90% expressed the mature cortical interneuron marker Sox6 and GABA. These results indicate that Nkx2.1::mCherry-expressing cells are bona fide MGE-like progenitors capable of giving rise to mature cortical

interneurons. Next, this study took advantage of the known developmental programs that differentially bias progenitors to produce PV<sup>+</sup> and SST<sup>+</sup> fated interneurons *in vivo*. First, a much larger percentage of all early born interneurons are SST<sup>+</sup> fated as compared to PV<sup>+</sup>, which are predominantly produced at later stages<sup>45,49,127</sup>. Second, higher levels of Shh signaling in dorsal MGE appear to bias progenitors to produce SST<sup>+</sup> interneurons<sup>45,49,127</sup>. Thus, by isolating early (DD12) Lhx6::GFP<sup>+</sup> precursors grown in the presence of high Shh, we achieved a 6.4:1 ratio of SST<sup>+</sup>:PV<sup>+</sup> interneurons (64% SST<sup>+</sup>, 10%PV<sup>+</sup>, 25% PV<sup>-</sup>/SST<sup>-</sup>)<sup>269</sup>. On the contrary, by isolating late (DD17) Nkx2.1::mCherry<sup>+</sup> progenitors grown in low Shh conditions, we achieved a ~2.9:1 ratio of PV<sup>+</sup>:SST<sup>+</sup> interneurons (19% SST<sup>+</sup>, 56% PV<sup>+</sup>, 25% PV<sup>-</sup>/SST<sup>-</sup>). It is worth noting that in this study, the low Shh condition indicates that no exogenous Shh was added. It was found that after exposure to XAV, the cultures alone generated sufficient levels of Shh to support moderate induction of Nkx2.1 and Lhx6. Around the same as this study was published, another group published a report of using the forced expression of lineage defining transcription factors to generate specific subpopulations of cortical interneurons and screen for genetic factors that could augment the differentiation and/or specificity of *in vitro*-derived cortical interneurons<sup>273</sup>. The authors used the same base protocol as in Watanabe 2005 but modified their mESC line with a construct containing the nestin promoter-enhancer sequence driving Nkx2.1 and a tetracycline-responsive transactivator protein (Nkx2.1::IRES-tTA2S). Dlx2 is then driven by a tetracycline response

element, which is bidirectional and can drive expression of a candidate gene of choice simultaneously. To identify putative cortical interneuron precursors, the authors also inserted a sequence containing the Dlx5/6 intergenic element to drive eGFP expression. Cells were then sorted for Dlx5/6-eGFP, transplanted into embryonic ventral telencephalon, and analyzed for fate in the cortex several weeks later. The base line, whereby nestin drives Nkx2.1 and Dlx2 without a candidate gene, resulted in the following fate enrichment: 35% PV<sup>+</sup>, 30% SST<sup>+</sup>, 25% CGE-like (reelin<sup>+</sup> or VIP<sup>+</sup>) and 10% unlabeled. Next, the authors tested the effects of 12 different candidate genes selected on the basis of being expressed in cortical interneuron progenitor zones but of unknown function. Of the 12 genes tested, LMO3 and Pou3f4 appeared to facilitate the differentiation of cINs in different ways. Whereas Pou3f4 improved the general efficiency of mESC-derived interneuron differentiation, LMO3 augmented the MGE-derived basket cell population, resulting in the following fate enrichment: 56% PV, 21% SST, 16% CGE-like and 7% unlabeled. Importantly, this result, which was gleaned from an in vitro mESC-system, reliably predicted the phenotype of the LMO3 null mouse, which was then shown in the same study to have a previously uncharacterized ~30% reduction in the number of PV<sup>+</sup> cortical interneurons<sup>273</sup>. While the aforementioned studies<sup>269,273</sup> made significant progress in generating cortical interneuron subgroups from mESCs, we hoped to build upon these studies further by leveraging recent data from our lab indicating that the location of neurogenic division within the MGE is a critical mechanism for determining

interneuron fate. Thus, the work described in this chapter complements this study and enhances our ability to generate PV+ interneurons from mESCs.

## **2.2 Atypical PKC inhibition Enhances the Generation of PV Cortical Interneurons from Embryonic Stem Cells**

### *Overview*

Parvalbumin-expressing (PV) interneurons comprise close to half of cortical interneurons and their dysfunction is implicated in neuropsychiatric disorders. Improved methods to generate PV-interneurons from stem cells would not only aid in the study of their development and function, but enable their use in cell-based therapies. Recent studies indicate that the location of neurogenesis within the medial ganglionic eminence (MGE) critically influences the fate determination of cortical interneuron subgroups, with PV interneurons originating from SVZ divisions. Importantly, the aPKC-CBP pathway regulates the transition from apical to basal progenitor and their differentiation into post-mitotic neurons. We find that aPKC inhibition enhances intermediate neurogenesis from stem cell derived MGE progenitors, resulting in a markedly increased ratio of PV to somatostatin-expressing interneurons. These findings confirm that the mode of neurogenesis influences the fate of MGE-derived interneurons and provide a means to further enrich for the generation of PV-interneurons from pluripotent stem cells.

## Introduction

Proper function of the cerebral cortex requires the coordinated activity of two distinct neuronal populations: excitatory projection neurons and inhibitory GABAergic interneurons (cINs). In both mice and humans, roughly half of all cINs originate within the medial ganglionic eminence (MGE) of the subcortical telencephalon and can be separated into two non-overlapping categories defined by their expression of either parvalbumin (PV) or somatostatin (SST)<sup>80,88</sup>. While SST interneurons primarily target the dendrites of their synaptic partners, PV interneurons mainly target the cell body, proximal dendrites, or the axon initial segment of pyramidal neurons<sup>83</sup>. Interneuron dysfunction is implicated in major neurological and psychiatric diseases including autism, schizophrenia, and epilepsy<sup>167</sup>.

Due to their remarkable capacity to migrate, survive, and integrate into cortical circuitry after transplantation, cINs are attractive candidates for use in cell-based therapies of disorders of cortical inhibition, such as epilepsy<sup>190,279</sup>. Although progress has been made in generating enriched populations of interneuron subgroups from pluripotent stem cells<sup>280,281</sup>, protocols to efficiently generate highly enriched samples of PV-interneurons are lacking.

We recently used *in vivo* fate mapping to demonstrate that PV interneurons originate primarily from divisions of intermediate progenitors in the SVZ of the MGE<sup>133</sup>. In addition, we found that MGE progenitors forced to undergo SVZ



divisions generate PV-expressing interneurons at the expense of those expressing SST. This finding is consistent with a previous study that loss of cyclin D2 (CCND2; CD2), which is expressed in intermediate progenitors throughout the telencephalon, results in reduced numbers of PV interneurons without affecting the SST-expressing subgroup<sup>130</sup>. Loss of CoupTF1, which results in increased expression of CD2 in the dorsal region of the MGE where most SST interneurons normally originate<sup>104</sup>, also results in supernumerary production of PV interneurons<sup>139</sup>. Together, these findings suggest that enhancement of intermediate progenitor-like divisions should enhance production of PV interneurons from stem cell differentiations.

The atypical protein kinase C (aPKC)-CREB-binding protein (CBP) signaling pathway regulates the differentiation of interneurons from ventral forebrain neural progenitors<sup>282</sup>. Activation of aPKC results in the phosphorylation of CREB, thereby promoting neural differentiation<sup>283</sup>. In addition, aPKC is an integral component of the aPKC/Par complex that regulates cell polarity, division orientation, and the localization of cell fate determinants<sup>284</sup>. Through antagonistic interactions with lethal giant larvae (Lgl), the aPKC/Par complex functions to asymmetrically localize the Notch inhibitor Numb, which subsequently regulates the proliferation and differentiation of neural progenitors<sup>285</sup>. Given the many roles of aPKC in regulating cell polarity and fate, we examined whether aPKC inhibition during directed differentiations of embryonic stem cells into post-mitotic interneuron precursors will bias progenitors to undergo SVZ-like divisions. We

find that a myristoylated PKC pseudosubstrate peptide inhibitor (aPKCi), applied to our “MGE” protocol that enriches for Foxg1 and Nkx2.1-expressing interneuron progenitors, significantly increases the fraction of these progenitors that express CD2. Moreover, treatment of stem cell differentiations with aPKCi greatly enriches for the generation of PV-expressing interneurons at the expense of those expressing SST. Taken together, our system provides a novel platform for further study of cortical interneuron genesis, fate determination, and for their use in the development of cell-based therapies.

## Results

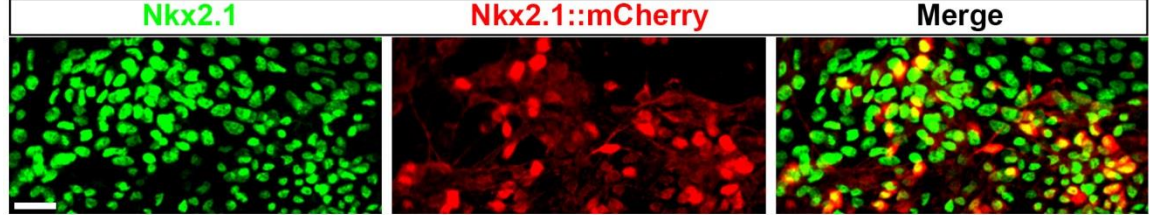
### *Generation of Nkx2.1-expressing interneuron progenitors*

Our previous study used a dual-reporter mouse embryonic stem cell (mESC) line for the isolation of interneuron-fated cells at the progenitor and post-mitotic stages<sup>269</sup>. This line expresses mCherry and GFP under the control of the Nkx2.1 and Lhx6 loci in bacterial artificial chromosomes, respectively. The line can be differentiated using a modified version of our previously established differentiation protocol (**Figure 2.1 A**)<sup>268,269</sup> into a highly enriched population of FoxG1 and Nkx2.1-expressing MGE-like progenitors. Although only ~11% of all Nkx2.1+ cells express mCherry by differentiation day (DD) 11, nearly all mCherry expressing cells also express Nkx2.1 protein, confirming the fidelity of the reporter (**Figure 2.1 B, C**). Thus, this system serves as an excellent platform for studying stem cell derived MGE-like progenitors in vitro.

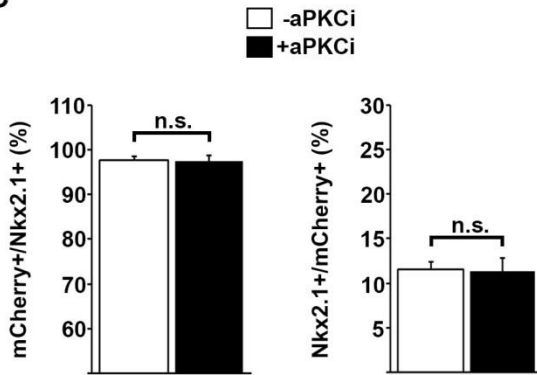
A

DD0	DD3	DD5	DD8	DD11
Neural Induction & V. Patterning		Growth & Expansion		Neural Specification
KSR:N2 (1:1)		KSR:N2 (1:1)		KSR:N2 (1:1)
+XAV		+XAV		+SAG
+LDN		+IGF-1		+/- aPKCi
Floating		Landing		Replating

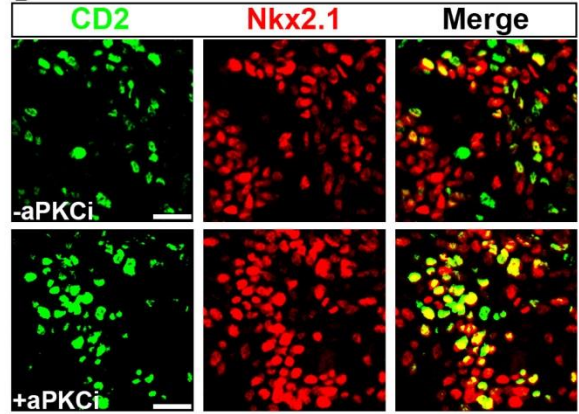
B



C



D



E

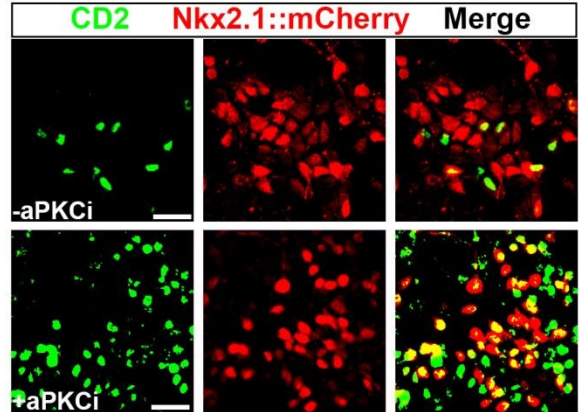
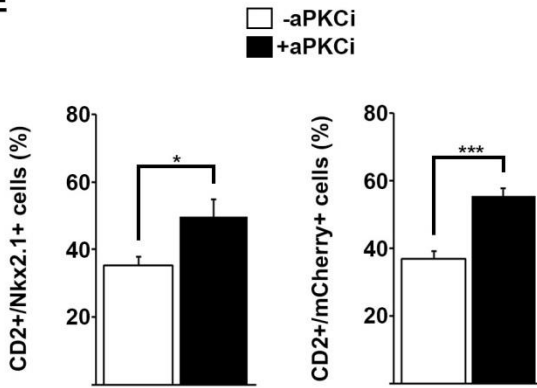


**Figure 2.1 aPKCi increases the proportion of CD2-expressing Nkx2.1 MGE progenitors.**

**(A).** Schematic of the differentiation protocol, with and without the addition of aPKCi from DD8-DD11. **(B).** Representative immunostaining of Nkx2.1 and Nkx2.1::mCherry from the JQ27 line at DD11 differentiated via the protocol shown in Fig 1A. **(C).** Quantification of the percentage of Nkx2.1::mCherry cells that also express Nkx2.1 protein, as well as the percentage of Nkx2.1+ cells that express Nkx2.1::mCherry. Neither of these measures is affected by aPKCi treatment. **(D).** CD2 with Nkx2.1::mCherry and Nkx2.1 immunofluorescence on DD11 cultures grown with and without aPKCi from DD8-DD11. **(E).** Quantification of the percentage of Nkx2.1 and Nkx2.1::mCherry-expressing cells that express CD2 shows a significant increase in the aPKCi treated condition. \* $p < 0.05$ ; \*\*\* $p < 0.001$  (pooled data from four independent experiments). Error bars indicate SEM. Scale bars 30  $\mu\text{m}$  in B, C.

*Atypical PKC inhibition increases the fraction of cyclin-D2 expressing Nkx2.1::mCherry progenitors*

We reasoned that if inhibition of aPKC biases progenitors toward intermediate neurogenesis, treatment of differentiations with the aPKCi beginning at DD8, when most of the cells in the culture express Nkx2.1, should increase the fraction of Nkx2.1::mCherry progenitors that also express CD2. Indeed, aPKCi significantly increased the percentage of CD2-expressing mCherry and Nkx2.1-positive progenitors (**Figure 2.1 D, E**). To determine whether the effect of aPKCi on CD2 expression by Nkx2.1+ progenitors is more broadly applicable to other stem cell lines and clones, we differentiated several additional mESC lines using the same protocol and found that aPKCi significantly increased the fraction of

Nkx2.1-expressing progenitors that also express CD2 (Figure 2.2).

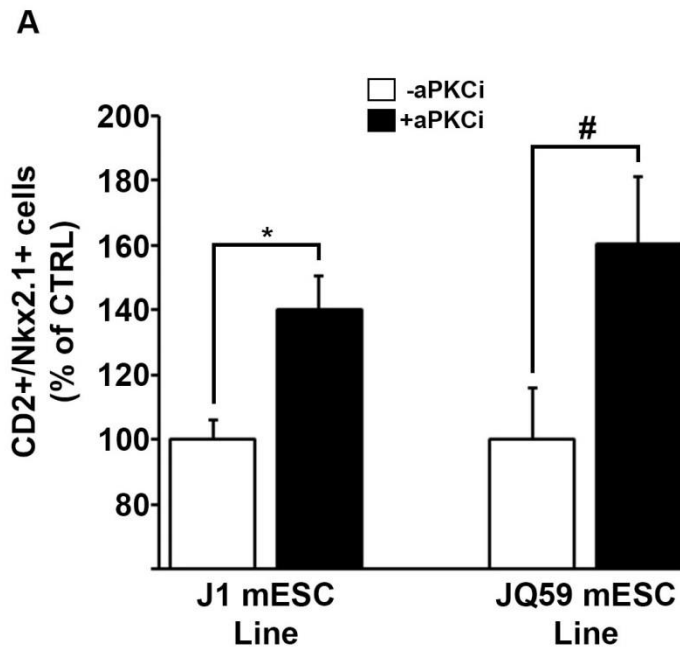


**Figure 2.2. aPKCi increases the proportion of CD2-expressing Nkx2.1 progenitors in two additional mESC lines.**

(A). Quantification of the proportion of Nkx2.1 progenitors that co-express CD2 at DD11. J1 (ATCC® SCRC-1010™) is the parent line of JQ27, used in this study. JQ59 is another J14 (Maroof et al 2010) subclone that also contains the Nkx2.1::mCherry BAC. The mCherry reporter expression in this line, however, is minimal. \* $p < 0.05$ ; #  $p < 0.05$  in Mann-Whitney U-test. Error bars indicate SEM.

To determine whether aPKCi treatment also influences progenitor proliferation, we pulsed cells for 30 minutes with the modified thymidine analogue EdU, which marks cells in S-phase, together with immunostaining for the proliferation marker Ki-67. Analysis of both markers showed no significant change in the fraction of EdU or Ki-67 expressing mCherry and Nkx2.1-positive progenitors with aPKCi

treatment (**Figure 2.3**). Together, these results suggest that aPKCi biases progenitors toward intermediate neurogenesis without affecting overall proliferation.

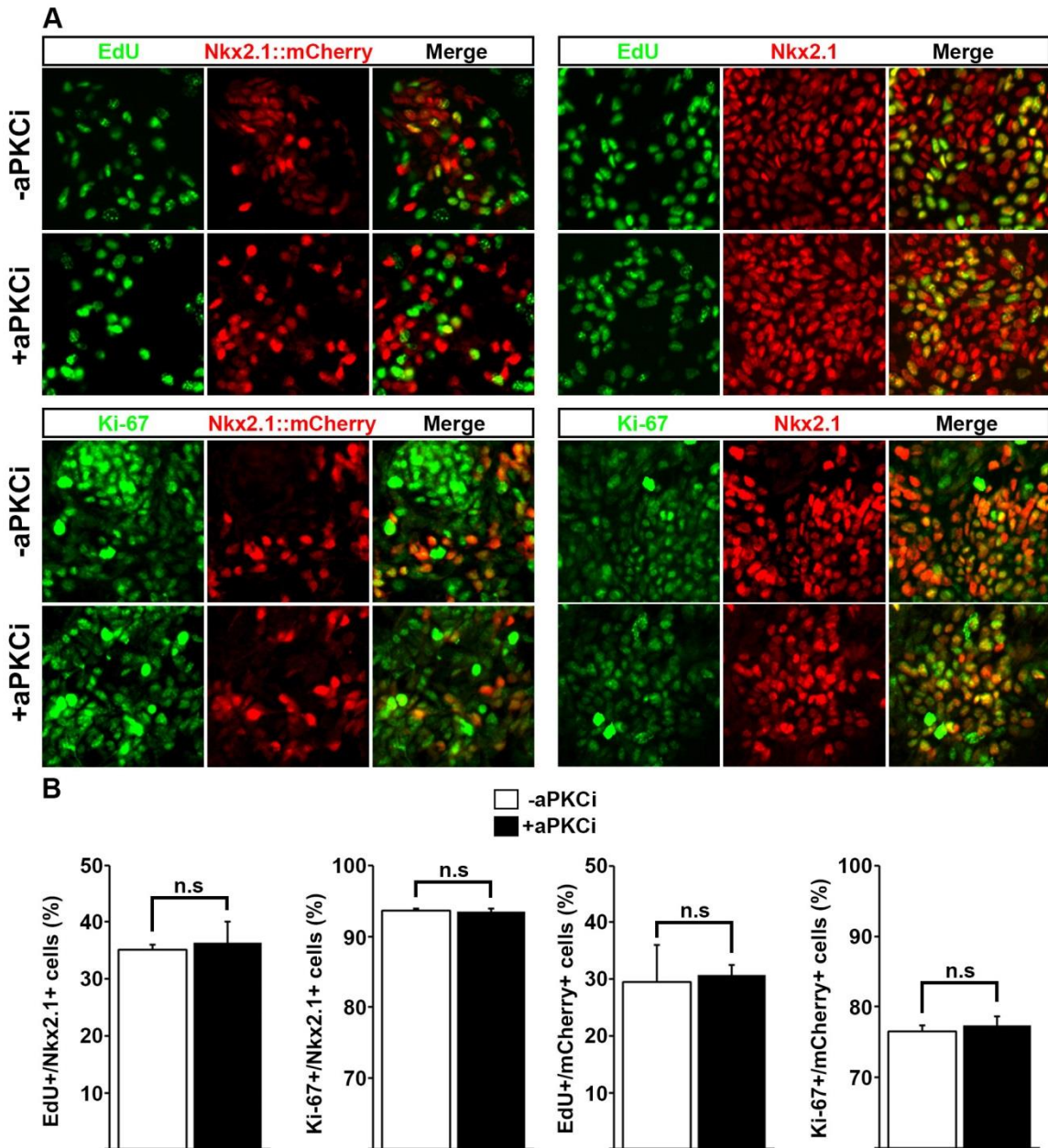


**Figure 2.3. aPKCi does not affect progenitor proliferation.**

**(A).** Representative images of EdU and Ki-67 together with Nkx2.1::mCherry or Nkx2.1 immunofluorescence on DD11 cultures grown with and without aPKCi. **(B).** aPKCi does not change affect the percentage of Nkx2.1:mCherry and Nkx2.1-expressing cells that label for EdU or Ki-67. \* $p < 0.05$ ; \*\* $p < 0.01$  (pooled data from three independent experiments). Error bars indicate SEM. Scale bars 30 $\mu$ m in A, B.

*Atypical PKC inhibition influences the mode of neurogenesis*

An additional benefit of our dual reporter mESC line is that the expression of mCherry and GFP enables us to evaluate whether the outcome of a division is proliferative or neurogenic. Using time lapse confocal microscopy, we found that from DD8 to 10 in some instances an Nkx2.1::mCherry progenitor divided into two mCherry-positive progenitors that then go on to divide again into Nkx2.1::mCherry+ cells (**Figure 2.4 A, B**). Other examples include symmetrical neurogenic divisions in which a mCherry-expressing progenitor divides to produce two Lhx6::GFP, post-mitotic interneuron precursors, which have visibly enhanced migratory activity (**Figure 2.4 C, D**). On rare occasions, more complex division schemes could be visualized, incorporating both symmetrical proliferative, symmetrical neurogenic, and asymmetrical neurogenic divisions (**Figure 2.4 E, F**).

Using this system, we hypothesized that aPKCi treatment should increase the fraction of Nkx2.1::mCherry daughter cells that divide symmetrically to produce two progenitors. Indeed, we found that aPKCi nearly doubled the percentage of Nkx2.1::mCherry progenitors that were observed to undergo a second division.



Together with the increased co-labeling of Nkx2.1-expressing progenitors with CD2, these results suggest that aPKCi biases interneuron progenitors to undergo SVZ-like divisions (**Figure 2.4 G**).

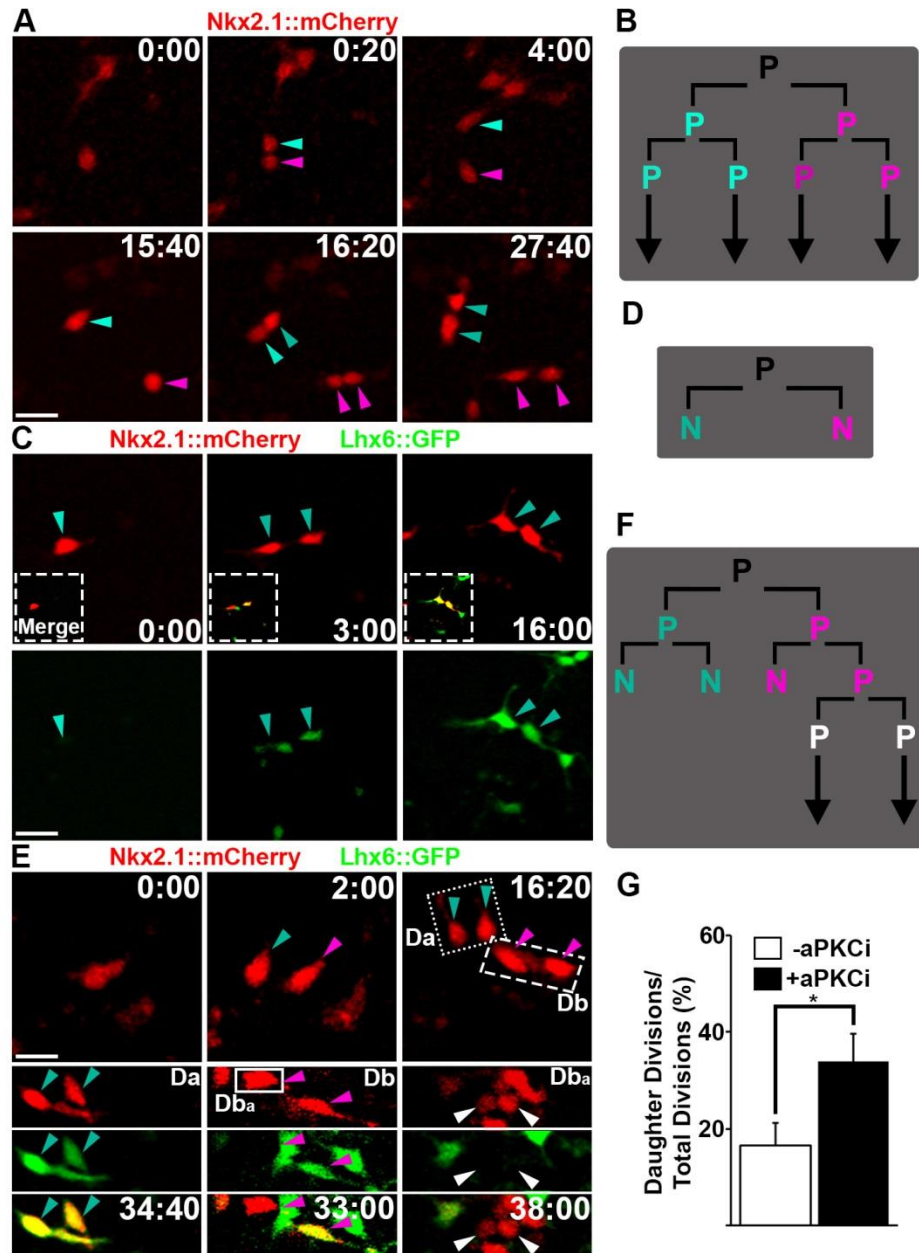




**Figure 2.4. Live cell imaging enables analysis of cell divisions and shows that aPKCi increases the proportion of Nkx2.1:mCherry daughter cells that undergo a second division.**

**(A).** A series of time-lapse images showing a single Nkx2.1:mCherry progenitor dividing symmetrically to produce two mCherry-expressing progenitors, which then go on to divide again during the 48 hour imaging session. Time is displayed as (hours:minutes). **(B).** Lineage relationships between cells in **A**. **(C).** A series of time lapse images showing a symmetrical neurogenic division, wherein one Nkx2.1::mCherry progenitor divides symmetrically to produce two Lhx6::GFP daughter cells. Merge of GFP and mCherry channels shown in dotted inset. **(D).** Lineage relationships between cells in **C**. **(E).** Time lapse imaging showing a more complex division scheme involving symmetrical proliferative, symmetrical neurogenic, and asymmetrical neurogenic divisions. **(F).** Lineage relationships between cells in **E**. **(G).** Quantification of the number of daughter cell divisions, defined by a Nkx2.1::mCherry daughter from a previous division that goes on to divide again. The number of daughter divisions is divided by the total number of Nkx2.1::mCherry divisions counted. The addition of aPKCi significantly increases the percentage of Nkx2.1::mCherry progenitors that divide again (pooled data from five independent experiments; 95 divisions counted in –aPKCi treated condition, 84 divisions counted in +aPKCi condition; \*p < 0.05). Error bars indicate SEM. Scale bars 30µm in A, C.

#### *Atypical PKC inhibition enhances PV fate specification*

Since directing MGE progenitors to undergo SVZ divisions directs them to produce PV-expressing cortical interneurons *in vivo*<sup>286</sup>, and since the aPKCi enhances the generation of SVZ-like progenitors *in vitro*, we next asked whether this treatment enhances the derivation of PV interneurons relative to SST interneurons in our stem cell system. mCherry progenitors differentiated in the presence or absence of aPKCi were isolated at day 11 via FACS and transplanted into neonatal mouse neocortex (**Figure 2.5 A**). Following transplantation, the mCherry reporter downregulates as the Lhx6::GFP reporter

becomes expressed in the post-mitotic interneuron precursors and is maintained in those cells thereafter (**Figure 2.5 B**)<sup>269</sup>. Thirty days post-transplantation, the fates of transplanted cells was assayed via immunostaining for GFP, parvalbumin (PV), and somatostatin (SST). aPKCi treated cultures resulted in a tremendous enrichment of PV-expressing interneurons at the expense of those expressing SST (**Figure 2.5 C, D**). Immunostaining for the MGE-derived cIN marker Sox6, together with GABA, confirms that aPKCi treated cells retain the appropriate lineage markers (**Figure 2.6**).

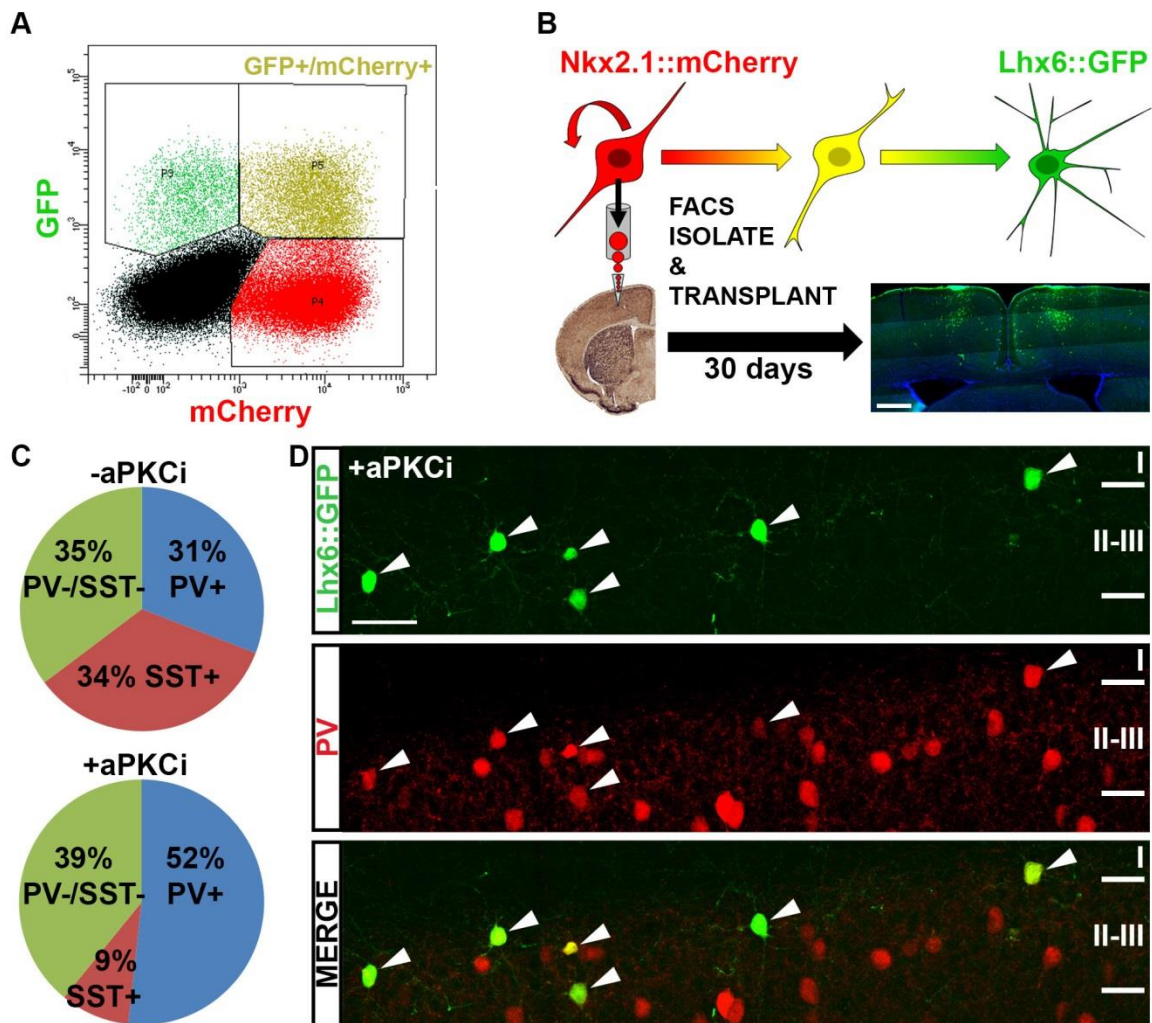


**Figure 2.5. Strategy to enhance the generation of parvalbumin (PV)-expressing interneurons from a dual Nkx2.1:mCherry-Lhx6:GFP mouse stem cell reporter line.**

**(A).** Representative FACS plot of the JQ27 line (Tyson et al., 2015) at DD11 shows segregation of mCherry-only (red), mCherry/GFP co-expressing (yellow), and GFP-only (green) expressing populations from non-fluorescent cells (black). **(B).** Schematic of reporter progression in mESCs differentiated towards Nkx2.1- and Lhx6-expressing fates, then subjected to FACS for mCherry on DD11, followed by transplantation into neonatal mouse cortex. After 30 days the animals are sacrificed and the fates of transplanted cells are assayed. **(C).** Quantification of SST or PV expression in Lhx6::GFP-expressing cells differentiated in the presence or absence of aPKCi from DD8-DD11 (-aPKCi 31.3±2.4% PV, 33.5±2.14% SST and 35.3±0.87% double negative; +aPKCi 51.9±4.5% PV, 9.03±1.4% SST, 39.1±3.6% double negative, SEM). The addition of aPKCi from DD8-DD11 significantly increases the ratio of PV to SST cells generated (n=4 independent differentiations, 8 brains total; P<0.005). **(D).** PV immunofluorescence on Lhx6::GFP expressing cells from the aPKCi condition 30 days post-transplant. PV, parvalbumin; SST, somatostatin. Scale bars 50 µm in D; 400µm in B.

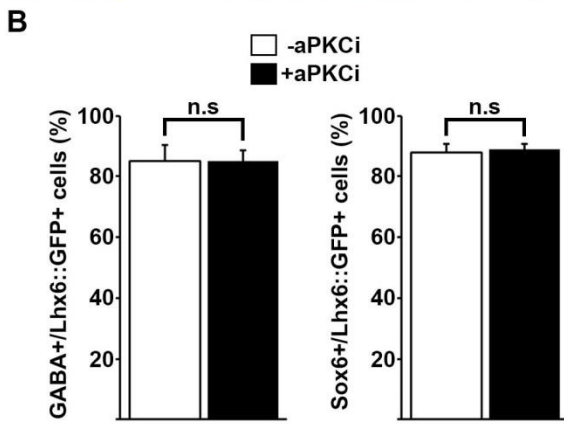
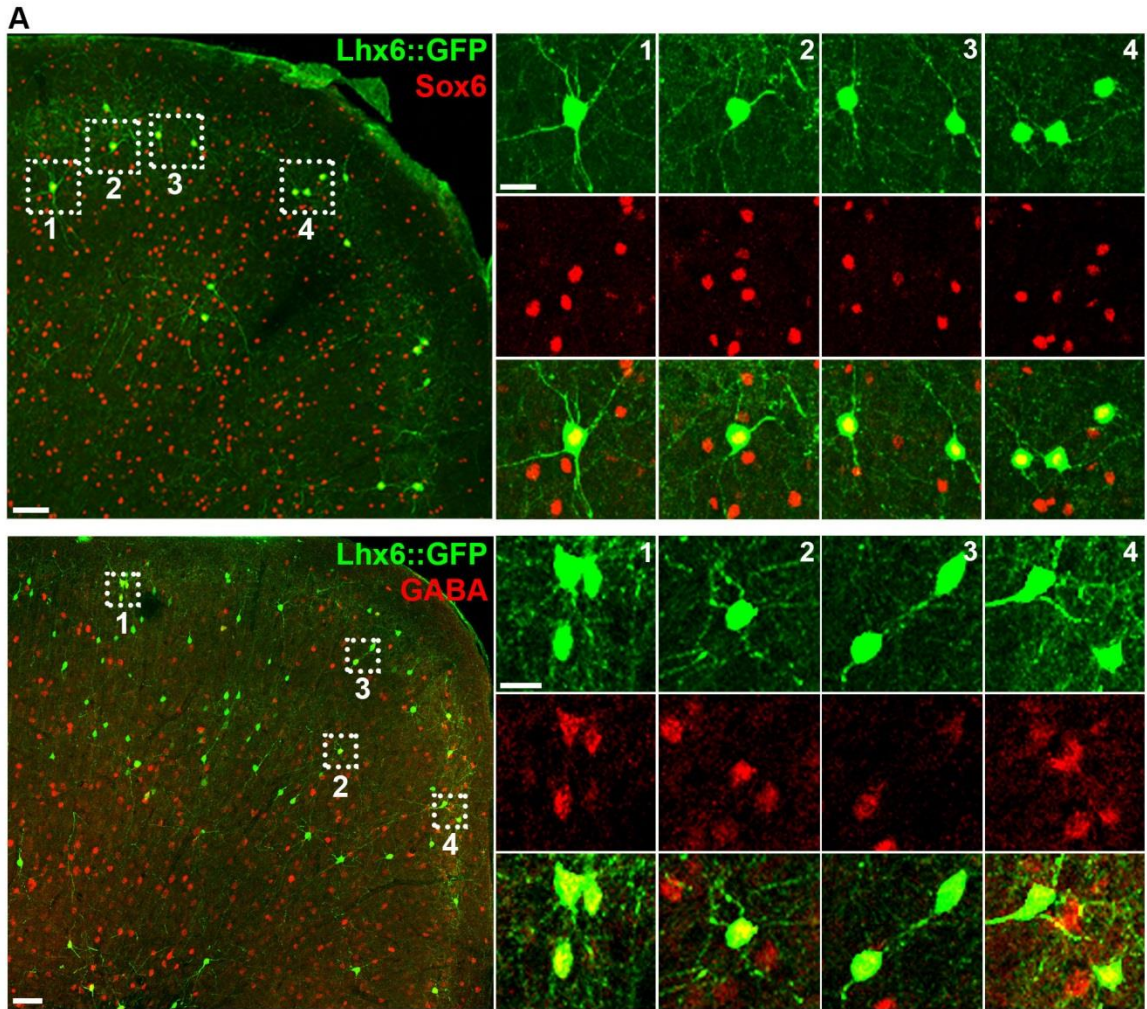


**Figure 2.6. aPKCi treated cells express Sox6 and GABA.**

**(A).** Representative brain sections containing transplanted Lhx6:GFP cells immunostained for Sox6, GABA, and GFP, with high-magnification images of individual cells expressing Sox6 and GABA. **(B).** aPKCi does not significantly change the percentage of transplanted cells that express Sox6 or GABA (pooled data from four independent experiments). Error bars indicate SEM. Scale bars 40 $\mu$ m in A; 10 $\mu$ m in insets.

## Discussion

Cortical interneurons represent a remarkably heterogeneous population of cells in terms of their morphology, connectivity, electrophysiology, and neurochemical profiles. As a consequence, interneuron subtypes differentially contribute to network processing that underlies a wide range of cortical functions. By extension, dysfunction of distinct interneuron subtypes is implicated in the specific pathobiology of major neurological and psychiatric diseases. Thus, considerable effort is being put forth to generate specific interneuron subgroups or subtypes from embryonic stem cells. The capacity to do so would not only allow for the study of factors that regulate the type, number, or function of interneurons, but would enable their use in cell-based therapies.

Our previous study showed that manipulations of sonic hedgehog (Shh) exposure and time in culture differentially enrich for PV- versus SST-fated mESC derived cINs<sup>280</sup>. While early born cells exposed to higher levels of Shh produced a ~6.4:1 ratio of SST to PV, increased duration in culture combined with lower levels of Shh generated a ~2.6:1 ratio of PV to SST. Another study using the

forced expression of transcription factors in a gain-of-function approach found that Lmo3 expression after the expression of Nkx2.1 and Dlx2 was able to achieve a 2.7:1 ratio of PV to SST<sup>281</sup>. In this study, we used aPKC inhibition to achieve a ~5.8:1 ratio of PV to SST. This is to our knowledge the greatest enrichment for PV expressing subtypes that has been obtained from mESCs to-date.

Although it remains unclear how aPKCi promotes intermediate neurogenesis in the context of our “MGE” differentiation system, there are several intriguing possibilities. First, the atypical PKC subgroup contains two isoforms, *iota* ( $\iota$  or  $\lambda$ ) and *zeta* ( $\zeta$ ), which have been shown to have numerous, distinct functions in the regulation of cell polarity, proliferation, and neural differentiation<sup>284,287,288</sup>. Loss of aPKC $\lambda$  in mouse stem cells enhances self-renewal through the activation of NOTCH1 and its downstream effectors<sup>289</sup>. Similarly, in dorsal neocortex, knockdown of aPKC $\lambda$  delays neural differentiation and expands the pool of Tbr2+ intermediate progenitors, whereas knockdown of aPKC $\zeta$  promotes radial glia self-renewal<sup>287</sup>. Taken together, these studies show that aPKC  $\lambda$  and  $\zeta$  largely promote stem cell differentiation through partially overlapping pathways. In our system, we use transient, partial inhibition of both aPKC isoforms to enhance the production of CD2+ intermediate progenitors. We favor the idea that partial inhibition of both isoforms promotes a balance between differentiation and self-renewal, resulting in the expansion of basal progenitors. Additional studies focusing on the selective loss of either isoform during directed differentiations of

stem cells into interneuron progenitors are needed to fully understand their individual roles in interneuron genesis. Based on the result of this study, such knowledge might have profound implications for enhancing the generation of interneuron subtypes from directed differentiations of stem cells.

In the field of cancer biology, aPKCs have generated considerable interest due to their roles in driving cellular proliferation. Interestingly, in basal cell carcinomas, aPKC $\lambda$  forms a complex with missing-in metastasis (MIM) that potentiates sonic hedgehog (Shh) signaling<sup>290</sup>. Genetic or pharmacological loss of aPKC $\lambda$  blocks Shh signaling and cancer cell proliferation. Previous studies from our lab have shown that lower levels of Shh signaling preferentially bias MGE progenitors to PV-expressing interneuron fates<sup>127,280</sup>. It is tempting to speculate that aPKCi may also bias progenitors to produce PV-fated interneurons through manipulation of Shh signaling. In fact, loss of Shh signaling in embryonic mice initially reduces proliferation in the MGE ventricular zone while simultaneously upregulating it in the MGE SVZ<sup>125</sup>. Taken together, our study provides evidence that aPKCs play a role in interneuron development and fate determination and may be doing so through interactions with the NOTCH and Shh signaling pathways.

Although our study significantly enhances the generation of PV-fated interneurons, we also find that between 35-40% of cells lack expression of either marker (**Figure 2.5 C**). This increase in non-labeled cells is approximately 10-15% greater than reported in our previous studies, which typically show around 25% of cells being non-labeled<sup>269</sup>. The non-labeled cells are presumably Lhx6<sup>+</sup>

on the basis of their being Lhx6:GFP<sup>+</sup>, and a substantial fraction also express Sox6 and GABA (**Figure 2.6**). Thus, these cells are more likely to represent MGE-like subtypes, as opposed to CGE-derived cells. In addition, staining for the CGE-derived interneuron marker CR showed that less than 1% of all cells were CR<sup>+</sup> (data not shown). Since PV is an activity dependent gene, it is possible that Lhx6:GFP<sup>+</sup> cells who have sub-optimally integrated fail to turn on PV appropriately. It would be interesting to do in situ hybridization for the potassium channel Kv3.1, which colocalizes with PV but not SST subtypes, on transplanted tissue.



# CHAPTER 3

## Function of the Zinc Finger SWIM Domain- Containing Proteins 5 & 6 in Forebrain Development

### 3.1 Introduction to Zinc-Finger SWIM Domain-Containing Proteins

#### *Overview*

Given evidence from our lab as well as others indicating that PV<sup>+</sup> interneurons primarily arise from cyclin D2-mediated divisions of intermediate progenitors in the MGE SVZ<sup>130,133</sup>, we set out to find candidate transcriptional regulators of intermediate progenitor cell identity and/or proliferation. A literature search for genes with patterns of expression restricted to the MGE SVZ led us to the zinc-finger SWIM domain-containing protein 5 (Zswim5). Zswim5 was identified in a microarray screen comparing gene expression profiles between the MGE and LGE<sup>291</sup>. qPCR analysis showed that Zswim5 expression in the MGE was 4 fold greater than in the LGE<sup>291</sup>. In situ hybridization for Zswim5 confirmed these

findings and showed that its expression is largely restricted to a narrow band of cells within the MGE SVZ<sup>291</sup>. Although no functional studies had been published on Zswim5, it belongs to a family of zinc-finger SWIM domain-containing proteins that are conserved across vertebrates<sup>292</sup>. In addition, RNAseq and microarray data indicate strong, restricted expression of Zswim5 in the human MGE<sup>293</sup>. Thus, Zswim5 represented an ideal candidate for the study of SVZ proliferation and its relationship to interneuron fate determination. In order to study Zswim5 function, we opted to generate Zswim5 loss-of-function mice. However, online gene expression atlases indicated that Zswim5 had a highly homologous paralogue, Zswim6, which was also expressed in the MGE<sup>293</sup>. Like Zswim5, no studies on Zswim6 function had been published nor was it associated with any diseases at the time. Thus, without additional data to indicate whether Zswim6 might compensate for Zswim5 loss-of-function, we opted to generate Zswim6 mutant mice as well. As will be described in this chapter, we found little to no involvement for Zswim5 or Zswim6 in the regulation of PV<sup>+</sup> interneurongenesis. Thus, we accepted our null hypothesis and set out to understand what other processes these genes might regulate, which eventually led us to focus on Zswim6 and its role in striatal development. The following chapter will consist of three parts. The first part describes what is known about SWIM domain-containing proteins, focusing on Zswim4, 5, 6, and 8. The second part will investigate our early hypothesis that Zswim5 and Zswim6 regulate interneuron development through the generation and characterization of Zswim5 and Zswim6

loss-of-function mice. The third part will include a thorough anatomical and behavioral characterization of Zswim6 mutant mice, with special emphasis on the role of Zswim6 in striatal development.

#### *SWIM Domain-Containing Proteins 4, 5, 6, and 8*

SWIM protein domains are zinc-finger-like domains found in bacteria, archaea, and eukaryotes<sup>292</sup>. As their name implies, zinc-finger domains bind zinc ions via a combination of cysteine and histidine residues. Although they share this commonality, zinc-finger domains are highly diverse in terms of their structure and function. The SWIM domain has the amino acid motif CxC<sub>n</sub>CxH, with n varying between 6 to 25 residues<sup>292</sup>. Alignment across multiple species revealed that SWIM domains are present in bacterial SWI2/SNF2 ATPases of the helicase superfamily II, in which the SWIM domain is located at the N terminus, upstream of the ATPase domain<sup>292</sup>. SWIM domains are also found in plant MuDR transposases, plant FAR1 nuclear proteins, vertebrate MEK kinase-1, and numerous uncharacterized proteins in prokaryotes and eukaryotes<sup>292</sup>. Structural analysis suggests that the SWIM domain adopts a  $\beta\beta\alpha$  structure, which may be similar to the classical C2H2 zinc-finger conformation<sup>292</sup>. Interestingly, in several species of bacteria, genes that encode for SWI2/SNF2 ATPases that lack the amino terminal SWIM domain are located adjacent to genes containing SWIM domains, likely within the same operon. This suggests a functional link between the two domains and that the origin of SWIM domain-containing ATPase proteins may be related to the fusion of adjacent genes<sup>292</sup>. Of note, several eukaryotic

SWIM domain-containing proteins also have an additional  $\alpha$ -helix domain downstream of the SWIM-domain. This feature is also found in bacterial SWIM domain-containing SWI2/SNF2 proteins, suggesting that eukaryotic proteins with this feature, such as Zswim5 and Zswim6, might functionally interact with chromatin-associated SWI2/SNF2 ATPases of the Trithorax group of chromatin remodelers/histone modifiers<sup>292</sup>.

In mammals, the SWIM domain-containing family of proteins has 8 members (Zswim1 to Zswim8). Of these, Zswim4/5/6 and 8 are paralogues of each other. With the exception of the SWIM domain, which is 37 amino acids long, Zswim1/2/3 and 7 have little to no significant homology with Zswim4/5/6 and 8. While Zswim4/5 and 6 are similar in structure and length (1100-1200 amino acids), Zswim8 is much larger (~1800 amino acids), though still shares considerable homology. An analysis of comparative genomics shows that Zswim4/5/6 and 8 all originated from the same ancestral gene found in bilateria approximately 937 million years ago. From this ancestral gene, Zswim8 split off and became EBAX-1 in *C.elegans*. A series of speciation and duplication events in early vertebrates formed Zswim4 and the ancestral gene for Zswim5 and Zswim6. Thus, Zswim5 and Zswim6 are closer to each other evolutionarily than Zswim4 (**Figure 3.1**).

## Gene Tree of Zswim Family Paralogues 4, 5, 6, & 8

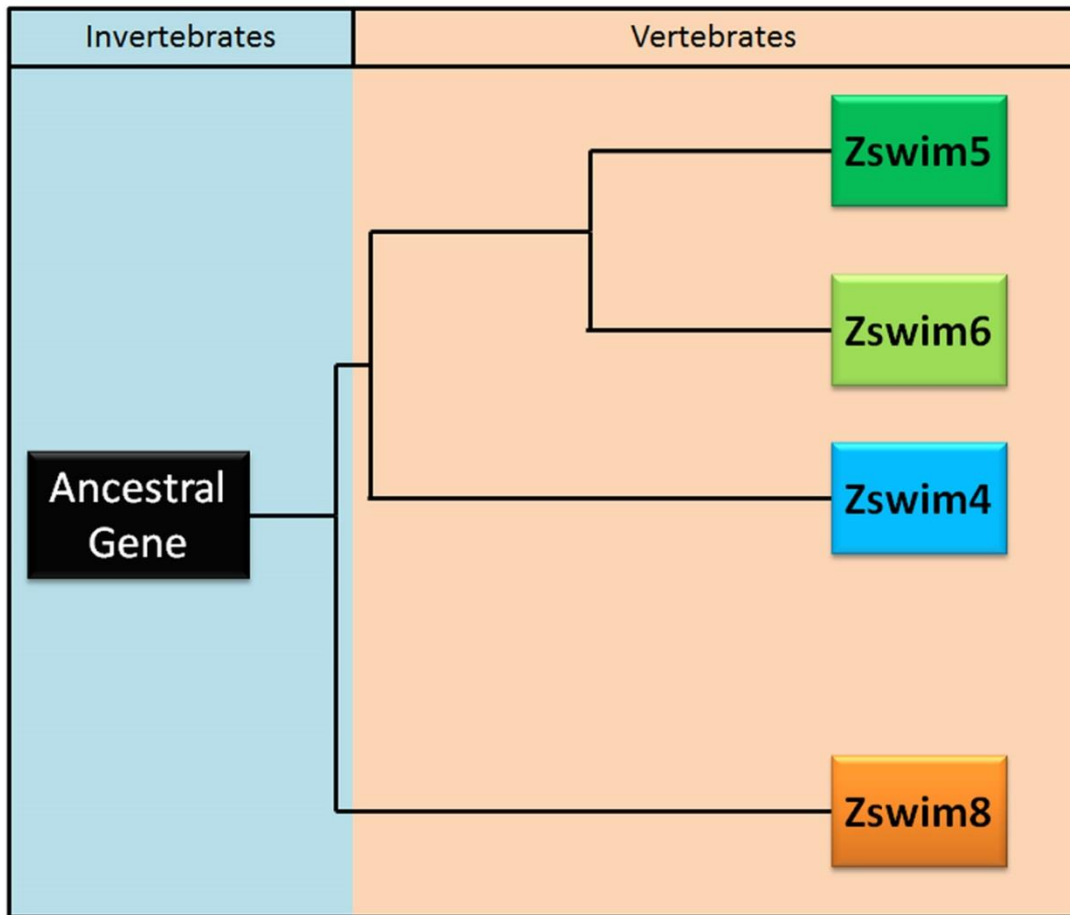


**Figure 3.1. Gene Tree for Zswim4, 5, 6, and 8 Gene Evolution**

The above diagram represents a simplified gene tree of that contained within the Ensemble Genome Browser and illustrates the evolutionary relationships between Zswim4, 5, 6, and 8.

While the function of Zswim4/5/6 and 8 in mammals is currently unknown, the homolog of Zswim8 in *C.elegans*, EBAX-1, has been studied. EBAX-1 is a substrate recognition subunit in the Elongin BC-containing Cullin-RING ubiquitin ligase (CRL) complex, which performs protein quality control by targeting unfolded or misfolded proteins to the proteasome for destruction<sup>1</sup>. During

*C.elegans* development, EBAX-1 cooperates with DAF-21/Hsp90 to control the protein quality of the SAX-3/Robo receptor, which is essential to ensure proper axon targeting<sup>1</sup>. In the absence of EBAX-1, AVM axons are significantly misrouted. EBAX-1 interacts with the CRL complex through its N-terminal BC-box and Cul2-box motifs, which are upstream of the SWIM domain and conserved across species<sup>294</sup>. In HEK293 cells, ZSWIM8 has been shown to interact with Elongin B/C proteins via its BC-box and the Cullin2 protein via its Cul2-box<sup>294</sup>. A screen for additional proteins that could direct the recruitment of Cul2 modules to Elongin BC-based ubiquitin ligases revealed that Zswim5 and Zswim6 also contained these motifs and could bind Elongin BC<sup>294</sup>. A follow-up analysis of mine revealed that Zswim4 also contained the BC-box and Cul2 motifs (**Figure 3.2**).

		BC-box		Cullin-box		
Zswim4	25	AARGRGR	EEALIDL	AKRVAESWAFEQVEERFSR	PEPVQKRIVFWSFPRSEREICMYSS	84
Zswim5	55	GARPHLQ	EDSLIDC	AKTVAEKWAYERVEERFER	PEPVQRRIVYWSFPRNEREICMYSS	114
Zswim6	69	GKTQS	EESLIDL	IARRVAEKWPFQERVEERFER	PEPVQRRIVYWSFPRSEREICMYSS	126

**Figure 3.2. Multiple sequence alignment of BC- and Cullin-boxes in ZSWIM4, 5, and 6.**

Protein sequences for human ZSWIM4, ZSWIM5, and ZSWIM6 were obtained from NCBI's protein sequence database and manually aligned to identify the BC- and Cullin-box domains. Amino acids that are identical to classical BC- and Cullin-box motifs are highlighted in yellow, very similar ones in blue, and similar amino acids in green.

The entire Elongin BC complex acts as an adaptor to link a substrate recognition complex (e.g. Zswim8) to Cullin2 and a ring-box protein, such as Rbx1. The ring-box protein binds to an E2 ubiquitin ligase, which catalyzes the reaction of ubiquitin onto the adaptor-linked substrate. In the case of Ebx-1, Hsp90 was shown to bind the SWIM domain. Aside from the BC-box, Cul2, and SWIM domains, Zswim4/5/6 and 8 also contain a conserved A domain downstream of the SWIM domain that aligns to cut8/STS1, which targets proteasomes to the nucleus<sup>295</sup>. The last ~75 amino acids of the C-terminus show similarity to structurally defined portions of four paired amphipathic helix Sin3 proteins, which have been shown to interact with RE1-silencing transcription factor (REST, or NRSF) to repress the expression of neuron-specific genes in nonneural cells and neuronal progenitors<sup>295</sup> (**Figure 3.3**).

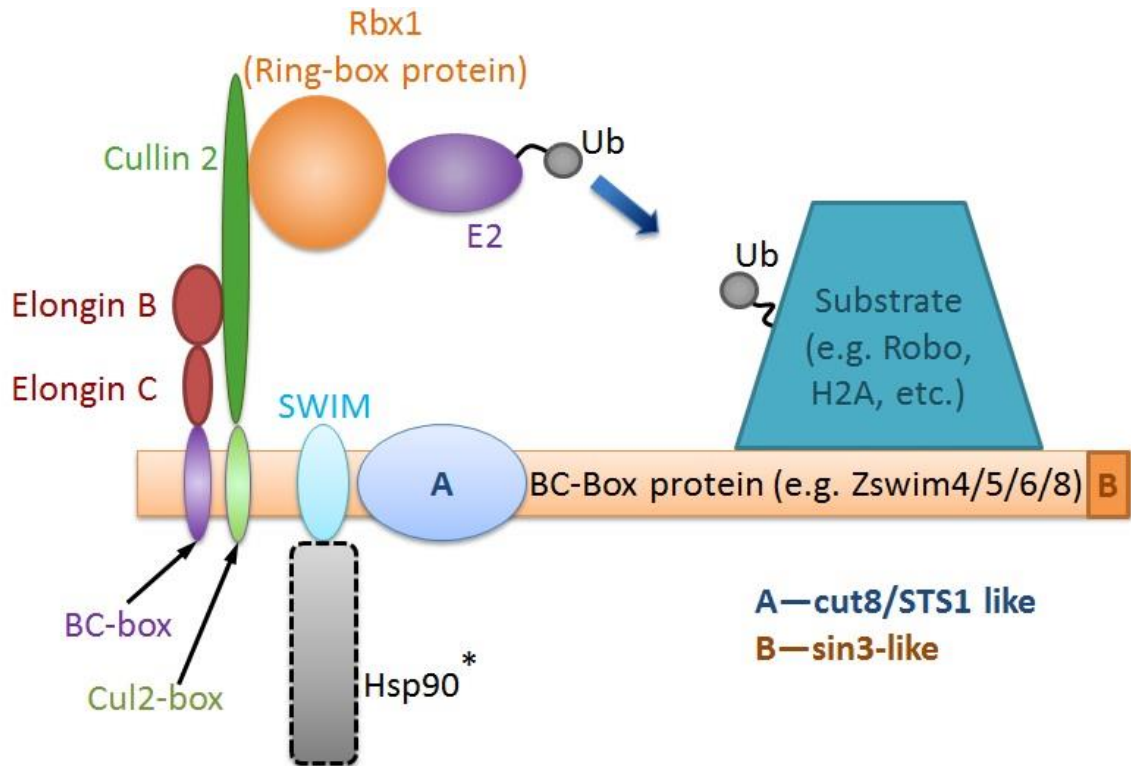


**Figure 3.3. Schematic illustration of putative Zswim-type cullin-RING E3 ubiquitin ligase**

The following schematic is derived from studies of Ebax-1/Zswim8 in *C.elegans*<sup>1</sup>. Ebax-1 encodes a conserved BC-box-containing protein and functions as part of a protein quality control mechanism that ensures proper axon guidance. Specifically, EBAX-1 functions as a substrate-recognition subunit for misfolded SAX-3 in an Elongin BC-containing Cullin-RING ubiquitin ligase (CRL) complex that promotes degradation of misfolded SAX-3/Robo receptor. The asterisk indicates that Hsp90 has been shown to bind Ebax-1 via its SWIM domain, but that this has not been tested for Zswim5 or Zswim6.

Evidence suggesting that Zswim4/5/6 and 8 might bind to ring containing proteins is interesting in light of their possible association with chromatin remodelers and/or histone modification complexes. The Polycomb group of transcriptional regulators is a group of proteins that bind to DNA and are traditionally thought to



repress gene transcription. However, this view has been recently challenged by new data indicating that Polycomb complexes can activate gene transcription in certain contexts<sup>296,297</sup>. Polycomb group proteins usually belong to one of two multi-subunit protein complexes, either Polycomb repressive complex 1 (PRC1), which adds an ubiquitin residue to histone H2A at Lys119, or PRC2, which catalyzes the addition of methyl groups to histone H3 at Lys27<sup>298</sup>. Of particular interest is the PRC1 complex, which is built around the RING domain-containing proteins RING1 and RING2. These proteins bind to six alternative Polycomb group RING finger (PCGF) proteins that together catalyze the transfer of ubiquityl moieties<sup>298</sup>. A major question in the field of gene regulation centers on how chromatin remodeling complexes such as Polycomb and Trithorax are dynamically directed to regions of the genome at the appropriate time in a cell type specific context to regulate gene expression. The ability to do so in part stems from the various compositions of Polycomb and Trithorax group complexes, of which upwards of 200 different permutations have been identified and continues to increase<sup>297,299</sup>. These complexes have been shown to bind transcription factors in a cell type specific manner that then recruit them to specific regions of the genome. For example, REST/NRSF has been shown to recruit Polycomb repressor complexes to distinct regions of the genome in mammalian cells, as has the autism susceptibility candidate 2 (Auts2)<sup>296,300</sup>. It is intriguing to speculate that Zswim proteins 4/5/6 and 8 might interact with these complexes in a cell type specific manner during brain development to recruit

them to specific genomic loci. As mentioned previously, Zswim proteins have been shown to bind RING-domain containing proteins to catalyze the transfer of ubiquityl moieties<sup>1,294</sup>. It would be interesting if Zswim proteins interacted with PRC1 complexes to regulate histone H2A ubiquitination during brain development. Some support for this idea comes from a 2012 study that did a mass spectrometry screen to identify proteins that interact with PRC1 complexes<sup>301</sup>. In this study, they found that Zswim6 immunoprecipitated with PRC1 complexes in HEK293 cells, albeit only a single peptide<sup>301</sup>. Furthermore, Zswim proteins are predicted to interact with mammalian SWI2/SNF2 complexes through interactions with their N-terminal SWIM domain<sup>292</sup>. To test this idea, I overexpressed Myc-tagged Zswim5 with HA-tagged Brg1 (the core ATPase subunit of Trithorax complexes) in HEK293 cells and found that both proteins were capable of immunoprecipitating the other (**Figure 3.4**).

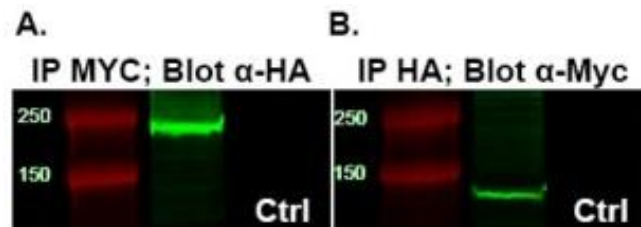


**Figure 3.4. Zswim6 co-immunoprecipitates with Brg1, the main ATPase subunit of SWI/SNF chromatin remodeling complex, in HEK293 cells.**

**(A)** Myc-Zswim6 was co-expressed with HA-Brg1 in HEK293 cells. Myc-Zswim6 was immunoprecipitated using anti-Myc magnetic beads and the eluant was run on western blot. The blot was then probed using an anti-HA antibody, which detects a clear band at ~220kD corresponding to HA-Brg1. The control indicates co-immunoprecipitation with nonreactive, non-antibody tagged magnetic beads.

**(B)** Myc-Zswim6 was co-expressed with HA-Brg1 in HEK293 cells. HA-Brg1 was immunoprecipitated using anti-HA magnetic beads and the eluant was run on western blot. The blot was then probed using an anti-Myc antibody, which detects a clear band at ~132kD corresponding to Myc-Zswim6. The control indicates co-immunoprecipitation with nonreactive, non-antibody tagged magnetic beads.

The C-terminus of Zswim proteins 4/5/6 and 8 also have structural similarity to Sin3 proteins, which have been shown to interact with REST/NSRF, SWI2/SNF2, and NURD complexes to regulate gene transcription<sup>302,303</sup>. Further support for this idea comes from analysis of Zswim5 and Zswim6 gene expression patterns across human brain development. Using the Allen Brain gene expression atlas of human brain development, it is possible to identify genes whose expression is correlated with a gene of interest within particular brain regions across development. Thus, I generated a list of 1000 genes whose expression is most highly correlated with Zswim5 and Zswim6 across all areas of the brain from early embryonic development up until adulthood. I then ran the top 1000 genes through the DAVID functional gene classifier to segregate them into functional groups by order of significance (**Table 3.1**).

<b>GO ANALYSIS FOR TOP 1000 GENES ASSOCIATED WITH ZSWIM5/6 EXPRESSION</b>			
<b>Annotation Cluster 1</b>	<b>Enrichment Score: 50.46</b>	<b>Gene Count</b>	<b>P_Value</b>
Nucleus		542	1.00E-123
Transcription		334	1.20E-93
Zinc-finger		297	2.70E-89
<b>Annotation Cluster 2</b>	<b>Enrichment Score: 35.89</b>	<b>Gene Count</b>	<b>P_Value</b>
Nuclear lumen		188	1.30E-54
Intracellular organelle lumen		191	7.10E-43
Organelle lumen		191	2.10E-41
<b>Annotation Cluster 3</b>	<b>Enrichment Score: 29.45</b>	<b>Gene Count</b>	<b>P_Value</b>
Zinc-finger region: C2H2-type 10		117	1.30E-66
Zinc-finger region: C2H2-type 11		102	1.40E-57
Zinc-finger region: C2H2-type 12		88	1.10E-49
<b>Annotation Cluster 4</b>	<b>Enrichment Score: 20.47</b>	<b>Gene Count</b>	<b>P_Value</b>
Chromatin modification		70	1.90E-27
Chromatin regulator		57	1.40E-25
Chromatin organization		75	3.50E-22
<b>GO ANALYSIS FOR TOP 50 GENES ASSOCIATED WITH ZSWIM5/6 EXPRESSION</b>			
<b>Annotation Cluster 1</b>	<b>Enrichment Score: 14.43</b>	<b>Gene Count</b>	<b>P_Value</b>
Transcription regulation		32	6.50E-19
<b>Annotation Cluster 2</b>	<b>Enrichment Score: 8.12</b>	<b>Gene Count</b>	<b>P_Value</b>
Zinc-finger		26	3.80E-14
<b>Annotation Cluster 3</b>	<b>Enrichment Score: 6.96</b>	<b>Gene Count</b>	<b>P_Value</b>
Regulation of RNA metabolic process		21	3.00E-08
<b>Annotation Cluster 4</b>	<b>Enrichment Score: 5.63</b>	<b>Gene Count</b>	<b>P_Value</b>
Zinc-finger region: C2H2-type 14		9	5.90E-09
<b>Annotation Cluster 5</b>	<b>Enrichment Score: 4.36</b>	<b>Gene Count</b>	<b>P_Value</b>
Nuclear lumen		13	2.30E-07
<b>Annotation Cluster 6</b>	<b>Enrichment Score: 4.29</b>	<b>Gene Count</b>	<b>P_Value</b>
Chromatin Regulator		11	1.30E-10

**Table 3.1. Functional gene ontology analysis for genes whose expression correlates with Zswim5 & Zswim6 expression during human brain development.**

The top 1000 genes whose expression most highly correlates with Zswim5 and Zswim6 during human brain development were obtained from the Allen Brain Atlas. For Zswim5 and Zswim6, correlated genes were ranked according to most correlated (#1, #2, etc.) to least correlated. The rank values for genes correlated with Zswim5 and Zswim6 were then combined to get a combined rank score. The 1000 genes with the lowest combined rank scores (most highly correlated with Zswim5 and Zswim6) were then run through a functional gene ontology analysis using the DAVID functional gene classifier. The top portion shows this analysis done for the top 1000 genes, and the bottom portion shows this analysis done on the top 50 genes. The same analysis done for genes correlated with either Zswim5 or Zswim6 (but not both) yielded similar results (not shown).

Functional annotation clustering revealed that the most significant cluster is related to transcriptional regulation and zinc-finger (C2H2-like) proteins. The second most significant cluster was related to proteins localized to the nucleus and the third most significant cluster is related to zinc-finger proteins. The fourth most significant cluster and of particular relevance is related to chromatin regulation, modification, and organization. Within just the top 50 associated genes, at least 32 have been shown to be involved in transcriptional regulation, chromatin remodeling, or histone modification (**Table 3.1**). I would argue that proteins that function together are more likely to be expressed together, lending further support to the notion that Zswim proteins may functionally interact with chromatin remodeling/modifying complexes. If this were true, we would expect Zswim5 to be predominantly localized in the nucleus, which is what we find when recombinant Myc-tagged Zswim5 is expressed in HEK293 cells (**Figure 3.5**).

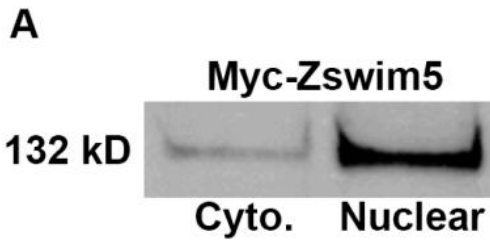


**Figure 3.5. Zswim5 predominantly localizes to the nucleus.**

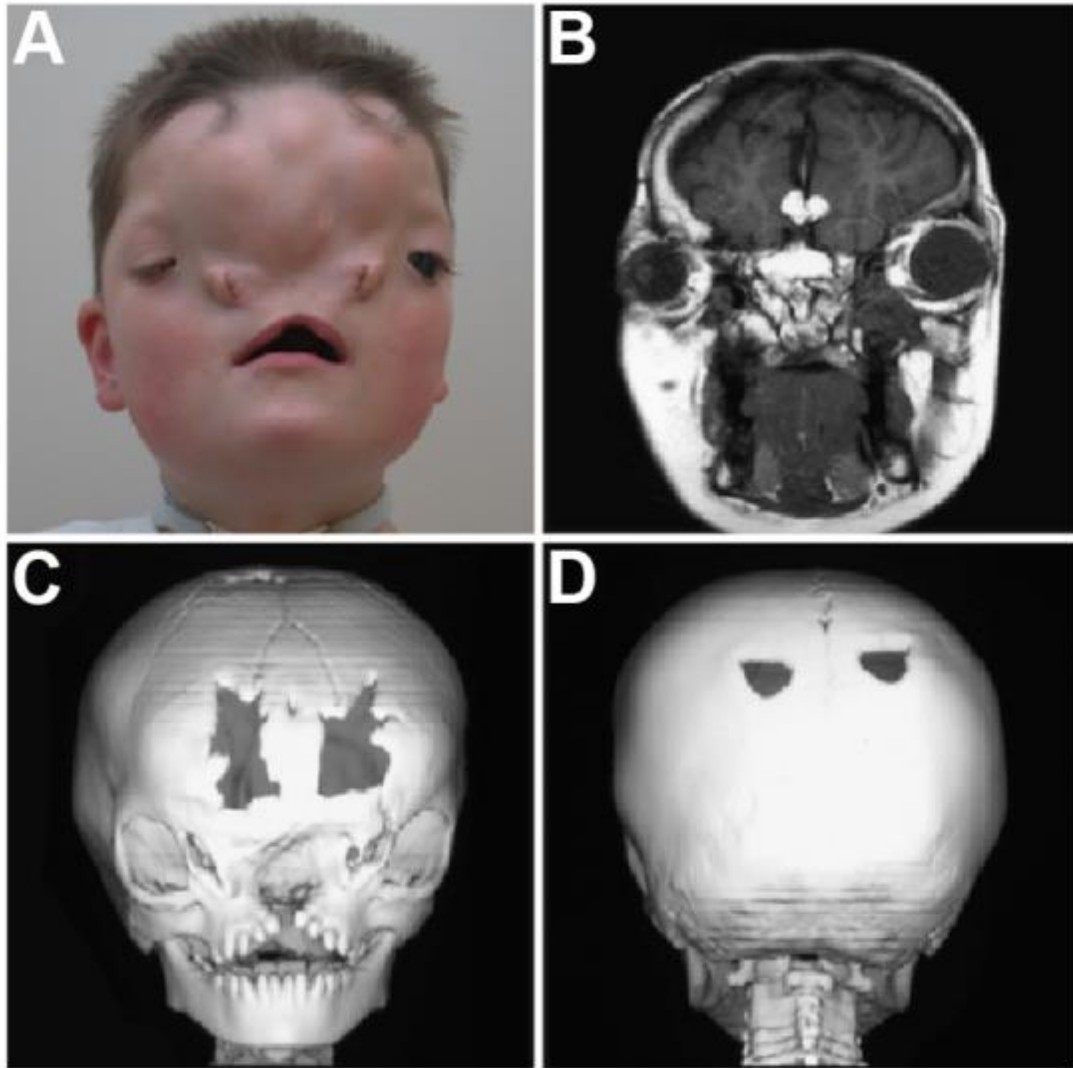
**(A)** Recombinant myc-tagged Zswim5 was expressed in HEK293 cells. Nuclear and cytoplasmic fractionation followed by detection of the myc-tagged protein via western blotting shows that the majority of Zswim5 protein is localized in the nucleus. Cyto, cytoplasmic.

In sum, multiple lines of evidence, both direct and indirect, implicate the involvement of Zswim4/5/6 and 8 in the regulation of gene expression through interactions with Polycomb, Trithorax, and other chromatin associated complexes.

#### *Zswim6 and Human Disease*

From a human disease standpoint, the potential of Zswim4/5/6 and 8 to participate in the process of chromatin modeling is interesting in light of evidence showing that mutations in proteins associated with chromatin remodeling are highly involved in the pathogenesis of major neurological and psychiatric diseases such as epilepsy, autism, and schizophrenia<sup>296,299,302,304-313</sup>. In a recent, large scale genome wide association study for schizophrenia, a single nucleotide polymorphism located ~50kB upstream of Zswim6 was identified as the 8<sup>th</sup> most significantly associated SNP in schizophrenia to date<sup>251</sup>. While little is known

about Zswim6 function, its dynamic expression during human brain development<sup>293</sup> and association with chromatin remodeling complexes makes it well suited to be a schizophrenia candidate gene. Additionally, two studies have identified the same, recurring point mutation in Zswim6 in patients with acromelic frontonasal dysostosis<sup>295,314</sup>, a rare disorder characterized by brain, limb, and craniofacial abnormalities. In at least 8 different probands a heterozygous cysteine to threonine mutation at position 3487 has been identified, leading to an arginine to tryptophan substitution at amino acid position 1163. Interestingly, this mutation occurs in the Sin3-like C-terminal domain of Zswim6. From the spectrum of clinical phenotypes, which include neurocognitive and motor delays, severe symmetric frontonasal dysplasia associated with median cleft face, widely spaced nasal alae, hypertelorbitism, bilateral tibial hemimelia, and preaxial polydactyly, together with changes in gene expression in patient cell lines, the authors of one of these studies concluded that this particular Zswim6 mutation results in Hedgehog pathway activation<sup>295</sup> (**Figure 3.6**).



**E**

Human	1138	LRQLLDATIGAYINTTHSRLTHISPRHYSEFIEFLSKARETFLMAHDGHI	1187
Bonobo	939	LRQLLDATIGAYINTTHSRLTHISPRHYSEFIEFLSKARETFLMAHDGHI	988
Mouse	1080	LRQLLDATIGAYINTTHSRLTHISPRHYSEFIEFLSKARETFLMAHDGHI	1129
Chicken	966	LRQLLDATIGAYINTTHSRLTHISPRHYSEFIEFLSKARETFLMAHDGHI	1015
Xenopus	1048	LRQLLDATIGAYINTTHSRLTHISPRHYSEFIEFLSKARETFLMAHDGLI	1097
Zebrafish	1053	LRQLLDATIGAYINTTHSRLTHISPRHYSEFIEFLSKARETFLMAQDGH	1102
Sea Squirt	1097	LRPLEAAIAAYVKT1HNKLSHISPRHYTEFIDFLNKARETFLLAAPDGHS	1146

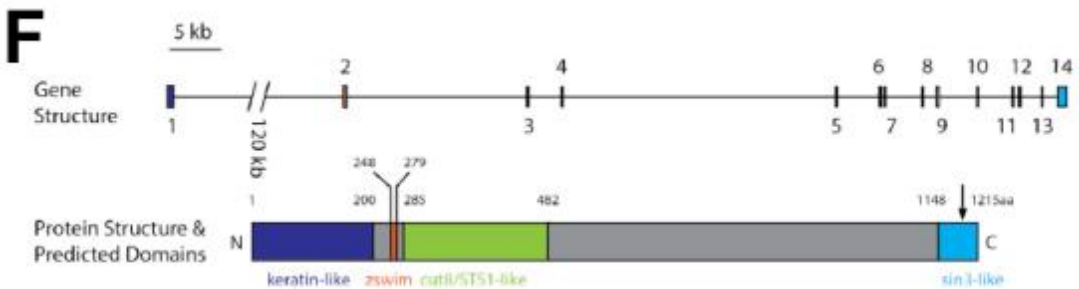




**Figure 3.6. Craniofacial phenotype of a Zswim6 human mutation patient, evolutionary comparative analysis, genomic structure, and predicted protein regions.**

**(A).** Anteroposterior view of the facial features of one patient shown to have a c.3487C>T mutation in Zswim6.

**(B).** Coronal MRI demonstrating a large interhemispheric lipoma from the patient shown in (A).

**(C and D).** Craniofacial CT scans showing disrupted cranial development, including disruption of the nasal structures and medial cleft palate (C), and symmetric parietal foramina (D).

**(E).** Protein alignments for the region surrounding the p.Arg1163Trp mutation (yellow) for multiple species shows that this region is highly conserved. Divergent residues are shown in red, and conservative substitutions are shown in green.

**(F).** Zswim6 contains 14 exons and spans a large genomic region. Only one transcript has been described. Analysis of Zswim6 protein structure indicates that Zswim6 has a low complexity, keratin-like N-terminal region, followed by the SWIM domain, a cut8/STS-1 like region, and a sin3-like region at the C-terminus. The location of the p.Arg1163Trp mutation is indicated by the black arrow.

**Modified from Smith et al. 2014**

Whether or not this proves true, it is interesting to note the similarities between patients with Zswim6 mutations and those with mutations in members of the SWI/SNF chromatin remodeling complex. *De novo* dominant mutations in different SWI/SNF proteins have been identified in individuals with Coffin-Siris (CSS) and Nicolaides-Baraitser (NCBRS) syndromes<sup>299,315,316</sup>. CSS is characterized by mild to severe intellectual disability, hypoplasia of the tips of the fingers and toes, and various craniofacial abnormalities<sup>315</sup>. NCBRS is characterized by severe intellectual disability, seizures, short stature, microcephaly, and facial coarseness<sup>316</sup>. Given the role of SWI/SNF proteins in

regulating gene expression in multiple tissues, it is not surprising that mutations in SWI/SNF proteins have pleiotropic effects of varying severity. While the association is tenuous at best, it is intriguing to link mutations in Zswim6 to its role as a putative chromatin modifier. As will be discussed in the forthcoming sections, the heterozygous point mutation identified in Zswim6 is likely a dominant gain-of-function mutation, since Zswim6 loss-of-function mice display a much different phenotype than the human c.3487C>T point mutation patients<sup>295</sup>.

### **3.2 Generation of Zswim5 and Zswim6 Knockout Mice and Characterization of their Role in Interneuron Development**

#### *Generation of Zswim5 Knockout Mice*

Over the course of these studies, we used two independently generated Zswim5 knockout mice. The first was obtained from the Knockout Mouse Project (KOMP) and the second was designed in collaboration with Ingenious Targeting Labs, who physically generated the mouse. The Zswim5 KOMP mouse (Z5-KOMP) was generated using homologous recombination, whereby exons 2 and 3 were replaced with a targeting cassette containing a lacZ reporter (**Figure 3.7 A**).

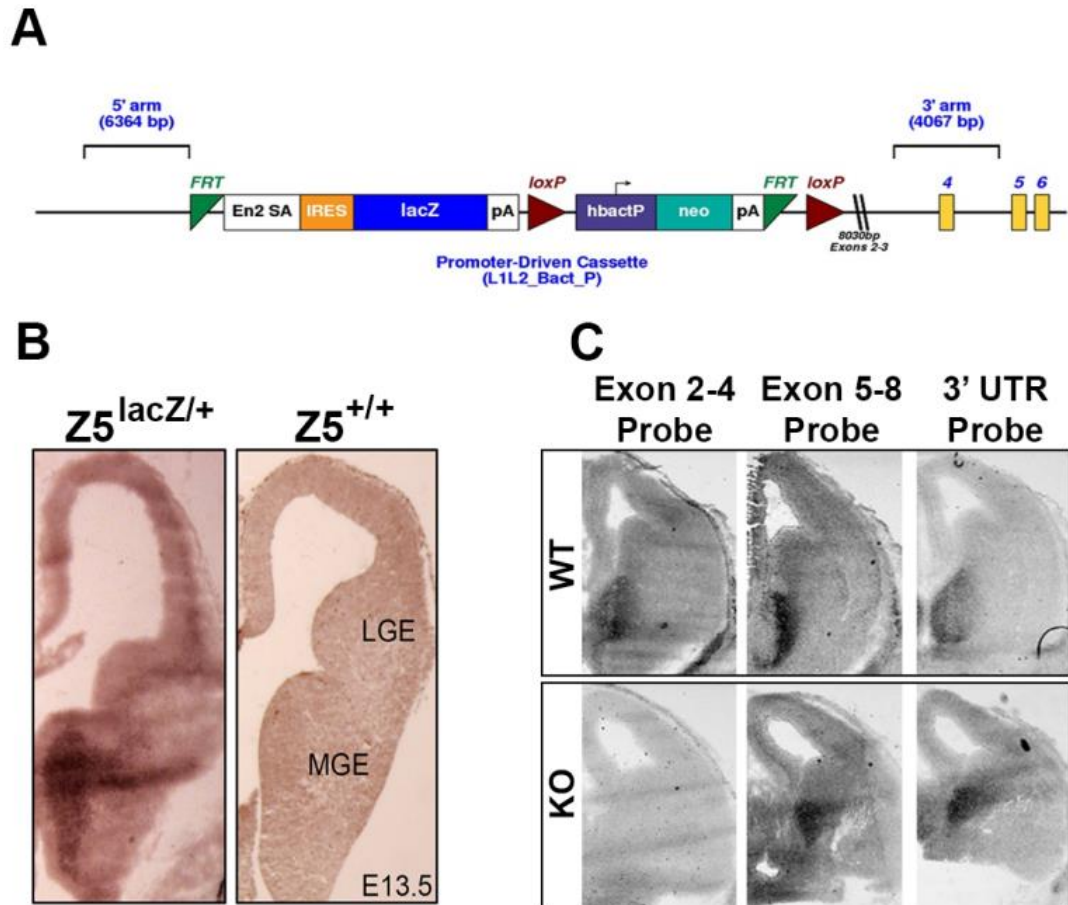


**Figure 3.7. Targeting strategy and characterization of Zswim5 knockout mouse obtained from the Knockout Mouse Project (KOMP).**

**(A).** Schematic of the Zswim5 locus after homologous recombination with a targeting construct electroporated into mouse embryonic stem cells. Exons 2 and 3 are replaced by the targeting construct, which contains a lacZ reporter gene. The neomycin (neo) insert was removed by crossing heterozygous mice to FLP-deleter mice before beginning our studies.

**(B).** Detection of  $\beta$ -galactosidase in embryonic day (E) 13.5 Zswim5<sup>lacZ/+</sup> and control mice shows that lacZ expression recapitulates Zswim5's endogenous expression.

**(C).** In situ mRNA hybridization of three different RNA probes to various regions of the Zswim5 transcript in wildtype and knockout mice. As expected, a probe spanning the exons removed in the knockout mouse (exon 2-4 probe) shows no signal, whereas probes to regions downstream of the deleted region detect the presence of residual transcript.

This results in a frameshift mutation that is predicted to cause nonsense mediated decay of the transcript. Importantly, there is only one known transcript for Zswim5. While a southern was not done to confirm the targeting, several other quality control measures were, including long range PCR and copy number testing (data not shown). In addition, lacZ staining on E13.5 Zswim5<sup>lacZ/+</sup> mouse forebrain confirms that the lacZ reporter recapitulates endogenous Zswim5 forebrain expression (**Figure 3.7 B**). To determine whether this mouse was a functional null, we first did in situ hybridization with a probe directed against exons 2 and 3, which were replaced with the targeting construct. As expected, knockout tissue showed no signal with this probe when compared to wildtype. However, in situ hybridization using several other probes downstream of the deleted exons showed that the transcript was still present in knockout mice (**Figure 3.7 C**). To determine whether alternative transcripts might be present that could still produce a functional protein, such as through exon skipping, we did 5' RACE and found no alternative transcripts (data not shown). With no evidence to suggest that an alternative transcript with protein-coding potential was being transcribed, we considered this mouse a functional null. From a biological standpoint, the in situ analysis we performed highlights the fact that not all transcripts may be subject to nonsense mediated decay to the same extent, and in the case of Zswim5, a substantial amount of mutant transcript remained. Since this mouse was a constitutive knockout, we wanted the ability to conditionally inactivate Zswim5 as well. Thus, we generated a conditional knockout (Z5-ITL) in

collaboration with Ingenious Targeting Labs. To generate this mouse we used homologous recombination to flank exon 3 with loxP sites (**Figure 3.8 A**), which upon Cre-recombinase mediated recombination is predicted to cause a frameshift deletion. Southern blot using 3' and 5' DNA probes indicates that the targeting construct inserted at the correct location (**Figure 3.8 B**). To confirm whether this strategy produced a null allele, we bred Zswim5 floxed mice to a CMV-Cre line (Jackson Laboratory Stock #006054) to produce a germline knockout. Using cDNA from the offspring, we did RT-PCR with a primer set containing a forward primer in exon 2 and a reverse primer in exon 3 and found no band at the expected length relative to control (**Figure 3.8 C**). Additionally, qPCR on E13.5 mouse forebrain showed that Zswim5 transcript was reduced by approximately 75% in knockouts relative to control. Together, these studies indicate that both Zswim5 mutant mouse lines are highly likely to be functional nulls (**Figure 3.8 D**).

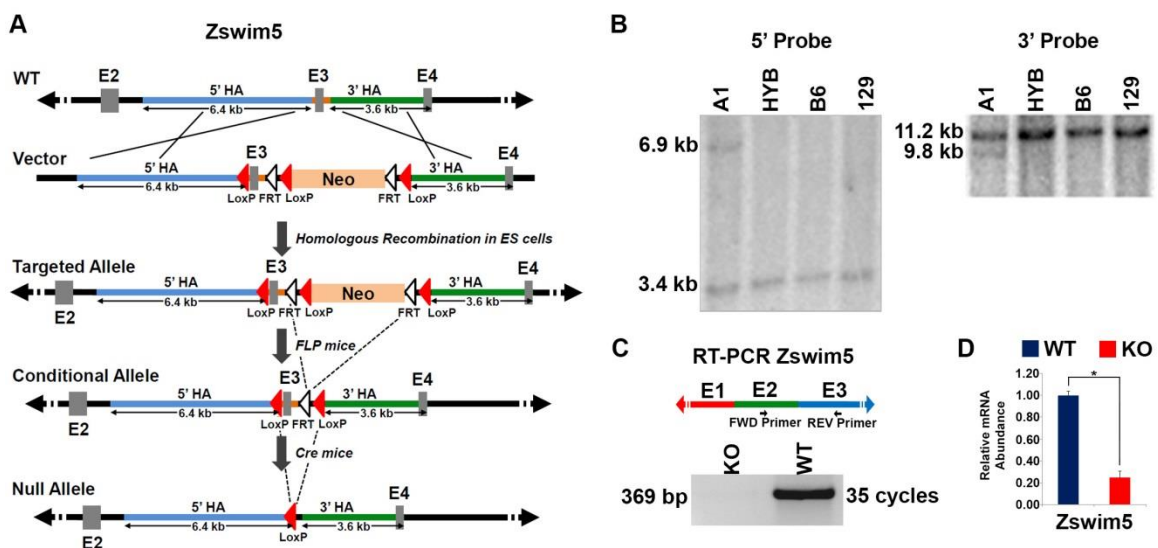


**Figure 3.8. Generation of Zswim5 knockout (KO) mice.**

**(A).** Schema of constructs used in generating a null allele for Zswim5 by flanking exon 3 with LoxP insertions, generating a mouse line, then crossing this line with Cre-deleter mice.

**(B).** Southern blot analysis to identify correctly targeting embryonic stem (ES) cell clones obtained from hybrid C57BL/6x129/SvEv ES cells electroporated with the targeting construct. One ES clone (A1) was identified in which there was the expected 5' and 3' recombinations. HYB, hybrid ES cell; B6, C57BL/6 ES cell; 129, 129/SvEv ES cell.

**(C).** RT-PCR reveals a loss of product created by primers flanking the exon 2 and 3 junction in the Zswim5 knockout.

**(D).** There is a 75% reduction in the relative abundance of Zswim5 mRNA in homozygous Zswim5 KO mice (N=3). Abbreviations: WT (wild type); Neo (neomycin resistance cassette); E (exon). \* $p < .001$ . Error bars indicate SEM.

*Study of Interneuron Development in Zswim5 Knockout Mice*

To begin our study of Zswim5, we first characterized its expression using in situ hybridization. We find that at E12.5, E14.5 and E16.5, Zswim5 mRNA is predominantly restricted to the MGE SVZ, with low levels of expression in the LGE SVZ and cortical plate (**Figure 3.9**). By P0, Zswim5 expression is undetectable (data not shown). Next, we turned our attention to analysis of Z5-KOMP mice. Observation of adult Zswim5 knockouts revealed no obvious behavioral, neurological, or anatomical phenotypes. We next examined whether loss of Zswim5 affected proliferation of MGE progenitors. We counted ventricular

and adventricular phospho-histone H3 mitotic figures and found a non-significant 14% and significant 9% decrease, respectively, in knockouts relative to controls (**Figure 3.10 A**). We also pulsed with EdU for 30 min at E13.5 to look at the

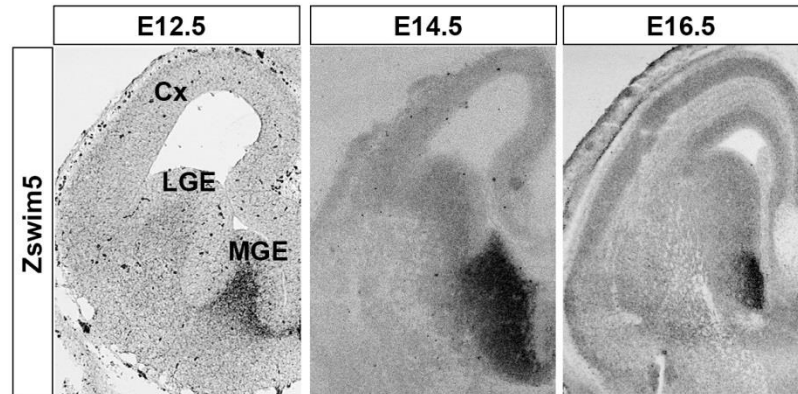


**Figure 3.9. Expression of Zswim5 in the developing mouse forebrain.**

In situ mRNA hybridization for Zswim5 shows strong expression in the medial ganglionic eminence (MGE) at embryonic day (E) 12.5, 14.5, and 16.5. Low levels of expression can also be detected in the lateral ganglionic eminence (LGE) and cortex (Cx).

fraction of progenitors in S-phase. Although we did not quantify the number of EdU+ progenitors, qualitatively there did not appear to be an obvious difference (**Figure 3.10 B**). This was also true for the SVZ marker cyclin D2 (**Figure 3.10 B**). Immunohistochemistry for Lhx6 also revealed no obvious changes in the production and/or specification of interneuron precursors (**Figure 3.10 B**). In agreement with these findings, we found no significant difference in the number of PV interneurons in the somatosensory cortex or hippocampus of P21 Z5-KOMP mutants (**Figure 3.11**). On the basis of these results, and the observation

that Zswim6 is also expressed in the MGE and may compensate for Zswim5 loss-of-function, we decided to turn our attention away from Zswim5 single knockouts and focus on Zswim5/Zswim6 double mutant mice.

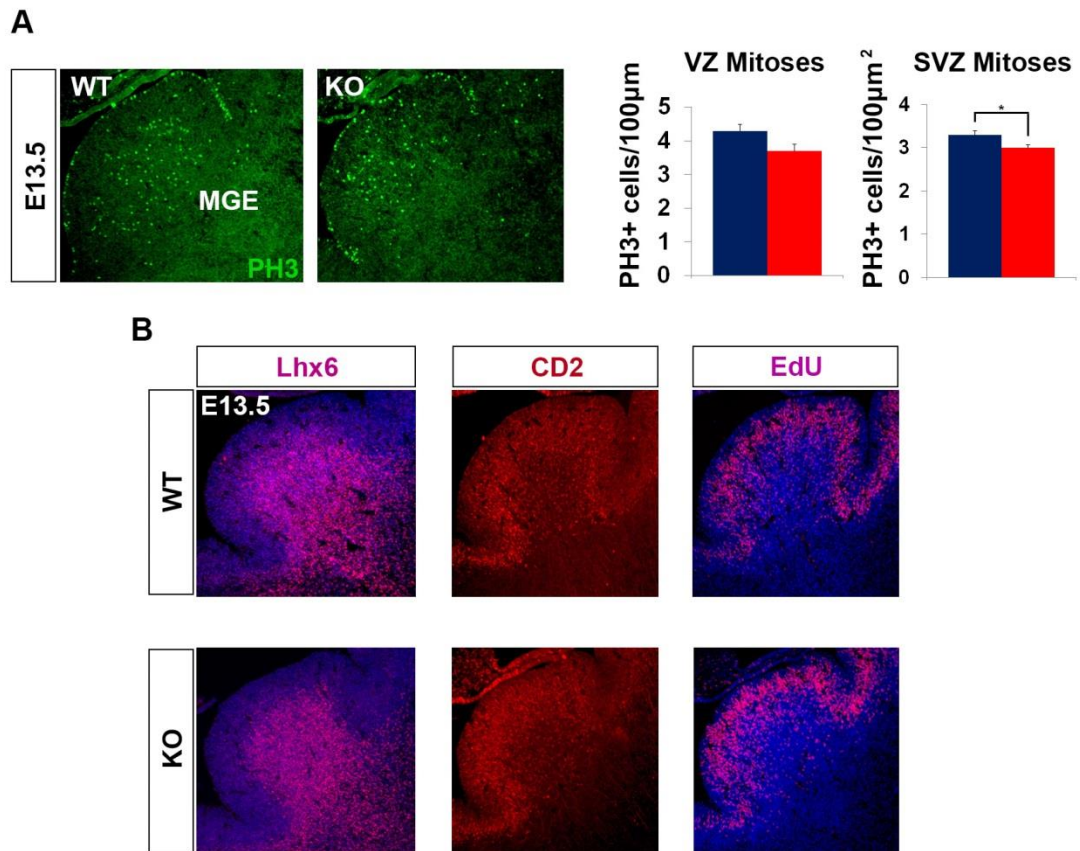


**Figure 3.10. Analysis of proliferation and molecular specification in the medial ganglionic eminence (MGE) of Zswim5 mutant mice.**

**(A).** Immunostaining for the M-phase marker phospho-histone H3 on embryonic day (E) 13.5 mouse forebrain sections shows that there is no change in ventricular zone (VZ) mitoses and a 9% reduction in subventricular zone (SVZ) mitoses.

**(B).** Immunostaining for Lhx6, a marker of post-mitotic, MGE-derived neocortical interneurons shows no gross differences between Zswim5 knockout mice (KO) and wildtype (WT) controls. Similarly, examination of the SVZ proliferation marker CD2 and the thymidine analogue EdU, which marks cells in S-phase, shows no gross changes in the KO relative to controls.



### Generation of Zswim5/Zswim6 Double Knockout Mice

Zswim5 and Zswim6 are highly homologous proteins. If one considers identical and identical/similar amino acids, they are 77% and 87% homologous, respectively.

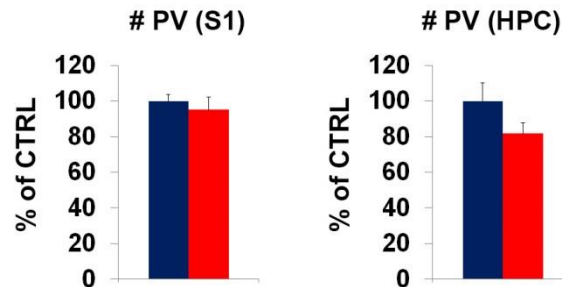


**Figure 3.11. Cortical parvalbumin interneuron numbers are normal in Zswim5 knockout mice.**

Counts of parvalbumin-expressing interneurons (PV) in primary somatosensory cortex (S1) and hippocampus (HPC) shows no difference in the number of PV interneurons in Zswim5 knockout mice relative to controls.

They are also expressed in largely overlapping patterns, increasing the likelihood of genetic compensation. In order to generate Zswim6 mutants, we adopted a conditional knockout strategy that was similar in approach to Zswim5. Since Zswim5 and Zswim6 were formed through gene duplication, they have a nearly identical genomic structure. The only major difference is that exon 1 in Zswim5 was split into two exons in Zswim6. Thus, exon 3 in Zswim6 is identical to exon 2 in Zswim5. Zswim5 has 14 exons in total and Zswim6 has 15, with exons 1 and 2 being equivalent to exon 1 in Zswim5. Like our Zswim5 conditional mutant, we

used homologous recombination to flank exon 4 of Zswim6 with loxP sites (**Figure 3.12 A**), which upon Cre-recombinase mediated recombination is predicted to cause a frameshift deletion. Southern blot using 3' and 5' DNA probes indicates that the targeting construct inserted at the correct location (**Figure 3.12 B**). To confirm whether this strategy produced a null allele, we bred Zswim6 floxed mice to a CMV-Cre line to produce a germline knockout. We then did in situ mRNA hybridization using a probe against the deleted exon to confirm its deletion (**Figure 3.12 C**). Using cDNA E13.5 KOs, we also did RT-PCR with a primer set containing a forward primer in exon 3 and a reverse primer in exon 4 and found no band at the expected length relative to control (**Figure 3.12 D**). Additionally, qPCR on adult mouse striatum showed that Zswim6 transcript was reduced by approximately 70% in knockouts relative to control (**Figure 3.12 E**). A more detailed analysis of Zswim6 single knockout mice will be provided in the following data section. In order to generate constitutive Zswim5/Zswim6 double knockouts, we bred each floxed line to CMV-cre line as previously described. After breeding out the CMV-cre allele, we bred the offspring together to generate Zswim5<sup>+/-</sup>Zswim6<sup>+/-</sup> compound heterozygotes. These were subsequently bred to generate Zswim5<sup>-/-</sup>Zswim6<sup>-/-</sup> double knockout mice.

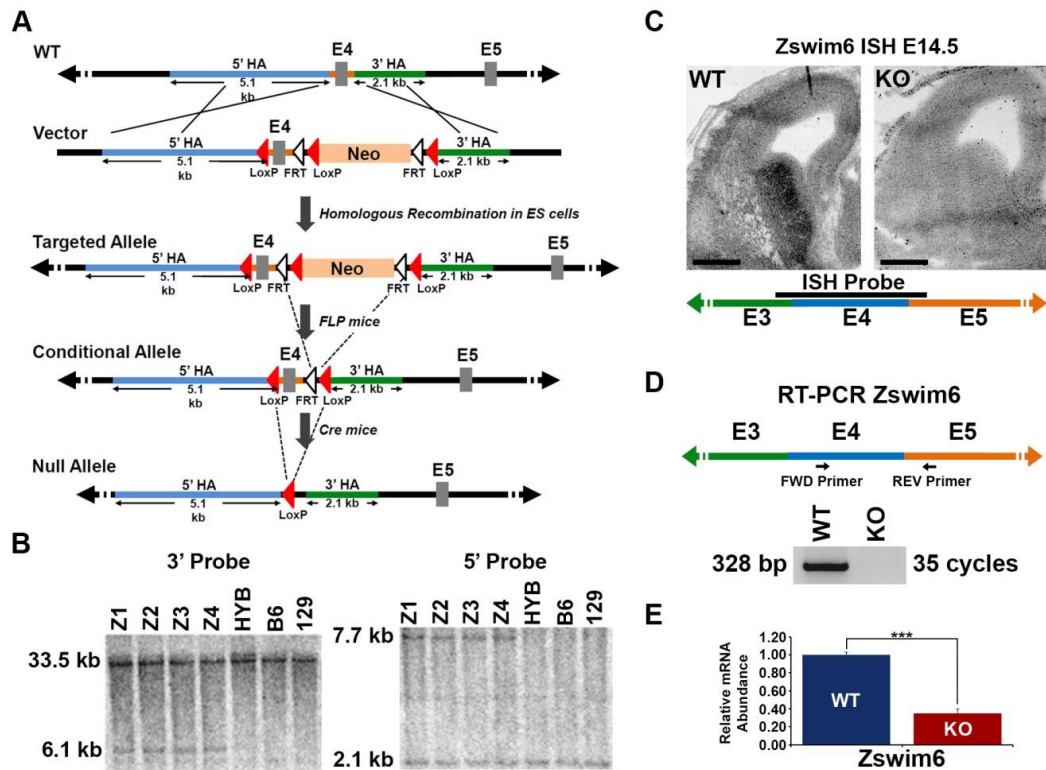


**Figure 3.12. Generation of Zswim6 null mutant mice.**

(A). Schema of constructs used in generating a null allele for Zswim6 by flanking exon 4 with LoxP insertions, generating a mouse line, then crossing this line with Cre-deleter mice.

(B). Southern blot analysis to identify correctly targeted embryonic stem (ES) cell clones obtained from hybrid C57BL/6x129/SvEv ES cells electroporated with the targeting construct. Four ES clones (Z1-Z4) were identified in which there was the expected 5' and 3' recombinations. HYB, hybrid ES cell; B6, C57BL/6 ES cell; 129, 129/SvEv ES cell.

(C). In situ hybridization (ISH) for Zswim6 using a probe spanning exon 3 to the beginning of exon 5 shows loss of expression in coronal sections from embryonic day (E) 14.5 forebrain of homozygous Zswim6 nulls.

(D). RT-PCR reveals a loss of product created by primers flanking the exon 4 and 5 junction in the Zswim6 KO.

(E). There is a significant reduction in the relative abundance of Zswim6 mRNA in homozygous Zswim6 KO mice (N=3). Abbreviations: WT (wild type); Neo (neomycin resistance cassette); E (exon). \*\*\*p<.001. Scale bar 400µm in C. Error bars SEM.

### *Study of Interneuron Development in Zswim5/6 Double Knockout Mice*

While Zswim5 knockouts have no observable phenotype, constitutive Zswim5/Zswim6 double knockouts die within the first 24-48 hours after birth. These mice have no obvious deformities, are well perfused without cyanosis, and have visible milk spots. Thus, their cause of death remains largely unknown. Since parvalbumin and somatostatin are not expressed in PV<sup>+</sup> and SST<sup>+</sup> fated cortical interneurons, respectively, until early adolescence in both mice and humans<sup>317,318</sup>, the early fatality of these double mutants precludes any analysis of adult cortical interneuron numbers. Thus, we took advantage of our mutant mouse lines' conditional potential and generated Nkx2.1-cre double mutants (Nkx2.1dKO)<sup>44</sup>. The Nkx2.1-cre line allows us to interrogate the function of Zswim5 and Zswim6 within Nkx2.1-expressing progenitors of the MGE and PoA<sup>44</sup>. While this line also expresses cre-recombinase in other tissues that express Nkx2.1, including the hypothalamus, thyroid, and lung, we did not examine these structures<sup>44</sup>. Nkx2.1dKO mice do not differ from their wildtype littermates in terms of survival or size (data not shown). Stereological analysis of cortical and striatal volumes showed no change in the volume of either structure (**Figure 3.13 A**). Next, we counted the number of PV<sup>+</sup> and SST<sup>+</sup> interneurons in the cortex and striatum of Nkx2.1dKO mice and found no difference in the number of either subgroup relative to controls (**Figure 3.13 C**). We also counted striatal ChAT<sup>+</sup> interneurons, which originate from Nkx2.1<sup>+</sup> progenitors in the MGE, and found a 20% decrease in their total number (**Figure 3.13 C**). Naturally,

we followed up on this finding by examining whether either of the single mutants showed a reduction in striatal ChAT<sup>+</sup> cells and found that neither of them did (Figure 3.13 B).

### Discussion

Here, we examined the role of Zswim5 and Zswim6 in the production of cortical and striatal interneurons. Analysis of Zswim5 single mutants showed no change in the number of PV<sup>+</sup> cortical interneurons. Armed with this data and knowledge of Zswim6 expression in the MGE, we opted to analyze Nkx2.1dKO mice in lieu of spending additional time and resources examining Zswim5 single mutants.

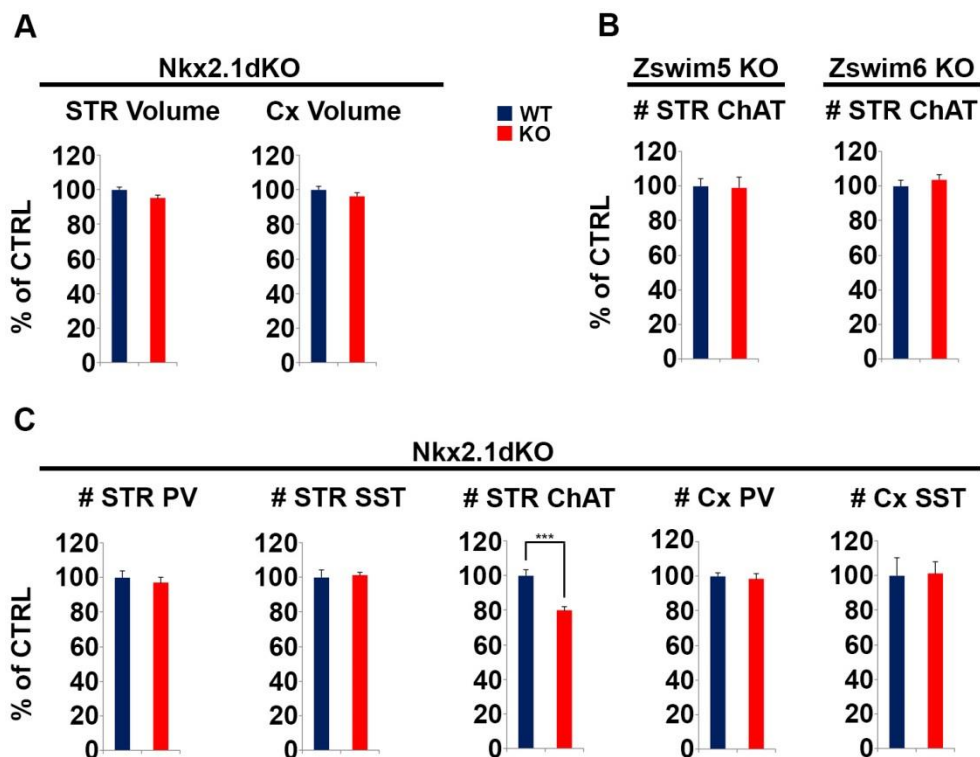


**Figure 3.13. Analysis of striatal and cortical volume and interneuron numbers in Nkx2.1-cre Zswim5/Zswim6 double knockout mice.**

**(A).** Nkx2.1-cre Zswim5/Zswim6 (Nkx2.1dKO) mice have no change in cortical (Cx) or striatal (STR) volume.

**(B).** Constitutive Zswim5 and Zswim6 single knockout (KO) mice have no change in the number of striatal cholinergic interneurons.

**(C).** Nkx2.1dKO mice have no change in cortical and striatal parvalbumin- (PV) or somatostatin (SST)-expressing interneurons but have a 20% decrease in the number of striatal cholinergic interneurons. \*\*\* $p < .001$ . Error bars indicate SEM.

The observation that constitutive double knockouts die shortly after birth suggests that Zswim5 and Zswim6 can at least partially compensate for loss of one another. In support of this, we found no change in the number of striatal ChAT<sup>+</sup> interneurons in either of the single mutants, but found a 20% reduction of ChAT<sup>+</sup> interneurons in Nkx2.1dKO mice. PV<sup>+</sup>, SST<sup>+</sup> and ChAT<sup>+</sup> interneurons are derived from common Nkx2.1<sup>+</sup> progenitors, which upon exit from the cell cycle express Lhx6, GABA, and, at least in a subset, Lhx7<sup>116</sup>. In cells that are fated to become cholinergic subtypes Islet1 is upregulated<sup>116</sup>. Islet1 is cross repressive with Lhx6 and causes it to downregulate in ChAT<sup>+</sup> fated cells. Interestingly, Lhx7 is required to maintain Islet1 expression, and lack of Lhx7 causes cells to revert into a default, GABAergic Islet1<sup>-</sup>/Lhx6<sup>+</sup> lineage<sup>114,116</sup>. Together, Lhx7 and Islet1 form a complex that activates a forebrain cholinergic transcriptional program<sup>115</sup>. A key question that remains to be addressed is the mechanism by which nascent Lhx6<sup>+</sup>, bipotential precursors that are destined to become cholinergic cells upregulate Islet1. It is intriguing to speculate that Zswim5 and Zswim6 might

participate in this process. In addition, further work is necessary to understand the ultimate fate of the missing ChAT<sup>+</sup> cells. We did not find an increase in the number of striatal PV<sup>+</sup> or SST<sup>+</sup> subtypes, suggesting that the missing ChAT<sup>+</sup> cells did not simply adopt a GABAergic identity. It remains to be resolved whether these cells die, migrate elsewhere, adopt another identity, were ever produced in the first place, or simply fail to express choline acetyl transferase. Regardless, this finding has important implications, since dysfunction of cholinergic transmission within the ventral telencephalon is thought to contribute to a number of disease processes including Alzheimer's, Parkinson's, Tourette's, schizophrenia, and addiction<sup>229,230,319-322</sup>.

### **3.3 Loss of the Schizophrenia Associated Gene Zswim6 Alters Striatal Development and Motor-Dependent Behaviors**

#### *Overview*

The zinc-finger SWIM domain-containing protein 6 (ZSWIM6) is a little studied protein with unknown function that has been associated with schizophrenia by two independent genome-wide association studies. More recently, a recurrent point mutation in ZSWIM6 has been identified in several cases of acromelic frontonasal dysostosis and thought to be causal in the disorder. Despite the growing number of studies implicating ZSWIM6 as an important regulator of brain development, its role in this process has never been examined. Here, we report

the generation of Zswim6 knockout mice and provide a detailed anatomical and behavioral characterization of the resulting phenotype. We show that Zswim6 is initially expressed widely during embryonic brain development but becomes restricted to the striatum postnatally. Loss of Zswim6 causes a reduction in striatal volume and changes in medium spiny neuron morphology. These are associated with alterations in motor behaviors including hyperactivity, impaired rotarod performance, repetitive hopping, and behavioral hyperresponsiveness to amphetamine. Together, our results show that Zswim6 is indispensable to normal brain development and support the notion that Zswim6 might serve as an important contributor in the pathogenesis of schizophrenia.

## **Introduction**

While neuropsychiatric disorders such as schizophrenia (SCZ) exhibit significant heritability, the underlying genetics are complex, involving multiple perturbations of modest effect size acting within critical temporal windows<sup>323</sup>. Efforts to understand the pathophysiology of SCZ are similarly complicated by the disorder's diverse, partially penetrant symptomology, organized loosely around positive (hallucinations/ delusions and movement abnormalities) and negative (altered affect, reduced pleasure and motivated action) behavioral domains. However, after many years of stagnation, advances in genomic sequencing, coupled to an appreciation for the scale at which studies must be conducted in order to identify common risk alleles of small effect, have started to uncover the genetic building blocks of polygenic diseases such as SCZ. While knockout



animal models offer admittedly limited insight into the complex nature of these disorders, they may be useful in identifying molecular pathways and neural circuits that are uniquely vulnerable to genetic insult and that have central functions in regulating behavioral output. Here, we contribute to the study of these variants through the generation and characterization of one such SCZ-associated risk gene, ZSWIM6. While to our knowledge no functional studies have been published on ZSWIM6, two independent genome-wide association studies have implicated it in SCZ<sup>251,324</sup> and several additional studies have documented its expression in developing and adult brain<sup>293,295,325,326</sup>. At least two clinical studies have also identified a recurrent point mutation in ZSWIM6 in cases of acromelic frontonasal dysostosis, a rare disorder characterized by multiple brain, limb, and craniofacial abnormalities<sup>295,314</sup>. And while few of the known protein domains within ZSWIM6 are well characterized, gene ontology studies suggest that ZSWIM6 may participate in the epigenetic regulation of gene transcription through interactions with chromatin remodeling complexes<sup>292</sup>— a process extensively implicated in SCZ pathogenesis<sup>305,308,309</sup>.

Recent evidence has implicated cortico-striato-thalamic circuit dysfunction in multiple neuropsychiatric diseases exhibiting motor and cognitive behavioral components<sup>223,327</sup>, reflecting the wide-ranging function of these pathways in motor control, decision-making and reward processing. Due in part to the dominance of the “dopamine hypothesis,” the striatum has long been considered a site of SCZ pathology, although how physiological dysfunction contributes to

specific behavioral abnormalities remains unclear. Here, through the generation of Zswim6 knockout (KO) mice, we provide evidence that further implicates striatal dysfunction in the manifestation of neuropsychiatric disease. We show that Zswim6 initially exhibits widespread early embryonic expression in many forebrain regions, but becomes progressively restricted to the adult striatum. Consistent with this highly restricted expression pattern, we observed that Zswim6 KO mice exhibit a range of motor abnormalities consistent with striatal dysfunction. Many of our findings are similar in nature to phenotypes observed in SCZ patients, suggesting that Zswim6 KO mice may serve as a useful model for studying SCZ-associated endophenotypes.

## Results

### *Expression of Zswim6 in the developing and adult forebrain*

To confirm previous reports and to examine Zswim6 across forebrain development, Zswim6 expression was evaluated by mRNA in situ hybridization. Zswim6 was detected in the subventricular zone (SVZ) of the LGE and MGE at E12.5 (**Figure 3.14 A-C**). Higher expression levels appeared in the LGE than MGE. By E14.5 this expression remained enriched in the SVZ (**Figure 3.14 E-G**), extending into more proximal regions of the MGE and LGE mantle regions. By E16.5, this expression expanded into the medial cortex, the developing amygdala, and portions of the thalamus and hypothalamus (**Figure 3.14 G-I**). In the telencephalon, the postnatal expression of Zswim6 became more restricted

to the striatum (**Figure 3.14 J**). Similar expression patterns have been identified in human samples (**Figure 3.15**).

#### *Generation of a Zswim6 null mouse*

These expression studies suggest that Zswim6 is expressed in the anlagen and postnatal tissue of several portions of the “limbic” forebrain. This expression pattern and the association of Zswim6 with schizophrenia led us to evaluate whether loss of Zswim6 would alter forebrain development and function. Gene targeting was used to create a null allele (**Figure 3.12 A**) in which exon 4 was flanked by LoxP sequences. Removal of exon 4 was predicted to result in a frameshift mutation. Southern blotting was used to identify correctly targeting embryonic stem cell clones (**Figure 3.12 B**). Crosses with a germline expressed Cre recombinase line (CMV-Cre) resulted in generation of an allele lacking expression of Zswim6 exon 4 by in situ hybridization and RT-PCR (**Figure 3.12 C, D**). The MGE of homozygous mutants expressed Zswim6 transcript at roughly 35% of control levels at E13.5 (**Figure 3.12 E**). Of note, in silico analysis

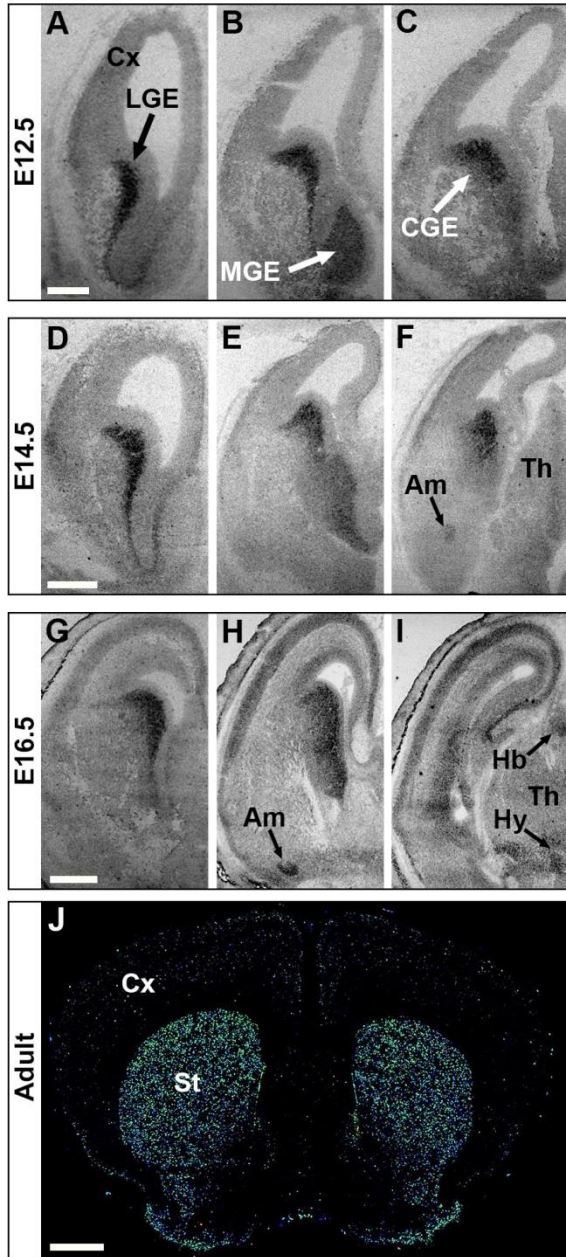


**Figure 3.14. Zswim6 expression during striatal development.**

At embryonic day (E) 12.5 (A-C) and E14.5 (D-F) Zswim6 is strongly expressed in the in the subventricular zone of the lateral and medial ganglionic eminences but at low to non-detectable levels not in the cerebral cortex. Low level expression can also be seen in the amygdala (arrow in F) and thalamus (G-I). At E16.5 this expression expands to the cortical plate and medial habenula (arrow in I) and increases in intensity in the amygdala, as well as the amygdala (arrow in H). (J) Image from the Allen Brain Atlas shows that expression of Zswim6 is present in the adult striatum but not in the overlying cerebral cortex. Abbreviations: LGE (lateral ganglionic eminence); MGE (medial ganglionic eminence); CGE (caudal ganglionic eminence); Cx (cortex); Th (thalamus); Am (amygdala); Hy (hypothalamus); St (striatum). Scale bars 300 $\mu$ m in A-C, 400 $\mu$ m in D-F, 500 $\mu$ m in G-I, 1000 $\mu$ m in J.

suggests that Zswim6 has a single transcript. Unfortunately, while the loss of exon 4 transcript and striatal-related phenotypes presented in this paper are highly encouraging that a Zswim6 null has been created, we were unable to confirm Zswim6 protein expression using commercial antibodies.

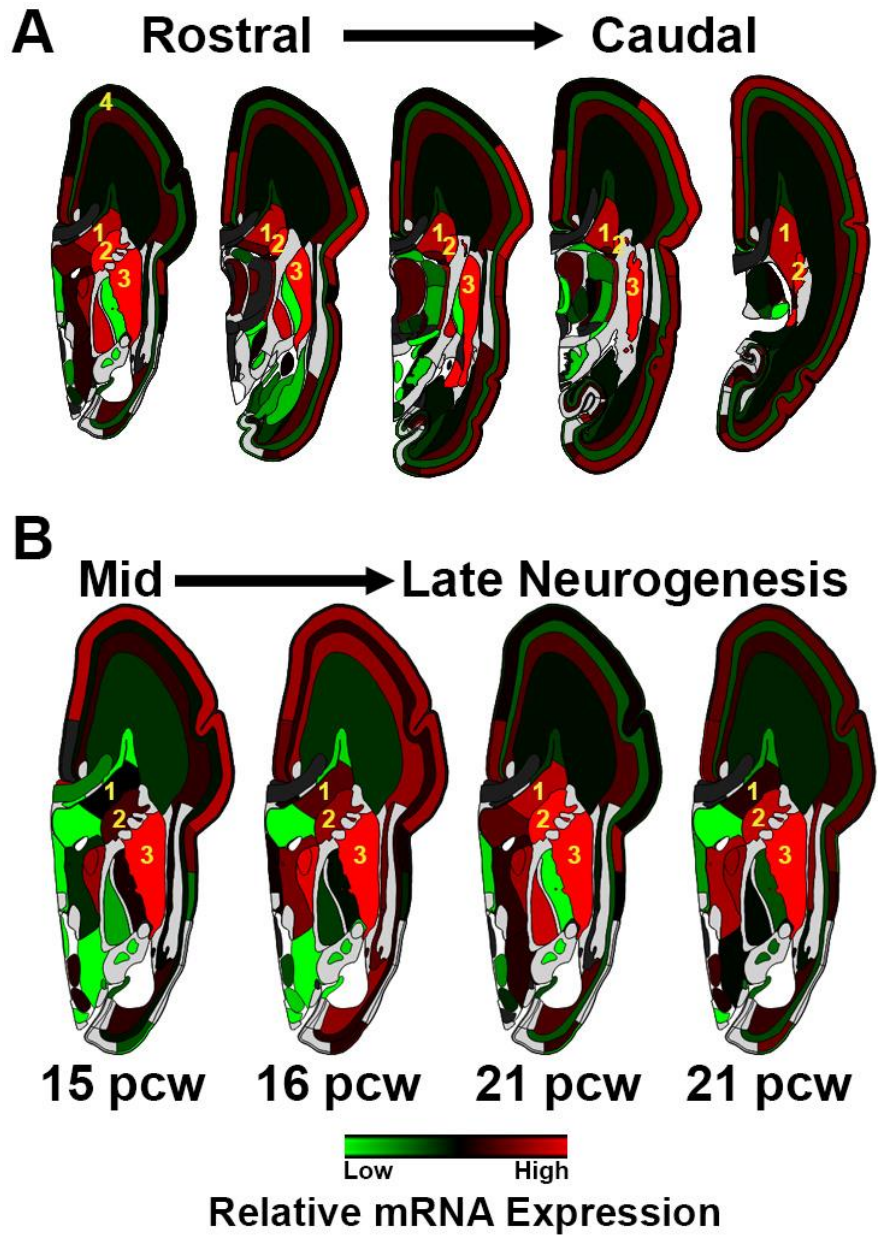


**Figure 3.15. Zswim6 expression during human fetal forebrain development.**

(A) and (B) are pseudocolored renderings from the Allen Brain Institute's human prenatal microarray study showing the relative expression levels of Zswim6 in different embryonic forebrain regions.

**(A).** Shows the relative expression of Zswim6 in different forebrain regions from a single post-conception week (pcw) 21 sample. The sections are arranged from rostral to caudal. Red indicates higher levels of expression, whereas lower levels are indicated in green. The "1" marks the lateral ganglionic eminence. "2" marks the caudate nucleus. "3" marks the putamen. "4" marks the cortex.

**(B).** Shows the relative expression of Zswim6 at three different embryonic time points at approximately the same coronal level. Each time point represents data from a single donor. The expression pattern in the anlage of the striatum is quite similar to that of Zswim6 in the mouse. The labeled structures are the same as in (A).

*Abnormal neocortical and striatal development in Zswim6 null mice.*

Zswim6 KO mice were born in Mendelian ratios, but showed increased neonatal mortality such that roughly 40% of Zswim6 KO mice survived to weaning (Fig. **Figure 3.16 A, B**). At postnatal day (PD) 21, their weight averaged about 80% of wild-type controls (**Figure 3.16 C**), although this normalized improved to 93% of controls by adulthood (**Figure 3.16 C**). Analysis of overhead-view surface area in adults showed a significant decrease for the Zswim6 KO cerebral cortex, and no such decrease for the cerebellum (**Figure 3.16 D**). Stereological analysis of cortical and striatal volumes by the Cavalieri method showed a 7% decrease of cortical volume and a 15% decrease in striatal volume (**Figure 3.16 D**).

To determine which components of forebrain volume were contributing to the above-mentioned phenotypes, we conducted stereological counting of immune-labeled neuronal subtypes in the dorsal striatum (striatum dorsal to the N.

Acumbens) of adult mice. Remarkably, relative to wild-type controls Zswim6 nulls

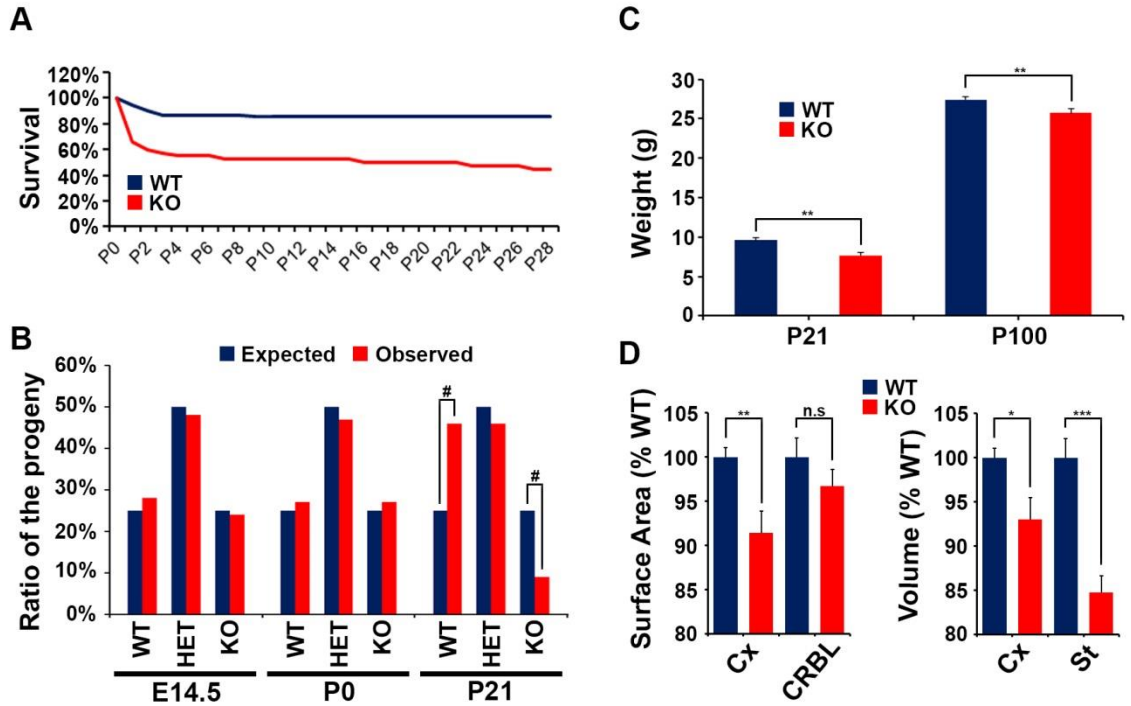


**Figure 3.16. Decreased early postnatal survival and forebrain size in Zswim6 null mutants.**

**(A).** Survival plot showing that the null mutant (KO) mice have a 40% mortality in the first few days after birth, followed by a very gradual decline through 4 weeks. Data is from approximately 100 mice from each group.

**(B).** Analysis of the % of litters that are wild type (WT), heterozygous (HET) or KO for Zswim6 at embryonic day (E) 14.5, P0, and P21 is consistent with loss of KO pups after birth (N=79 mice for P21, chi-square with 2 degrees of freedom = 27.911).

**(C).** Zswim6 KOs also show a small decrease of weight relative to controls at P21 that persists into adulthood (N=10).

**(D).** Overhead surface area of the cerebral cortex (Cx) shows a significant decrease in the Zswim6 KOs, but no change in the cerebellum (N=5). Volumetric measurements based on analysis of coronal tissue sections show a significant reduction of volume in both the Cx (N=5 WT, 6 KO) and the striatum (St; N=5).

showed a 17% reduction in the number of nuclei labeling with CTIP2, a marker of medium spiny neurons (**Figure 3.17 A**). However, the density of these neurons was not changed. In contrast, there was no change in the number of two major

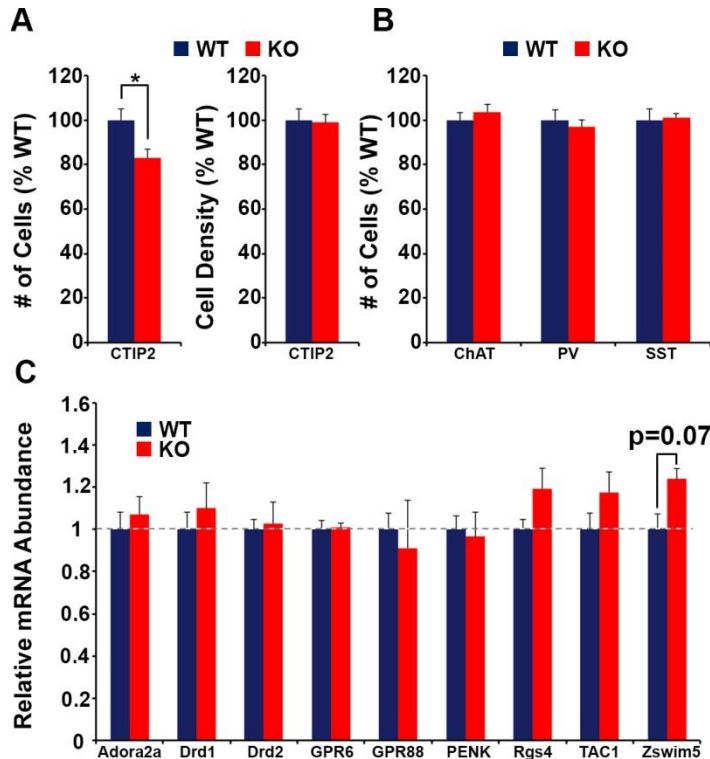


**Figure 3.17. Zswim6 null mutants have a reduced number of medium spiny neurons.**

**(A).** Cell counts for the medium spiny neuron marker CTIP2 in adult Zswim6 KOs relative to WT controls shows a significant reduction of cell number in the KOs. On the other hand, cell density is unchanged, consistent with the reduced total dendritic length (N=3; see Fig. 5) combined with cell loss.

**(B).** In contrast to the effects on medium spiny neurons, cell counts for several populations of striatal interneurons (choline acetyl transferase, ChAT; parvalbumin, PV; somatostatin, SST) are unchanged (N=3).

**(C).** Semi-quantitative RT-PCR for striatal transcripts, including the dopamine receptors Drd1 and Drd2, were not altered in the Zswim6 KOs (N=3). Interestingly, in the KOs there was a trend for increased levels of Zswim5, which might be compensation by this close homologue to Zswim6. \* $p < .05$ . Error bars indicate SEM.



subclasses of GABAergic striatal interneurons (**Figure 3.17 B**), defined by parvalbumin (PV) and somatostatin (SST). In addition, there was no change in the number cholinergic interneurons defined by their expression of choline-acetyl transferase (**Figure 3.17 B**). There were no gross alterations in the expression of

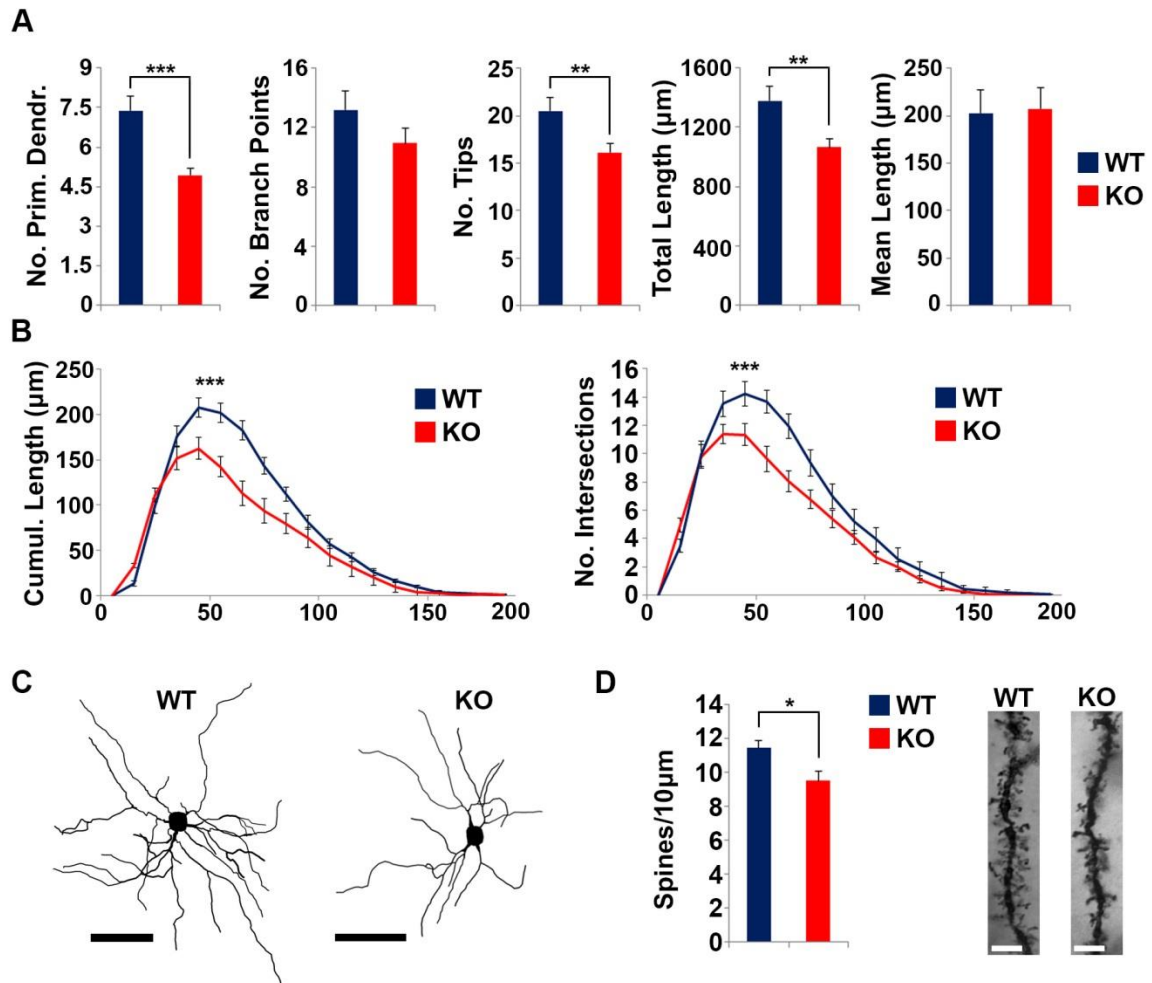


**Figure 3.18. Dendritic abnormalities in striatal medium spiny neurons of Zswim6 null mutants.**

**(A).** The number of primary dendrites, dendritic ends (tips), and total length were decreased in the KOs, whereas there was an insignificant trend towards a reduced number of branch points, and no difference in mean length (N=3, 7 MSN/animal).

**(B).** Consistent with the results in (A), Scholl analysis revealed decreased cumulative length and number of intersections in the KOs.

**(C).** Shows an example of the reconstructions from Golgi-stained sections used in these analyses.

**(D).** Spine density was also decreased on the medium spiny neurons of Zswim6 KOs. Scale bars 50µm in C, 5µm in D. \*p<.05, \*\* p<.01, \*\*\*p<.001. Error bars indicate SEM.

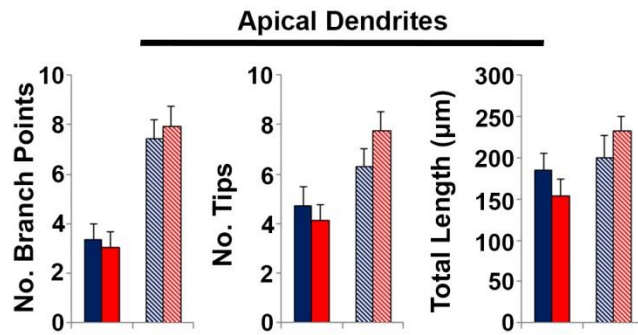
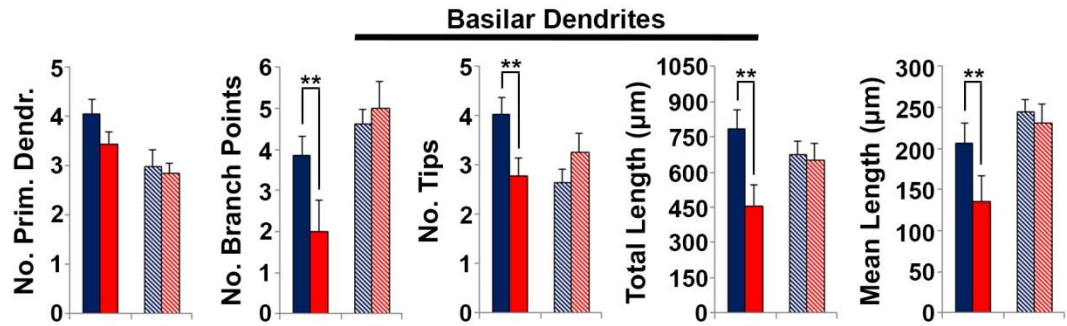
dopamine receptors DRD1 or DRD2 by in situ hybridization (data not shown), and no gross change in tyrosine hydroxylase or DARPP32 (data not shown). Finally, there were no statistically significant changes in the expression of striatal genes evaluated by qPCR (**Figure 3.17 C**), including GPR88, PENK, Adora2a, Drd1, Drd2, Rgs4, TAC1, and GPR6. Interestingly, there was a non-significant trend for Zswim5 upregulation, by 20%.

In addition to neuronal number, another important component to striatal size is dendritic arborization. Indeed, reconstructions of Golgi-stained neurons revealed a significant decrease in dendritic number, tips, and total length (**Figure 3.18 A, C**). There was no change in the number of branch points or mean dendritic length. Sholl analysis revealed that Zswim6 KOs have reduced cumulative dendritic length and decreased Sholl intersections (**Figure 3.18 B**). Spine density was reduced in the KOs by about 15% (**Figure 3.18 D**).

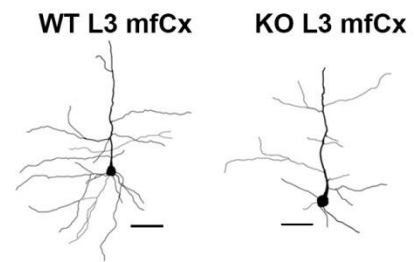
These results suggest that the reduction of striatal volume involves both a reduction in the number of medium spiny neurons, and a reduction in their dendrites. To determine whether the dendritic arborization phenotype is specific to the striatum, we examined layer 3 pyramidal neurons of the medial frontal cortex. While the apical dendrites of Zswim6 KO pyramidal neurons were unchanged from controls, the basilar dendrites had reduced dendritic complexity and length (**Figure 3.19 A, B**). This result contrasted to that of layer 3 of somatomotor cortex, which was not altered in the Zswim6 KO brains (**Figure 3.19 A**). As for the striatum, Sholl analysis of the medial frontal cortical layer 3 pyramidal neuron basilar dendrites revealed that Zswim6 nulls have reduced cumulative dendritic length and decreased Sholl intersections (**Figure 3.19 C**). Again, these differences were not found in the basilar dendrites of layer 3 pyramidal neurons in somatomotor cortex (**Figure 3.19 C**). Spine density on medial frontal cortical layer 3 pyramidal neuron basilar dendrites was reduced by about 13% (**Figure 3.19 D**).

**A**

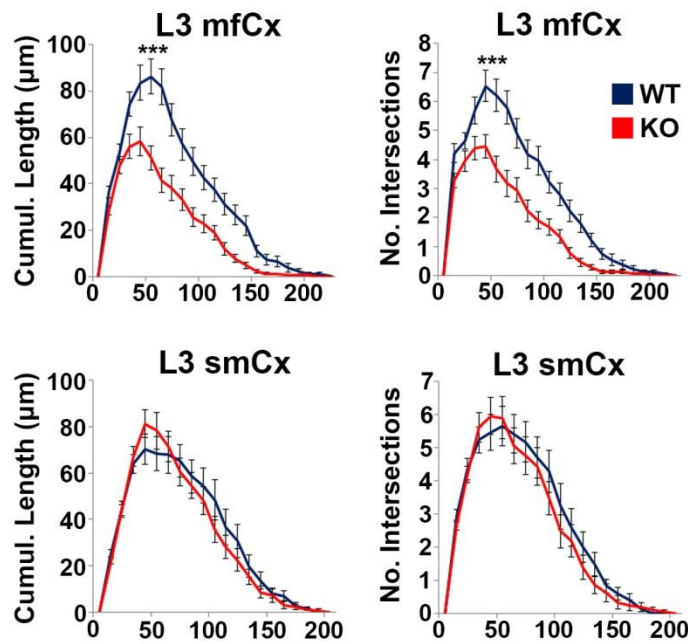
■ WT Layer 3 mfCx ■ KO Layer 3 mfCx ▨ WT Layer 3 smCx ▩ KO Layer 3 smCx



**B**



**C**



**D**

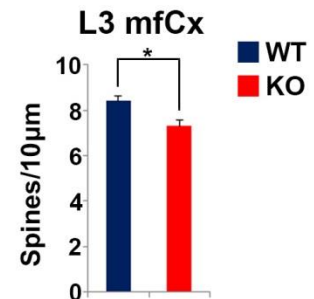


**Figure 3.19. Zswim6 null mutants have decreased dendritic complexity in medial frontal cortex but not somatomotor cortex.**

**(A).** For pyramidal neurons (PN)s of the medial frontal cortex (mfCx), the Zswim6 KOs had a significant decrease of branch points, tips, total length and mean length in the basilar dendritic tree, whereas the apical trees were not affected. In contrast, the basilar dendrites were unchanged in the KOs somatomotor cortex (smCx) (N=3, 6 PN/animal)

**(B).** Shows an example of the reconstructions from Golgi-stained sections used in these analyses.

**(C).** Sholl analysis of the basilar dendrites revealed decreased cumulative length and number of intersections in the mfCx of the KOs, but no change in the smCx.

**(D).** Spine density was also decreased on the basilar dendrites of Zswim6 KO mfCx pyramidal neurons . Scale bar 50 $\mu$ m in B. \*\* p<.01, \*\*\*p<.001. Error bars indicate SEM.

To evaluate potential mechanisms behind the reduction of striatal medium spiny neurons, we quantified markers of proliferation during embryonic development. Counts of the m-phase marker PH3, and the S-phase marker EdU, showed no differences in the LGE between Zswim6 KO embryos and wild-type controls (**Figure 3.20**). In addition, there was no gross difference in the density of cells expressing cyclin-D2, expressed primarily in subventricular zone progenitors (data not shown). While these analyses cannot definitely rule out the presence of a relatively subtle proliferation deficit, they do suggest that the adult striatal phenotype in Zswim6 KO embryos is not secondary to a major proliferation deficit. In addition, we also investigated the presence of cleaved caspase-3 as an indicator of apoptosis in Zswim6 KO and control mice at E14.5, P0, P21, and P60 and found no increase in its expression (data not shown).

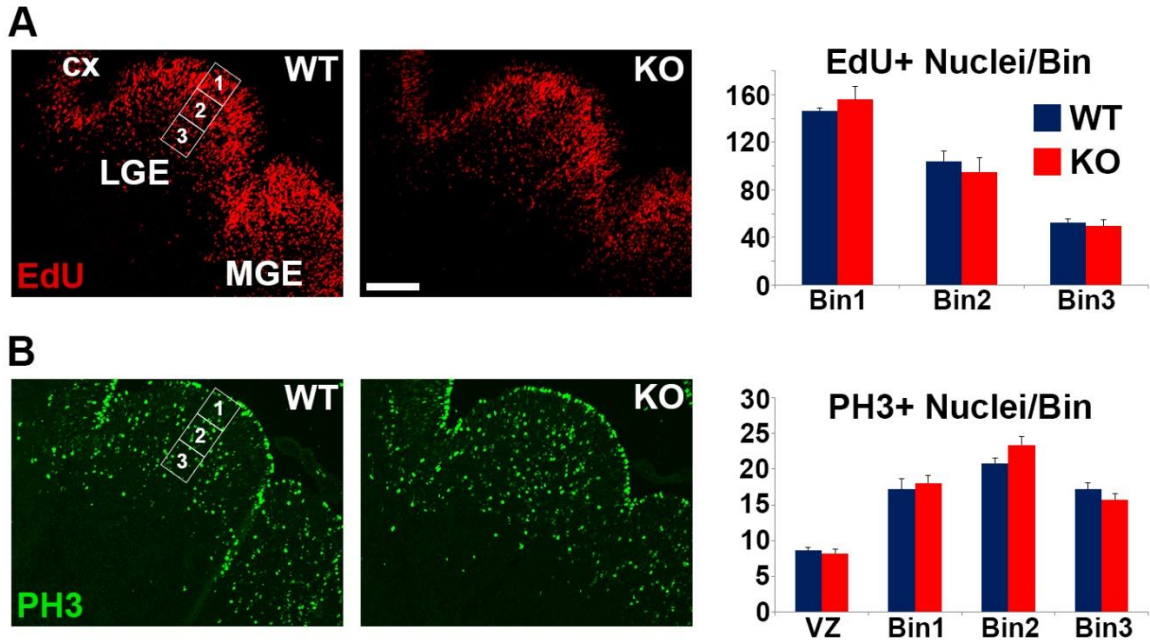


**Figure 3.20. No evidence for reduced proliferation by striatal progenitors in *Zswim6* null mutants.**

**(A).** At embryonic day (E) 14.5, mice were pulsed with the thymidine analogue EdU 30 minutes before fixation and the location of s-phase cells identified by histochemistry. The boxed region shows the areas for which EdU+ nuclei were counted in the lateral ganglionic eminence, the origin of medium spiny neurons of the adult striatum. There were no differences in EdU expression in the *Zswim6* KOs.

**(B).** PH3 labels m-phase cells. Again, there were no differences in this marker of proliferation in either the ventricular zone (bin 1) or subventricular zone (bins 2 and 3) of the KOs relative to WT controls (N=5). Scale bar 300 $\mu$ m. Error bars indicate SEM.

### *Loss of *Zswim6* results in behavioral deficits*

To determine whether the alterations in medium spiny neuron number and arborization are accompanied by behavioral abnormalities in *Zswim6* nulls, mice were subjected to a battery of tests. Consistent with an alteration of striatal function, *Zswim6* nulls had a performance worse than controls on the rotarod

(**Figure 3.21 A**). In the open field test they showed increased horizontal beam breaks, increased rearing, and decreased thigmotaxis (**Figure 3.21 B**). Hyperactivity was also apparent in the force plate test, and hind limb jumping was greatly increased (**Figure 3.21 C**). In agreement with the open field findings, Zswim6 nulls also had fewer low mobility bouts and spent less time in the center of the arena (**Figure 3.21 C**). In the elevated zero maze the Zswim6 nulls showed a non-significant trend towards increased time in the open arm, and an increased average speed (**Figure 3.21 D**). Remarkably amphetamine, at a dose (2mg/kg) that did not alter the activity of controls, significantly increased the activity of the Zswim6 nulls (**Figure 3.21 E**). This result is consistent with enhanced striatal dopamine signaling in these mutants.

We also attempted to assess sensorimotor gating by measuring prepulse inhibition (PPI) of the acoustic startle reflex. However, during the initial acoustic habituation trials, we discovered that Zswim6 nulls have a dramatically blunted response to increasing auditory stimulation, indicating a potential for hearing loss (**Figure 3.22 A**). Follow-up brainstem auditory evoked response testing (ABR) on three Zswim6 nulls revealed that two animals had normal ABR thresholds to a 16 kHz pure tone, which is the frequency at which mice hear best, while one animal had no response (**Figure 3.22 A, C, D**). Overall, knockout mice did not appear to have altered thresholds over a 20 kHz range (**Figure 3.22 C**).

## Discussion

To our knowledge this is the first paper to describe a loss of function model of the schizophrenia-associated gene *Zswim6* in mice. *Zswim6* is strongly expressed within the subventricular and mantle zones of the striatal anlage. Broadly, it has a dynamic expression pattern in multiple regions, including the medial frontal cortex, medial habenula, and the amygdala. This expression pattern in regions of the “limbic” forebrain is particularly intriguing in light of the association of *Zswim6* with schizophrenia.

*Zswim6* null mutants are born at Mendelian ratios, but roughly half fail during the neonatal age range. The cause of this death is not clear, but the *Zswim6* mutants lag behind their littermates in weight through weaning and into adulthood, then appear to breed normally. Due to the strong persistent expression of *Zswim6* in the adult striatum, where the close homologue *Zswim5* is weakly expressed, and due to the relevance of striatum to the pathology of schizophrenia, we focused on striatum and related phenotypes in this study.

Striatal volume was reduced by 15% in *Zswim6*<sup>-/-</sup> adults. This occurred in part due to a reduction in the number of medium spiny neurons (**Figure 3.17**). To examine the mechanism of reduced medium spiny neuron number, proliferation was examined in embryonic *Zswim6* mutants. No gross change was found at E14.5 (**Figure 3.20**), although an alteration in proliferation that caused a 15% difference in neuron number could be very difficult to detect. There was no



increase in the expression of the apoptosis marker cleaved caspase 3 at E14.5, P0, P21 or in adults (data not shown).

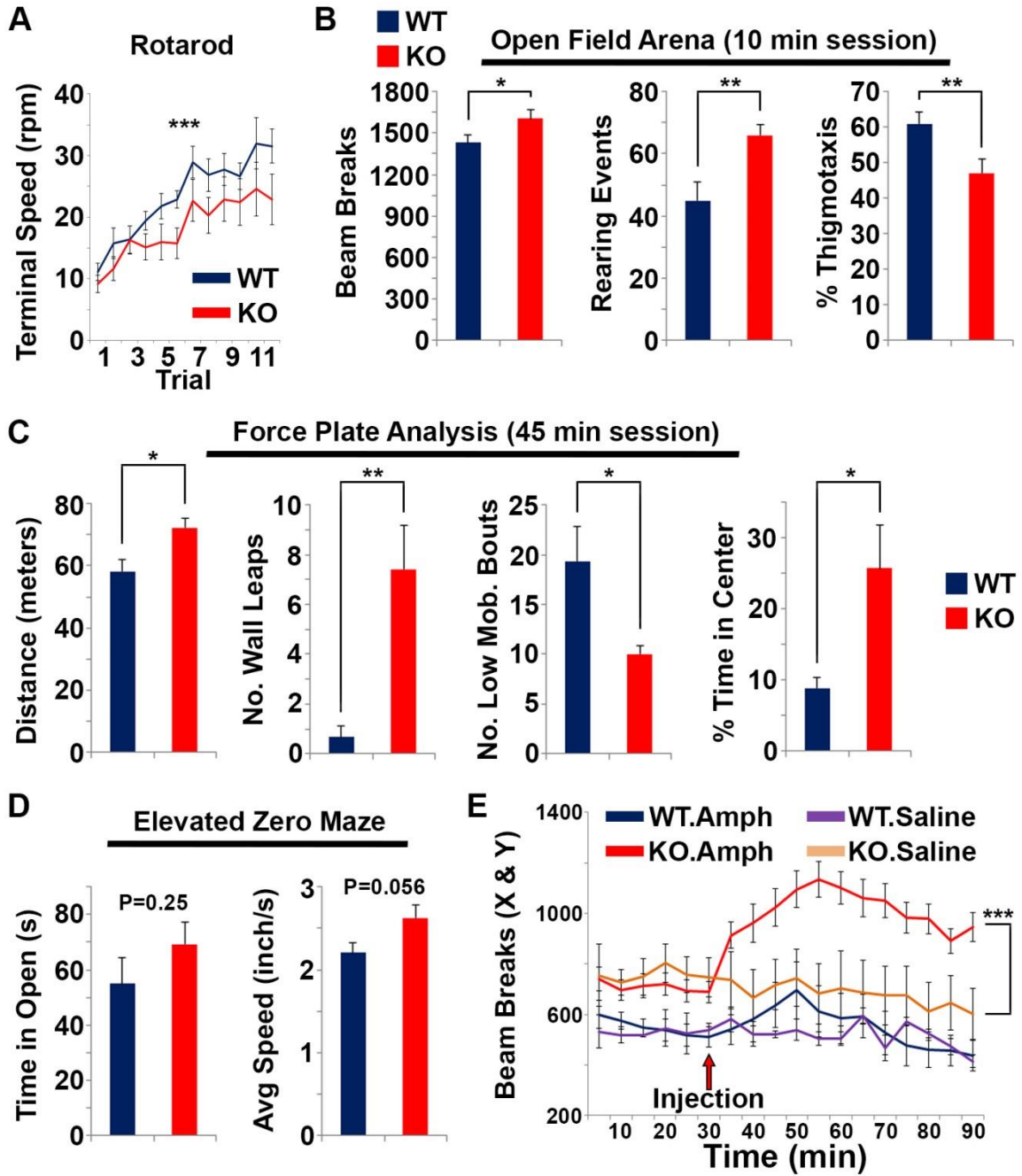


**Figure 3.21. Behavioral defects in Zswim6 null mutants.**

**(A).** Zswim6 KOs achieved significantly lower terminal speeds on the rotarod test (N=14 WT, 15 KO).

**(B).** In the open field the KOs had more beam breaks, more rearing events, and decreased thigmotaxis (N=16 WT, 19 KO).

**(C).** Force plate analysis showed greater distance traveled, increased hind limb jumps, decreased low mobility bouts, and increased time in the center (N=9 WT, 7 KO).

**(D).** In the elevated zero maze there were non-significant trends towards increased percent time in the open sections and increased average speed for the KOs (N=12 WT, 13 KO).

**(E).** Amphetamine (2mg/kg; administered at 30 minutes) did not alter motility of controls (dark blue and purple lines show wild-types treated with amphetamine or saline, respectively; N=12 WT-amph, 13 KO-amph, 4 WT-saline, 4 KO-saline). In contrast, 2mg/kg amphetamine significantly increased the motility of the Zswim6 KOs over its moderately elevated baseline. \*p<.05, \*\*p<.01, \*\*\*p<.001. Error bars indicate SEM.

To determine whether striatal volume loss could also be secondary to defective dendritic arborization in the Zswim6 mutants, adults were subjected to Golgi-Cox staining (**Figure 3.18**). Indeed, there was a significant reduction in total dendritic length and in the number of dendrites per cell. Spine density was also significantly decreased, suggesting a loss of synaptic input.

To determine whether this effect is striatal specific, we also examined the neocortex. Neocortical volume was less affected than that of the striatum in Zswim6 mutants, but was significantly reduced by about 7% (**Figure 3.16**).

Analysis of layer 3 pyramidal neurons of medial frontal cortex revealed reduced total length of the basilar dendrites in the mutants, whereas the apical dendrites

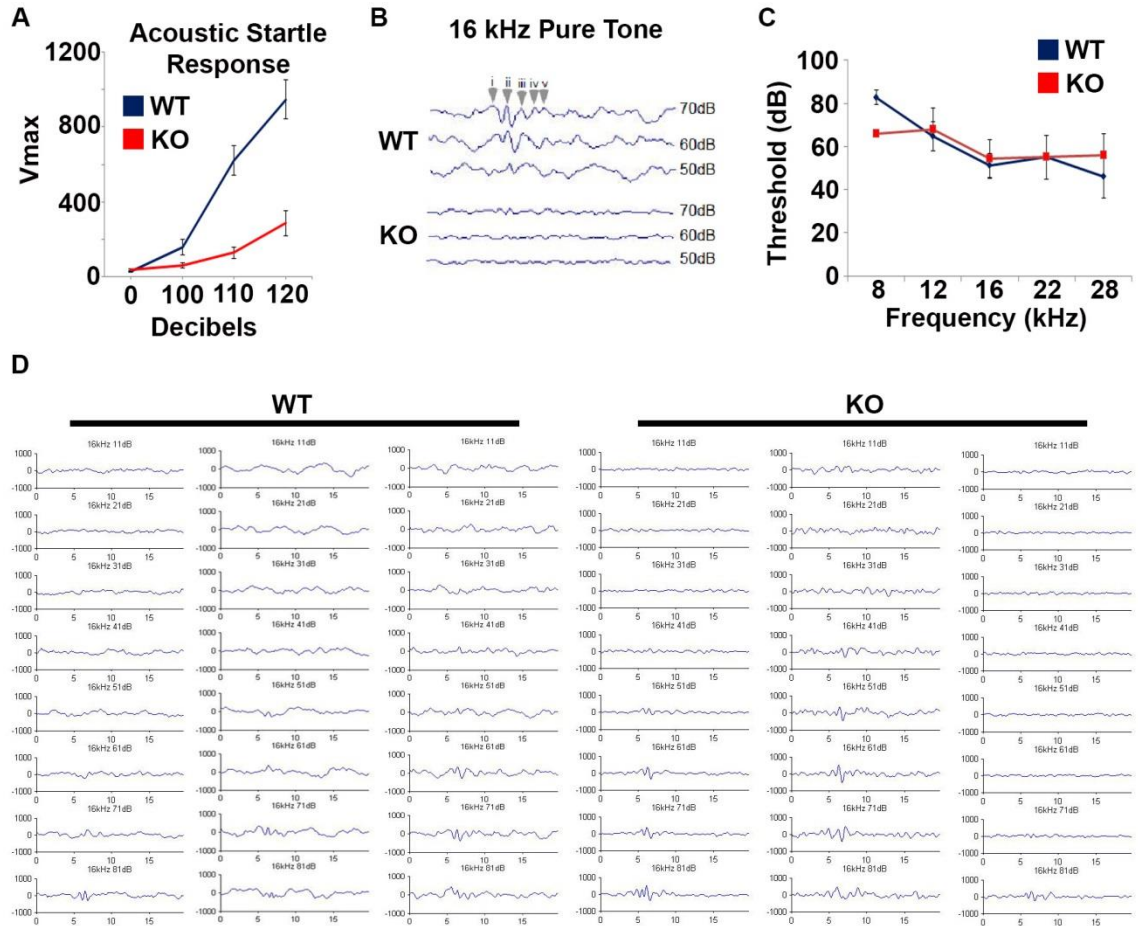


**Figure 3.22. Brainstem auditory evoked response testing on Zswim6 knockout mice.**

**(A).** Zswim6 knockout (KO) mice have a dramatically reduced startle response to increasing auditory stimulation.

**(B).** Electrophysiological tracings of brainstem responses to a 16 kHz pure tone played at three different sound intensities shows that one Zswim6 knockout has no response, indicating a potential for deafness.

**(C).** KO mice have on average normal auditory thresholds at different frequencies.

**(D).** Electrophysiological brainstem responses to a 16 kHz pure tone for three WT and three KO mice.

were not affected (**Figure 3.19**). Interestingly, layer 3 pyramidal neurons in the somatomotor region were unchanged in the mutants, suggesting that the deficits may be most pronounced in areas such as the medial frontal cortex and striatum most associated with neuropathological findings in schizophrenia. How Zswim6 loss of function results in these abnormalities is unclear although, since the targeting construct included the capacity to generate conditional mutants, future studies will be able to evaluate whether, for example, striatal or cortical specific loss of this putative chromatin regulator alters gene expression and cortico-striatal circuitry during development.

Based on the findings of striatal defects Zswim6 mice were subjected to a battery of behavioral tests. Remarkably, they showed defects in the rotarod, increased rearing and hind limb jumping behavior, and hyperactivity in the open field which was further increased by a dose of amphetamine that did not alter the activity of

controls (**Figure 3.21**). These alterations are consistent with defects in striatal functioning.

In sum, we have generated null mutant mice for the schizophrenia-associated gene *Zswim6*. While our analysis is not exhaustive, loss of *Zswim6* results in striatal and cortical abnormalities that are consistent with schizophrenia-associated endophenotypes, including spine density reduction in frontal cortex and hypersensitivity to amphetamine. We thus conclude that this appears to be a useful model for studying the function of a schizophrenia-associated gene at the molecular, functional circuitry, and behavioral levels.

# CHAPTER 4

## Ongoing Studies & Future Directions

### 4.1 Overview

The work in this dissertation largely seeks to identify novel molecular-genetic pathways that regulate the production of distinct neuronal subtypes from within the embryonic subpallium. We harnessed information gleaned from studying the development of cortical interneurons *in vivo* to enhance the production of PV cortical interneurons from embryonic stem cells *in vitro*. In an effort to identify new genes that control interneurongenesis, specifically within the SVZ, we inadvertently discovered novel genetic regulators of striatal ChAT interneurons and MSN. With an enhanced ability to produce PV cortical interneurons, we can now begin to explore with greater precision the pathways that regulate PV vs SST cortical interneuron development, as well as use enriched populations of cortical interneuron subtypes for cell-based transplantation assays. In addition, we also provide evidence for the role of Zswim6, and to a lesser extent Zswim5,

in the development and function of the telencephalon. As a significant schizophrenia candidate gene, insight into Zswim6 function will hopefully take us closer to understanding the biological pathways that are affected in different neuropsychiatric disease states. With rapidly evolving technologies that enable quicker and higher resolution genome editing, genetic sequencing, and epigenetic profiling on multiple scales, combined with greater access to large genetic patient datasets, we are now poised to answer some of the most challenging questions in neuroscience. The following chapter will discuss our ongoing efforts to build upon the work presented in this thesis, as well as describe future directions that these projects could move in.

## **4.2 RNA and Epigenetic Profiling of mESC-Derived Fate Committed Cortical Interneurons**

Evidence from fate mapping studies has shown that interneuron subtypes have distinct spatiotemporal origins. Knowledge of the transcriptional programs that direct interneurongensis will likely reveal how different interneuron fates are determined. In addition, many studies have demonstrated that neuronal fate determination occurs before or around the time of cell cycle exit, often based on the functions of transcription factors expressed selectively within the proliferative zones. However, cortical interneurons undergo an extended period of migration prior to their maturation into interneurons with subgroup or subtype-defining features. In mouse, migration from the MGE, LGE, and CGE into the overlying cortex takes approximately one week. A highly similar migration occurs in

humans<sup>328,329</sup>, where it may require 4 to 8 weeks. During this time, interneuron morphology and migratory behavior is indistinguishable across interneuron subgroups. However, the mechanisms by which distinct neuronal fates are maintained during the migration period, when they may no longer express the genes initially required for their fate determination, is largely unknown. A major advance that our current mESC study makes is the ability to strongly enrich for either PV or SST subtypes, using a single cell line and without the need for forced gene expression. We are thus in a unique position to profile early post-mitotic, differentially fate-committed cortical interneurons *in vitro*.

We hypothesize that the mechanism by which interneuron fate potential is maintained throughout the extended migration period depends upon either a RNA transcript(s) and/or epigenetic landscape(s). In order to identify these molecular memory traces, we have begun collecting differentially fated Lhx6:GFP<sup>+</sup> cortical interneuron precursors for RNA-seq and ATAC-seq. RNA-seq will allow us to identify RNA transcripts that are differentially expressed between PV and SST-fated populations. ATAC-seq will enable us to identify regions of open and closed chromatin that correlate with expressed transcripts, enhancers, and, potentially, regions of the genome that are poised to be expressed (e.g. open) but remain inactive until migration has ended. For the latter possibility, our hypothesis is that genes driving subgroup-selective differentiation after the migratory phase will be “poised” for transcription in newly born Lhx6:GFP<sup>+</sup> cells from one subgroup and “closed” for transcription in the other. Ultimately, this



would be combined with chromatin signature analysis by ChIP-seq to compare “poised” and repressed loci across the PV- and SST-fated cells. A similar approach has recently been used to correlate cell type-specific transcriptomes with an atlas of open chromatin to identify novel genes and transcriptional regulatory elements that confer cell-type identity, while simultaneously retaining cell-fate plasticity, in purified populations of human pancreatic  $\alpha$ - and  $\beta$ -cells<sup>330</sup>. To test whether this approach will be useful in identifying novel transcripts and/or epigenetic landscapes specific to PV and SST subtypes, we have collected PV- and SST-fated cells for this purpose. To enrich for SST-subtypes, we used a modified version of our previously published protocol<sup>280</sup>. We grew cells under high Shh conditions from DD8-12 and then collected Lhx6:GFP-only expressing cells on DD12. During cell sorting, 3 x 125,000 cells were collected for RNA-seq, followed by 4 x 50,000 cells for ATAC-seq. To confirm that the collected cells are enriched to become SST subtypes, we sorted additional cells for transplantation into neonatal neocortex. Only those differentiations that produce the intended ratio (i.e. 6:1 SST:PV for the SST-enriched protocol and greater than 5:1 PV:SST for the PV-enriched protocol) will be used for downstream analyses. To enrich for PV-subtypes, we grew cells under low Shh conditions (SAG from DD8-10, combined with aPKCi from DD8-16) and collected Lhx6:GFP::Nkx2.1:mCherry double-positive cells on DD16. We collected cells 5 days later than the PV-protocol described in this dissertation in an attempt to further enrich for PV, since previous work from our lab has shown that increased time in culture enhances

the genesis of PV subtypes at the expense of SST subtypes. Upon confirmation of cell fate, members of Zhaolan Zhou's lab at the University of Pennsylvania will proceed with preparing DNA and RNA libraries for ATAC-seq and RNA-seq, respectively, from the sorted populations. Bioinformatic analyses will then be used to identify transcripts enriched in either the SST or PV-fate cells. Gene expression analyses including qPCR, immunohistochemistry, and in situ hybridization will be used to confirm the expression of any candidate genes identified in this analysis. In parallel with the RNA-seq data, bioinformatic analyses of the ATAC-seq data will be used to identify regions of open and closed chromatin. We anticipate that a large number of genes will be co-expressed in both populations and that these will correlate with regions of open chromatin. However, we also anticipate finding regions of chromatin that are open in one population but closed in the other, and then correlate this with RNA-seq data to identify regions that are poised for transcription but not yet active. We will then use previously published gene expression datasets of mature PV and SST populations to see if any poised regions (e.g. closed in one population and open in the other but not transcribed) become active upon terminal differentiation. Follow-up analyses would show that poised regions identified on the basis of RNA-seq and ATAC-seq data are defined by the simultaneous presence of histone modifications associated with both gene activation and repression (e.g. H3K4me3 and H3K27me3, respectively)<sup>331</sup>. Meanwhile, the same regions of chromatin in the other cell population should be defined by the

presence of histone modifications associated with gene repression. Finally, gene and chromatin loci “hits” will be tested functionally in mESC differentiations. Candidate genes will be knocked down via RNAi or CRISPR-Cas9 mediated mechanisms to determine their influence on cell fate. Meanwhile, candidate genomic loci will be activated or repressed using CRISPR-Cas9 mediated gene activation and/or repression.

### **4.3 Notch Inhibition to Enhance the Generation of SST-subtypes from Embryonic Stem Cells**

As mentioned earlier, a previous study from our lab used electroporation of a dominant-negative version of the Mastermind-like-1 protein (dnMAML) to block notch signaling within apical MGE progenitors and force them out of the cell-cycle<sup>133</sup>. The result was a remarkable enhancement of SST-interneurongenesis at the expense of PV subtypes. In parallel with our current effort to enhance SVZ-like neurogenesis in vitro via aPKC inhibition, we are using notch inhibition in our stem cell system to promote early cell cycle exit, and by extension, SST-fate specification. To do so, we are using the well-established  $\gamma$ -secretase inhibitor DAPT to block notch signaling *in vitro*<sup>332,333</sup>.  $\Gamma$ -secretase is required to cleave the notch intracellular domain (NICD), which translocates to the nucleus to activate notch effector genes. When  $\gamma$ -secretase is inhibited, NICD is prevented from entering the nucleus and notch signaling is effectively eliminated. We hypothesize that interneuron progenitors forced to undergo cell-cycle exit will preferentially produce SST-fated interneurons at the expense of PV subtypes

secondary to intermediate progenitor cell depletion. To this end, we added DAPT to our stem cell cultures from DD10-12 and then collected Lhx6:GFP<sup>+</sup> and Lhx6:GFP::Nkx2.1:mCherry double-positive cells on DD12 for transplantation. Of note, time lapse video microscopy shows that GFP is expressed at cell cycle exit, when Nkx2.1 is downregulated in cortical interneurons, but that there is a brief window when mCherry perdures, enabling the isolation of newly born, post-mitotic GFP<sup>+</sup>/mCherry<sup>+</sup> cells<sup>269</sup>. In agreement with our *in vivo* findings, we find that the addition of DAPT (10 $\mu$ M) to our mESC cultures from DD10-12 causes a ~2 fold increase in the fraction of GFP<sup>+</sup> and GFP<sup>+</sup>/mCherry<sup>+</sup> cells together with a 27% decrease in the fraction of mCherry-only expressing cells (**Figure 4.1**). These results are consistent with a dramatic increase in cell cycle exit. These experiments are currently ongoing.

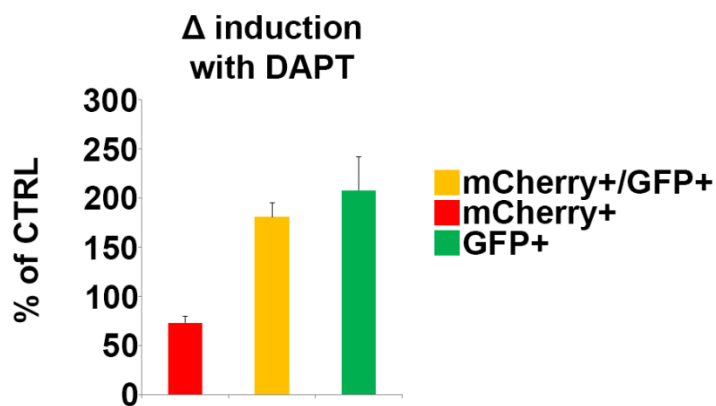


**Figure 4.1. DAPT forces progenitors to exit the cell cycle.**

We added the notch inhibitor DAPT from differentiation days 10-12 during directed differentiations of our Nkx2.1:mCherry::Lhx6:GFP dual reporter mouse embryonic stem cell line and measured the percentage of mCherry<sup>+</sup> (Nkx2.1<sup>+</sup> progenitors), mCherry<sup>+</sup>/GFP<sup>+</sup> (early post-mitotic precursors), and GFP<sup>+</sup> (later post-mitotic precursors) cells via FACS. DAPT causes a ~ two-fold increase in the percentage of mCherry<sup>+</sup>/GFP<sup>+</sup> and GFP<sup>+</sup> cells and a corresponding ~25% reduction in the percentage of mCherry<sup>+</sup> progenitors.

#### **4.4 Embryonic Stem Cell-Derived Interneuron Based Therapy for Epilepsy**

Now armed with the ability to generate enriched populations of PV expressing interneurons from mESCs, we are exploring the potential for using mESC derived cortical interneuron transplantation as a cell based therapy for Dravet syndrome. Dravet syndrome, also known as Severe Myoclonic Epilepsy of Infancy (SMEI), is a malignant seizure disorder in which affected children develop medication resistant seizures, developmental delay, and severe to profound intellectual impairment. About 10-15% of children with Dravet syndrome will eventually die from status epilepticus or sudden unexpected death in epilepsy (SUDEP). Approximately 80% of SMEI cases are due to mutations in the gene SCN1A<sup>334</sup>. Importantly, several studies have shown that loss of SCN1A causes impaired action potential firing of inhibitory interneurons with little to no effect on the activity of excitatory neurons. This suggests that interneuron dysfunction, particularly of PV subtypes, is the cause of seizures in Dravet syndrome<sup>185,186</sup>. Based on these studies, we hypothesize that transplantation of mESC-derived PV interneuron precursors into neonatal cortex and hippocampus will mitigate the

development of epilepsy in transgenic mice engineered to harbor a mutation in SCN1A (Scn1aRH) that is associated with cases of Dravet syndrome. Furthermore, we hypothesize that transplants enriched for PV interneurons will more efficiently modify epilepsy in Scn1aRH mouse pups than either mixed transplants or those enriched for SST-subtypes. To this end, we will perform stereotaxic injections into five sites bilaterally (frontal, parietal, and occipital neocortex, and dorsal and ventral hippocampus) at P0 and P1. We will inject four different treatment conditions: (1) PV-enriched interneuron cell transplants; (2) SST-enriched interneuron cell transplants; (3) freeze-killed interneuron cell transplants; and (4) untransplanted negative controls. Based on our previous studies, we anticipate that mESC-derived interneurons will occupy appropriate cell type-specific niches and integrate functionally into host cerebral cortical brain circuits, thereby augmenting cortical inhibition. Approximately four weeks post-transplantation, intracranial EEG electrodes will be surgically implanted into Scn1aRH mice and controls. In conjunction with video monitoring, EEG data from P28-P35 will be analyzed to determine whether interneuron cell transplants delay the onset, frequency, or duration of seizure activity in Scn1aRH mice, as well as quantify the rate of epilepsy-associated cell death. We are also developing several additional variants of our Nkx2.1:mCherry::Lhx6:GFP line that will enable us to pharmacologically or optogenetically control the activity of transplanted cells. By using the PiggyBac transposon system, we can insert stable transgenes into our dual reporter mESC line. We have begun generating a dual reporter line

that expresses the inhibitory DREADD (designer receptor exclusively activated by designer drugs;<sup>335,336</sup>), hM4DG<sub>i</sub>, which enables us to “turn off” transplanted interneurons in the intact animal *en masse* to allow for confirmation of continued presence of the cell graft as required for seizure suppression. We have also started the generation of another line engineered to express the red-shifted channelrhodopsin ChrimsonR<sup>337</sup>, which will allow “on-demand” recruitment of transplanted interneurons to terminate ongoing seizures in Scn1aRH mice using a closed-loop stimulation system coupled to a wireless EEG transmitter. To date, we have done two rounds of PV-enriched interneuron cell transplants into Scn1aRH mice and controls. For reasons that we do not fully understand, our first series of injections were largely unsuccessful in that we failed to achieve large numbers of cell engraftment in the cortex. We injected upwards of 400,000 cells into each animal over the course of two days, and upon immunohistological examination of the transplanted tissue found fewer than 1000 cells within the cortex, with many cells engrafted into the amygdala and ventricular walls. Reasons for the poor outcome may be related to the number of cells we injected (too many cells may elicit an immunogenic response leading to decreased survival), the age of the cells we injected (cells taken from later stage cultures have reduced survival relative to progenitors isolated from early stage cultures), incorrect targeting (differences in cortical thickness between mouse strains may have caused our injections to enter the ventricles rather than the cortex), or the volume of solution that we injected. For our second experiment we injected at

only one time point (P1), bilaterally into the cortex with 100,000 cells per injection site. We are currently awaiting results from this experiment. If successful, this project will help us determine whether mESC-derived interneuron transplants have the potential to help human patients with SCN1A mutations. In addition, we will hopefully gain insight into whether PV-enriched, SST-enriched, or mixed cell transplants are more or less efficacious in mitigating seizure activity.

#### **4.5 Ongoing Studies and Future Directions for Understanding Zswim6 Function**

The data presented in this thesis suggest that Zswim6 plays an important role in brain development and function. However, there are many questions that remain to be addressed. As a schizophrenia candidate gene, it is important to determine whether Zswim6 acts predominately during embryonic development to regulate the production of forebrain derivatives or during postnatal periods to regulate the function of MSN and their associated circuits (or both). Although schizophrenia typically manifests in the late teens and early 20's, it is thought to have a strong developmental component that affects the formation of essential brain circuits. Zswim6 is expressed at high levels in the developing striatum and limbic regions, including the cortex. Postnatally, its expression becomes restricted to the striatum. Does Zswim6 function in progenitors to regulate the production of different neuronal subtypes? Or does it act as a transcriptional regulator in mature MSN to fine tune gene expression? The changes in morphology and spine density that we found on adult MSN and frontal cortex pyramidal neurons



begs the question as to whether those changes are also present during adolescence. If not, then this supports a predominantly later occurring phenotype that more closely mimics the biological changes that occur in the context of schizophrenia. We are currently measuring striatal volume and analyzing MSN/frontal cortex neuronal morphology on P21 mutants and controls. Another way we are addressing the time frame and neuronal circuits that Zswim6 predominantly functions in is by breeding our Zswim6 conditional line to several cre-recombinase expressing lines. These include the DRD1-cre and A2a-cre lines, which perturb Zswim6 expression in direct and indirect pathway MSN, respectively. These lines will not only enable us to determine whether loss of Zswim6 function in post-mitotic MSN is sufficient to recapitulate the behavioral changes found in our Zswim6 constitutive knockout, but which striatal subdomains are most important for Zswim6 function. Such an approach was recently used to understand the synaptic basis of repetitive behaviors observed in mice harboring mutations in the autism-associated gene neuroligin-3 (NL3)<sup>338</sup>. Despite NL3 being expressed throughout the brain, the authors showed that conditional loss of NL3 within D1-expressing MSN of the nucleus accumbens was sufficient to recapitulate the repetitive motor routines observed in NL3 mutant mice. On the contrary, loss of NL3 within D2-expressing MSN was insufficient to induce the behavioral phenotype<sup>338</sup>. If we discover that loss of Zswim6 within either of these circuits is capable of recapitulating our behavioral phenotypes, then we can further dissect which striatal subdomains are involved

through the use of adenoviral injections that either rescue or knockdown Zswim6 expression. For example, if we find that Zswim6 knockdown within D1-expressing MSN is capable of recapitulating our behavioral findings, then we can cross our Zswim6 constitutive knockout to the DRD1-cre line and inject an adenovirus that expresses Zswim6 in a cre-dependent fashion into different striatal subdomains to rescue the phenotype. Alternatively, we can inject a cre-recombinase expressing adenovirus into different striatal subdomains of Zswim6<sup>F1/F1</sup> mice to determine which regions are capable of recapitulating the phenotype. We have also started to breed our Zswim6 constitutive knockout to DRD1-tomato and DRD2-EGFP lines, which allow for the unambiguous identification of all major striatal cell types. We intend to use these lines to do whole cell voltage clamp recordings of MSN to explore how loss of Zswim6 function affects their excitatory and inhibitory synaptic parameters, as well as potential alterations in synaptic plasticity. Using these same lines, we can also FACS isolate mature DRD1- and DRD2-expressing MSN for gene profiling. If Zswim6 functions as a chromatin modifier, then we would expect to find changes in gene expression that correlate with changes in chromatin accessibility. Given that the striatum plays important roles in decision-making and reward processing, we hypothesize that loss of Zswim6 will cause additional phenotypes in the initiation or persistence of goal-directed actions, which are particularly affected in schizophrenia<sup>339,340</sup>. To test this, Zswim6 mutant mice will be subjected to an operant choice paradigm that enables us to determine whether Zswim6 mutants exhibit deficits in their ability to

use reinforcing stimuli (e.g. rewards) to reliably reinforce future behavior. In addition to behavioral experiments, it would be interesting to determine how Zswim6 functions on a biochemical level. To start, one might identify Zswim6 binding partners using mass spectrometry. Previous studies have found that Zswim6 is expressed in HEK293 cells<sup>294,301</sup>. Thus, while its binding partners in HEK293 cells may differ from those in the brain, we can still learn a great deal about the type of complexes it is capable of forming. Ultimately, we eventually want to determine whether Zswim6 function in mice is similar to its function in human. To do so, one might use CRISPR-Cas9 to inactivate Zswim6 in human stem cells, then differentiate these cells into distinct neuronal subtypes, including MSN, for which there are established differentiation protocols<sup>341,342</sup>.

At present, a shortcoming of this study is our inability to explain the reduction in MSN number that we observe in adult Zswim6 knockout mice. Although we did not find a decrease in proliferation at E14.5, this was the only age we analyzed. Measuring proliferation at other time points may reveal a subtle proliferation defect. Along the same vein, we only looked for apoptosis at P0, P21, and in adult. It is possible that MSN undergo apoptosis during a very narrow time window that we have missed in our analysis. It will be important to quantify MSN number using the aforementioned cre-recombinase lines to determine whether loss of MSN is due to a lack of production, apoptosis, or a combination of the two, as well to determine whether the decreased number of MSN contributes significantly the phenotypes we observe.

Another potential shortcoming of this study is the possibility of inner ear defects in Zswim6 mutant mice, since inner ear dysfunction has been shown to cause hyperactivity by inducing specific molecular changes in the striatum<sup>343</sup>. However, it is unclear whether hyperactivity due to inner ear defects is secondary to hearing loss, vestibular dysfunction, or a combination of the two. Zswim6 mutant mice do not exhibit circling behavior, a hallmark of vestibular dysfunction, suggesting that if they have inner ear dysmorphogenesis, it primarily affects their hearing ability. Zswim6 is expressed at low levels in many developing brain areas related to hearing, including the cochlear membrane, spiral ganglion cells, cochlear nucleus, thalamus, and auditory cortex (D.J. Epstein, V.E. Abraira, personal communication)<sup>293,325</sup>. Despite the widespread expression of Zswim6, its relative significance in these regions, if any, remains to be determined. For future studies, it will be important to determine whether Zswim6 mutant mice are indeed deaf. We will need to perform brainstem auditory evoked response testing (BAER) on a large (N=12-15) cohort of mice. In addition, we can also do BAER testing using various cre-recombinase expressing lines (e.g. nestin-cre) to perturb Zswim6 function in particular circuits. Such an analysis would help determine whether Zswim6 causes neural/sensorineural or conductive hearing loss, if at all.

# CHAPTER 5

## Materials and Methods

### 5.1 Materials and Methods for mESC Studies

#### *Mouse Embryonic Stem Cell Culture.*

Mouse ES cells (the JQ27 mESC-Nkx2.1::mCherry:Lhx6::GFP line) were grown on mouse embryonic fibroblasts (MEF CF-1 MITC7M, GSC-6101M, Global Stem) in standard mESC medium (knock-out DMEM (Invitrogen), 15% FBS (Invitrogen-Thermo Fisher Scientific), supplemented with L-glutamine, MEM nonessential amino acids,  $\beta$ -mercaptoethanol, and LIF (1.4ul/mL [107 U/mL] ESG1107, Millipore). To eliminate MEFs, mESCs were replated on a 0.1% gelatin coated plate for 1-2 days prior to differentiation.

#### *Telencephalic mESC Differentiation.*

For neural induction, mESCs were harvested and floated on non-tissue culture treated plates in a 1:1 mixture of KSR (10828-028, Invitrogen) and N2 media (DMEM:F12, 11330, Invitrogen, with N2 07156, Stemgent) supplemented with LDN-193189 (250nM, 04-0074, Stemgent) and XAV939 (10 $\mu$ M 04-0046, Stemgent) as described previously (Maroof et al 2010 & Watanabe et al., 2005). At differentiation day 3 (DD3), embryoid bodies (EBs) were enzymatically dissociated using Accutase (A1110501, Invitrogen) and single cells were replated onto poly-L-Lysine (P6282, Sigma)- and laminin (L2020, Sigma)-coated plates at (37,500 cells/cm<sup>2</sup>) in the same media supplemented with Y-27632 (10nM, 1254, Tocris). For the dorsal/ventral (D/V) patterning, cells were treated with KSR/N2 media supplemented with FGF-2 (10 ng/ml, DD5–9, 233-FB, R&D Systems), IGF1 (20 ng/ml, day 5–9, 291-G1-200/CF, R&D Systems) from DD5 to DD8. At DD8, cells were replated on PLL- and LN-coated plates at 200,000 cells/cm<sup>2</sup> and treated with KSR/N2 media supplemented with SAG (30 nM, EMD Biosciences, Inc.) and protein kinase C  $\zeta$  Inhibitor (PKCi) (2  $\mu$ M, EMD Biosciences, Inc.). Cells were cultured until DD11 and then processed for FACS or IHC. For DAPT experiments, DAPT was added to a final concentration of 10 $\mu$ M from DD10-12. Cells were then sorted on DD12 and transplanted.

### *Cell Sorting.*

Samples at DD11 or later were treated with Accutase (Invitrogen) for 15 min, centrifuged at 900 rpm for 5 min, and resuspended in Hiberante E (Invitrogen) supplemented with B27, glutamax, and Y-27632 (10nM, 1254, Tocris). After

filtration twice through a 40µm filter, samples were kept on ice until FACS (Aria II, BD Biosciences) and analyzed using FACS Diva software (Version 6.1.3).

#### *Cortical Transplantation.*

Transplantation of neural precursors into the somatosensory cortex of cooling-anesthetized neonatal pups was conducted as described previously (Maroof et al 2010 and Wonders et al., 2008). After sorting for Nkx2.1::mCherry progenitors, cells were resuspended in neurobasal medium (NBM) supplemented with Y-27632 (10 nM), glutamax, and B27 at 30,000 ~ 50,000 cells/µL. About 6 µL of cell suspension medium was bilaterally injected into the somatosensory cortex at the following coordinates from bregma (2.0 mm anterior, 2.5 mm lateral, 1.0 mm deep), targeting cortical layers 3–6 of CD1 pups at P0-2. Mice were perfused and analyzed 30 days post-transplant. Care of animals was in accordance with institutional guidelines at The Children's Hospital of Philadelphia.

#### *Immunohistochemistry.*

Samples were fixed in 4% paraformaldehyde in PBS and blocked in 5% BSA in 0.1% PBST. For antibodies requiring the use of antigen retrieval (mouse-Nkx2.1), samples were pretreated with 1mM EDTA in PBS for 5 min at 65°C. After washing, samples were incubated in primary antibodies, followed by secondary antibodies with DAPI for nuclear staining. Primary antibodies used were chicken anti-GFP (Abcam, ab13970; 1:1000), rabbit-Nkx2.1 (1:1000, Abcam ab76013), mouse anti-Nkx2.1 (Abcam, ab76013; 1:200), rabbit anti-PV

(Swant, PV-25; 1:2000), rat anti-SST (Millipore, 14224; 1:200), rabbit anti-GABA (Sigma-Aldrich, A2052; 1:1000), rabbit anti-Sox6 (Abcam, ab30455; 1:2000), rabbit anti-cyclinD2 (Santa Cruz, M-20, 1:5000), rabbit anti-Ki-67 (Thermo, RB-9043, 1:200), and rat anti-RFP antibody (Chromtek, 5F8; 1:400). Secondary antibodies were conjugated to Alexa fluorophores (488, 568 or 680, Invitrogen). EdU signals were detected with the Click-iT EdU Alexa Fluor 647 imaging kit (Invitrogen, Carlsbad, CA, USA).

#### *In Vivo Fate Quantification.*

30 days post-transplantation, mice were perfused and fixed with 4% paraformaldehyde in PBS. Fixed brains were sectioned in the coronal plane at 50 $\mu$ m on a vibrating microtome (Leica). To identify the fate of the transplanted cells, sections including somatosensory cortex, rostral to the hippocampal commissure and caudal to the genu of the corpus collosum, were incubated with the aforementioned antibodies. Generally, 12-15 sections were evaluated per marker. Transplanted animals were excluded if there were fewer than 25 total GFP+ cells present, and only GFP+ cells engrafted in cortical layers 2-6 were included in fate analysis. Each condition was repeated on 4 separate occasions, with a minimum of two transplanted mice per condition. Therefore, a statistical n represents counts from multiple transplants of one differentiation experiment. Statistical significance was determined using a two-tailed Student's t-test.



### *Live Imaging Analysis.*

At DD8, cells were replated on PLL- and LN-coated chamber slides (Nunc Lab-Tek II Chambered Coverglass #1.5 Borosilicate) at a density of 200,000 cells/cm<sup>2</sup>. Time-lapse images were acquired every 15 minutes over the course of 48 hours with an Olympus Fluoview (FV10i) confocal microscope at 37°C, 5% CO<sub>2</sub> at 10x magnification. T-stacks were compiled in ImageJ with GFP and mCherry channels pseudocolored green and red, respectively. Only cells that could be visualized throughout the entire imaging session were included in the daughter cell analysis. The percentage of daughter divisions was calculated as follows: % daughter division = # daughter divisions/(mCherry parent division + daughter division). At least 20 divisions were counted for each condition across five independent experiments. Statistical significance was determined using a two-tailed Student's t-test.

### *Cell Counting.*

For CD2, EdU, and Ki-67 co-expression analyses, multichannel stacks were generated in ImageJ. For each experiment, at least 500 clearly labeled Nkx2.1 or RFP cells were marked using the ImageJ cell counter plugin. After marking, these cells were examined for CD2, EdU, or Ki-67 co-expression by alternating between channels. Each condition was repeated on at least 3 separate occasions. Statistical significance was determined using a two-tailed Student's t-test.

## 5.2 Materials and Methods for Zswim5 and Zswim6 Studies

### *Mouse Lines*

This study was carried out in strict accordance with the recommendations in the Guide for the Care and Use of Laboratory Animals of the National Institutes of Health. The protocol was approved by the Institutional Animal Care and Use Committee at The Children's Hospital of Philadelphia (Protocol Number: 2012-4-1004). ABR measurements were performed under anesthesia (ketamine (100mg/kg)/xylazine (10mg/kg) cocktail). Adult mice were euthanized by isoflurane overdose, followed by cervical dislocation. All efforts were made to minimize suffering. Behavioral experiments were performed during the first 3 hours of the light phase (7:00-11:00am) and animals were allowed to acclimate to the procedure room for at least 15 minutes before beginning experiments. Primers used for genotyping animals and for generating in situ hybridization probes are summarized in (**Table 5.1**).

**Table 5.1. List of primers used in this study.**

Mouse lines	Primer Name	Sequence	Floxed Allele	WT Allele	KO or Cre Allele	Purpose
Zswim6	Z6-3G-FWD	catggaagtacttgggtccga	893	716	~300	Genotyping
	Z6-3G-REV	ttctccatgtgggaaaactagaaag	893	716	~300	Genotyping
	DelExonP1-F	TGGCCATCAGCTTTGATCGT		328	no band	Confirm KO
	DelExonP1-R	TCGTCAATACTAGCACCCGC		328	no band	Confirm KO
	3'UTR_ISH-F	tacattacgcctttgcagtg		524		ISH
	3'UTR_ISH-R	ACATGAGTGAAGAAGTACAACC		524		ISH
	Exon3-5_F	GCAAGCCAGAGCAGGTCAAAC		478		ISH
	Exon3-5_R	TCATCCCAGAGCTGCCTATACTTG		478		ISH
	Zswim5	Z5-2G-FWD	atgccgtggaatgtagaacagat	1031	846	~380
Z5-2G-REV		ctgatttcgaggctgggctta	1031	846	~380	Genotyping
DelExonP1-F		CGGCTGTGGGAATAAGGACA		369	no band	Confirm KO
DelExonP1-R		CCCCAATGATACCGAGACC		369	no band	Confirm KO
3'UTR_ISH_F		TCAGGACAAGGACTCTGAAAC		550		ISH
3'UTR_ISH_R		ATCTTCAGGCCACAGTTTCTG		550		ISH
Exon2-4_F		GAGCCAGCAGTGACTTACAAGG		504		ISH
Exon2-4_R		cctggctccattagaatctctc		504		ISH
Exon5-8_F		GGATGGAAACTATGGGCATGAG		484		ISH
Exon5-8_R		CAAAGTGAGAAACAGGCAGCCAA		484		ISH
Nkx2.1-Cre	P1	CCACAGGCACCCACAAAAATG		no band	666	Genotyping
	P2	GCCTGGCGATCCCTGAACAT		no band	666	Genotyping
KOMP-Zswim5	CSD-F	tgtagaagatgctggaattgtgc		~420	~270	Genotyping
	Exon2REV	GTTGATTTCTGAGTTGGAGGAC		~420	~270	Genotyping
	Lar3	cacaacgggttcttctgtaagtcc		~420	~270	Genotyping

We worked with Ingenious Targeting Laboratories (Ronkonkoma, New York, USA) to make the Zswim5 and Zswim6 conditional knockouts. For Zswim6, a 13.75-kb Zswim6 genomic fragment was subcloned from a C57BL/6 BAC clone to construct the targeting vector using homologous recombination. A FRT-LoxP-Neo-FRT-LoxP cassette was inserted downstream of exon 4 and the third single LoxP site was inserted upstream of exon 4. The region flanked by the second and third LoxP sites is approximately 569bp. Exon 4 encodes amino acids 337-386 and its deletion causes an early stop. The short homology arm extends 2.1kb to the 3' end of the FRT-LoxP-Neo-FRT-LoxP cassette, whereas the long homology arm extends 5.1kb from the 5' side of the third loxP site. The linearized

targeting vector was then electroporated into iTL BA1(C57BL/6X129/SvEv) hybrid embryonic stem cells.

A 16.64kb genomic fragment of the *Zswim5* gene was used to construct the targeting vector. A FRT-LoxP-Neo-FRT-LoxP cassette was inserted downstream of exon 3 and the third single LoxP site was inserted upstream of exon 3. The first and second LoxP sites thus flank a 620bp genomic region that includes exon 3. Exon 3 encodes amino acids 321-370 and its deletion causes an early stop. The short homology arm extended 3.6kb to the first LoxP site and the long homology arm extended 6.4kb downstream of the LoxP-Neo-LoxP cassette.

Targeted embryonic stem cells were microinjected into C57BL/6 blastocysts. Resulting chimeras with a high percentage agouti coat color were mated to C57BL/6 FLP mice to remove the Neo cassette. Heterozygous mice confirmed for somatic neo deletion were then bred to wild type C57 mice to remove the FLP transgene. To generate germline null alleles, *Zswim5*<sup>+/-</sup> and *Zswim6*<sup>+/-</sup> mice were bred to CMV-cre mice (The Jackson Laboratory Stock NO: 006054) to generate *Zswim5*<sup>+/-</sup> and *Zswim6*<sup>+/-</sup> animals.

#### *Tissue Preparation for Immunohistochemistry*

Following euthanasia with isoflurane, mice were perfused with 4% paraformaldehyde (PFA) in PBS and post-fixed in 4% PFA overnight. Brains were then embedded in 4% low-melting-point agarose, cut in 50µm sections with a vibrating microtome (Leica), and stored in antifreeze solution (30% ethylene

glycol and 30% glycerol in 1x PBS) at -20°C until processing. Embryonic samples for in situ RNA hybridization and immunohistochemistry were processed identically (see section *Tissue Preparation for In Situ RNA Hybridization* below)

### *Immunohistochemistry*

Brain sections were pre-incubated for one hour in blocking buffer (5% bovine serum albumin with 0.1% Triton-X-100). Sections were then incubated overnight at 4°C with the following primary antibodies: rabbit anti-PV (Swant, PV-25; 1:2000), rat anti-SST (Millipore, 14224; 1:200), rat anti-CTIP2 (Abcam, ab18465, 1:500), goat anti-ChAT (Chemicon, ab144P, 1:200), rabbit anti-phospho-Histone H3 (Millipore, 06-570, 1:400), rabbit anti-cyclinD2 (Santa Cruz, M-20, 1:5000), rabbit anti-DARPP32 (Abcam, ab40801, 1:1000), mouse anti-TH (Millipore, MAB318, 1:200). Secondary antibodies were conjugated to Alexa fluorophores (488, 568 or 680, Invitrogen). DAPI (300nM) was applied concurrently with secondary antibodies to label cell nuclei. EdU signals were detected with the Click-iT EdU Alexa Fluor 647 imaging kit (Invitrogen, Carlsbad, CA, USA).

### *Cell Counting*

Stereological analysis for CTIP2 was conducted on a Nikon E600 microscope equipped with a motorized stage and Stereoinvestigator software (MicroBrightField). CTIP2 cell counts were obtained using the Optical Fractionator Probe and systematic random sampling at 40x magnification. Optical dissector frame and counting grid sizes of 60µm x 60µm and 700µm x

700 $\mu$ m, respectively, were used. Striatal contours were delineated as described by Franklin and Paxinos (2008). Starting from the genu of the corpus callosum, every 5<sup>th</sup> section was evaluated for a total of 6 sections.

For PV, SST, and ChAT cell counts, 10x montages of entire brain sections were generated using Stereoinvestigator's Virtual Tissue module. Starting from the genu of the corpus callosum, every 5<sup>th</sup> section was imaged for a total of 6 sections. Images were opened using ImageJ and the striatum was delineated as described by Franklin and Paxinos (2008). Using the ImageJ cell counter plugin, striatal interneurons from each brain section were counted and then summated. Statistical significance was determined using a two-tailed Student's t-test.

For PH3 and EdU counts, image stacks were opened in ImageJ and three 120 $\mu$ m x 120 $\mu$ m boxes were drawn beginning at the apical surface and extending outward from LGE along a line that was approximately equidistant from the pallial-subpallial angle and MGE-LGE sulcus (as shown in **Figure 3.20**).

#### *Volumetric Analyses and Surface Area*

Volumetric analyses were done using the Cavalieri estimator on Stereoinvestigator (MicroBrightField). We used a total of 11, 50 $\mu$ m thick sections in our analysis, where section 3 of 11 along the rostrocaudal axis corresponded to the first section in which the genu of the corpus callosum could be identified, and used every 5<sup>th</sup> section from that point. Cortical contours were drawn using the pial surface as the outside boundary and terminated laterally at a point that

was perpendicular to the midline. For surface area analyses, we took overhead images of adult brains using a dissection microscope fitted with a digital camera. Images were then opened in ImageJ and analyzed using the area measure tool. Statistical significance for volumetric and surface area analyses were determined using a two-tailed Student's t-test.

#### *Quantitative PCR (qPCR) Analysis*

Following euthanasia with isoflurane, Zswim6 mice were decapitated and their brains rapidly dissected. Brains were then sectioned at 400 $\mu$ m in ice cold PBS using a vibrating microtome. Dorsal striatum was carefully dissected and placed in TRIzol reagent (Invitrogen) for RNA extraction using the PureLink RNA Mini kit (Invitrogen). cDNA was synthesized using the VILO cDNA synthesis kit (Invitrogen). qPCR was conducted using Taqman Gene Expression Assays (Applied Biosystems). Each sample was run in triplicate, along with probes for GAPDH on the same plate, on a Stratagene MX3005P real-time PCR machine (La Jolla, CA) following the manufacturer's recommended protocol. Data were analyzed using the comparative  $C_T$  method. Statistical significance was determined using a two-tailed Student's t-test.

#### *Golgi-Cox Staining and Neuron Reconstruction*

Golgi-Cox staining was performed using the FD Rapid GolgiStain kit (FD NeuroTechnologies). Brains were incubated in a potassium dichromate solution for 2 weeks in the dark, then with silver nitrate for another two days before being

cut into 150µm sections with a vibrating microtome (Leica). Golgi staining was then performed on slides. Cell bodies and dendrites of striatal MSN and layer 3 cortical pyramidal neurons from each group were traced and analyzed using Neurolucida (MicroBrightField). Only MSN within the dorsal striatum were traced. We delineated medial frontal cortex as the region bounded dorsolaterally by motor cortex extending along the midline from 2.65mm-2.09mm rostral to Bregma as defined in Franklin and Paxinos (2008). We considered somatomotor cortex to encompass a 500µm region on either side of the boundary between primary motor and somatosensory cortices extending from the genu of the corpus callosum to where the anterior commissure connects at the midline, using as reference Franklin and Paxinos (2008). Morphological differences were analyzed using a two-tailed Student's t-test. For Sholl analyses, a two-way ANOVA was used to determine significance using Prism 5 (GraphPad).

#### *B-Galactosidase Staining*

Embryos were flash frozen in liquid nitrogen, sectioned at 12µm using a cryostat, and stored at -80°C. On the day of staining, the sections were fixed for 5 minutes in 0.2% glutaraldehyde, 2% formalin, 5mM EGTA and 2mM MgCl<sub>2</sub> in 0.1M phosphate buffer (pH 7.3) for 4 hours. They were then washed three times in rinse buffer (0.1% sodium deoxycholate, 0.2% IGEPAL, 2mM MgCl<sub>2</sub> in 0.1M phosphate buffer (pH 7.3) and incubated in the dark at 37°C in staining solution (1 mg/ml Salmon gal (Lab Scientific) and 0.4 mM 5-bromo-4-chloro-3-indolyl phosphate (TNBT) in rinse solution). The reaction was monitored every 10



minutes to determine the onset of staining (approximately 1 hour) and then quenched using 4% PFA in 1x PBS for 10 minutes.

### *Spine Density Analysis*

For spine quantification, dendrites were traced using Neurolucida (MicroBrightField) and divided into 10 $\mu$ m segments using a 100x oil-immersion objective. For each analysis, we counted spines from a minimum of 10 neurons from each animal. For MSN, we counted spine density at a distance of 60-150 $\mu$ m from the soma and analyzed a minimum of 40 $\mu$ m from each neuron; both primary and secondary dendrites were included. A total of 2400 $\mu$ m of dendrite were analyzed from each group and the reported average is the spine density for each group between 60-150 $\mu$ m. For layer 3 pyramidal neurons, spine quantification was done on the basilar dendrites at a distance of 10-110 $\mu$ m from the soma with a minimum of 50 $\mu$ m analyzed from each neuron. A total of 3000 $\mu$ m of dendrite was analyzed from each group. Statistical significance was determined using a one-tailed Student's t-test, where each data point represented the average number of spines per 10 $\mu$ m for the dendritic range (e.g. 60-150 $\mu$ m for MSN) that we analyzed.

### *Tissue Preparation for In Situ RNA Hybridization*

For embryonic samples, embryos were fixed overnight at 4°C in RNase-free 4% PFA in 1x PBS. Embryos were then washed two times in 1x PBS and cryoprotected by immersion through sucrose (15 and 30% sucrose in 1x PBS;

solutions were changed once embryos had sunk). Afterwards they were embedded in freezing compound and stored at -80°C until sectioning. For adult samples, mice were perfused with 4% PFA in 1x PBS and post-fixed in 4% PFA overnight. Brains were then embedded in 4% low-melting-point agarose, cut in 50µm sections with a vibrating microtome (Leica), and stored in antifreeze solution (30% ethylene glycol and 30% glycerol in 1x PBS) at -20°C until processing. On the day of in situ hybridization, sections were mounted onto Superfrost Plus slides (Fisher Scientific, Pittsburgh, PA) and allowed to dry at room temperature for 2 hours before processing.

#### *In Situ RNA Hybridization*

We generated cDNA templates for riboprobe synthesis for Zswim5 and Zswim6 by nested PCR incorporation of T7 and Sp6 RNA polymerase promoters using the primers listed in (**Table 5.1**). Template cDNA was obtained from E13.5 mouse brain. cDNA plasmids for DRD1 and DRD2 were gifts from Kenneth Campbell. Following incubation in prehybridization buffer for 2 hours at 60°C, sections were incubated with digoxigenin-labeled riboprobes for 16 hours at 58°C. After rinsing, sections were incubated with an alkaline phosphatase conjugated sheep anti-digoxigenin antibody (Roche, 1:2000) in blocking buffer at 4°C for 16 hours and developed in nitroblue tetrazolium/5-bromo-4-chloro-3-indolyl phosphate solution (7µl/ml in 10% polyvinyl alcohol; Roche) in the dark for 12-48 hours. Fresh developing solution was exchanged every 24 hours. After developing, material was rinsed, and alkaline phosphatase activity was quenched

by fixation in 4% PFA containing 0.125% glutaraldehyde. Sections were then rinsed, cleared in 50% glycerol in 1x PBS, and mounted using aqueous mounting media.

#### *Brainstem Auditory Evoked Response (BAER) Testing*

BAER testing was done in collaboration with Maria Geffen's lab at the University of Pennsylvania as described in<sup>344</sup>.

#### *Rotarod*

For high speed rotarod performance testing a five-station Rotarod treadmill (IITC) was used. Rotarod testing consisted of three trials per day over the course of 4 days. Days 1 and 2 consisted of 4-40rpm trials over a 300 second period with a constant rate of acceleration. Days 3 and 4 consisted of 8-80rpm trials over a 300 second period. A trial was terminated when a mouse fell off, made one complete backward revolution while hanging on, or after 300 seconds (maximum speed, no further acceleration). On day 1, mice were allowed to acclimate to the rod for 1 minute before beginning the first trial. On each testing day, mice were left in the room for 15 minutes to acclimate before testing. The machine was wiped down with 70% ethanol in between each trial. Groups were compared using the Mann-Whitney U test.

#### *Open Field*

Locomotor activity was assessed with the automated Photobeam Activity System

(San Diego Instruments). After acclimating to the room for 15 minutes, mice were individually placed in a 16 x 16 inch arena outfitted with photocells to detect horizontal and rearing activities over the course of 10 minutes. The arena was cleaned with 70% ethanol in between trials. For amphetamine-sensitivity testing, mice were placed in the open field arena for 30 minutes before being injected with either a 2 mg/kg D-amphetamine hemisulfate salt (Sigma) solution prepared in isotonic saline at a concentration of 0.2 mg/ml or isotonic saline as control. Immediately after injection, mice were placed back into the arena for an additional 1 hour. For the 10 min open field sessions, both groups were compared using a one-tailed Student's t test (paired). For the amphetamine-sensitivity testing, the effect of amphetamine on ambulation was determined using a two-way mixed regression analysis performed in Stata.

#### *Elevated Zero Maze*

Mice were individually placed on a 2.5 inch wide circular track with an external diameter of 20 inches, raised 24 inches above the floor (San Diego Instruments). The track had two open and two walled quadrants of equal dimensions. Mice were placed in the center of a closed quadrant to begin a 5 min trial. A highly trained scorer, blind to group designation, graded the digitally recorded trials for time spent in the open quadrants. Mice were scored as within a segment when all four paws were within that segment. Transitions between quadrants were also noted as a measure of general locomotor activity. Groups were compared using a two-tailed Student's t test (paired).

## Force Plate Actometer

Force-plate actometer assays<sup>345,346</sup> were performed using standard approaches. Each trial was 45 minutes in length.

## *Co-immunoprecipitation and Western Blot*

The coding sequence for Brg1 was subcloned from pMX-Brg1 (Addgene plasmid #25855) into a plasmid containing 3 sequential HA tags (Addgene plasmid #12555). Zswim6 was cloned from cDNA obtained from E13.5 embryonic brain and subcloned into a Myc-tag containing plasmid (Addgene plasmid #19400). Both plasmids were transfected into HEK293 cells using Lipofectamine 2000 (Invitrogen). 48 hours post-transfection, cells were lysed in a low-stringency buffer (50mM NaCl, 1mM MgCl<sub>2</sub>) on ice for 20 min, followed by 4 seconds of low-power sonication, and then centrifuged for 5 min at max speed at 4°C. Supernatants were then incubated with either anti-HA (Thermo Cat #88836) or anti-Myc magnetic beads (Thermo Cat #88844) for 100 minutes at room temperature. Beads were then washed two times with lysis buffer followed by one wash with ddH<sub>2</sub>O. Bound proteins were eluted by heating the beads to 95°C in sample loading buffer containing DTT. The control indicates co-immunoprecipitation with nonreactive, non-antibody tagged magnetic beads (Thermo Cat #88826). Samples were then run on 4-12% Bolt™ Bis-Tris gels using the Bolt™ Mini Gel Tank and transferred onto nitrocellulose membranes using the iBlot Transfer System. After transfer, blots were allowed to dry for one

hour before rehydration in 1x TBS. Blots were incubated in Odyssey Blocking Buffer in TBS for 1 hour then incubated overnight at 4°C with anti-Myc (Thermo, MA1-980, 1:1000) or anti-HA (Cell Signaling, #3724, 1:1000) antibodies. The next day, blots were washed 3 times for 10 minutes in TBS with 0.1% Tween-20 and then incubated with IRDye 800CW secondary antibodies (1:10,000). Blots were washed 3 times for 10 minutes in TBS with 0.1% Tween-20 and then imaged using the Li-COR imaging system.

#### *Nuclear-Cytoplasmic Fractionation*

Recombinant myc-Zswim5 was expressed in HEK293 cells using Lipofectamine 2000 (Invitrogen). 48 hours post-transfection, HEK293 cells were collected for nuclear-cytoplasmic fractionation using the NE-PER Nuclear and Cytoplasmic Extraction Kit (ThermoFisher). Equal amounts of nuclear and cytoplasmic fractions were then run on western blot using the aforementioned protocol.

## REFERENCES

- 1 Wang, Z. *et al.* The EBAX-type Cullin-RING E3 ligase and Hsp90 guard the protein quality of the SAX-3/Robo receptor in developing neurons. *Neuron* **79**, 903-916, doi:10.1016/j.neuron.2013.06.035 (2013).
- 2 Rakic, P. Specification of cerebral cortical areas. *Science* **241**, 170-176 (1988).
- 3 Tomassy, G. S., Lodato, S., Trayes-Gibson, Z. & Arlotta, P. Development and regeneration of projection neuron subtypes of the cerebral cortex. *Sci Prog* **93**, 151-169 (2007).
- 4 Molyneaux, B. J., Arlotta, P., Menezes, J. R. & Macklis, J. D. Neuronal subtype specification in the cerebral cortex. *Nature reviews. Neuroscience* **8**, 427-437, doi:10.1038/nrn2151 (2007).
- 5 Petroff, O. A. GABA and glutamate in the human brain. *The Neuroscientist : a review journal bringing neurobiology, neurology and psychiatry* **8**, 562-573 (2002).
- 6 Trevelyan, A. J. & Watkinson, O. Does inhibition balance excitation in neocortex? *Progress in biophysics and molecular biology* **87**, 109-143, doi:10.1016/j.pbiomolbio.2004.06.008 (2005).
- 7 Utter, A. A. & Basso, M. A. The basal ganglia: an overview of circuits and function. *Neurosci Biobehav Rev* **32**, 333-342, doi:10.1016/j.neubiorev.2006.11.003 (2008).
- 8 Rektor, I., Bockova, M., Chrastina, J., Rektorova, I. & Balaz, M. The modulatory role of subthalamic nucleus in cognitive functions - a viewpoint. *Clin Neurophysiol* **126**, 653-658, doi:10.1016/j.clinph.2014.10.156 (2015).
- 9 Smith, Y., Raju, D. V., Pare, J. F. & Sidibe, M. The thalamostriatal system: a highly specific network of the basal ganglia circuitry. *Trends Neurosci* **27**, 520-527, doi:10.1016/j.tins.2004.07.004 (2004).
- 10 Kemp, J. M. & Powell, T. P. The cortico-striate projection in the monkey. *Brain* **93**, 525-546 (1970).
- 11 Bolam, J. P., Hanley, J. J., Booth, P. A. & Bevan, M. D. Synaptic organisation of the basal ganglia. *J Anat* **196 ( Pt 4)**, 527-542 (2000).
- 12 Kreitzer, A. C. & Malenka, R. C. Striatal plasticity and basal ganglia circuit function. *Neuron* **60**, 543-554, doi:10.1016/j.neuron.2008.11.005 (2008).
- 13 Parent, A. Extrinsic connections of the basal ganglia. *Trends Neurosci* **13**, 254-258 (1990).
- 14 Gerfen, C. R. The neostriatal mosaic: multiple levels of compartmental organization in the basal ganglia. *Annu Rev Neurosci* **15**, 285-320, doi:10.1146/annurev.ne.15.030192.001441 (1992).
- 15 Gerfen, C. R. The neostriatal mosaic: compartmentalization of corticostriatal input and striatonigral output systems. *Nature* **311**, 461-464 (1984).

- 16 Gerfen, C. R. The neostriatal mosaic. I. Compartmental organization of projections from the striatum to the substantia nigra in the rat. *J Comp Neurol* **236**, 454-476, doi:10.1002/cne.902360404 (1985).
- 17 Herkenham, M. & Pert, C. B. Mosaic distribution of opiate receptors, parafascicular projections and acetylcholinesterase in rat striatum. *Nature* **291**, 415-418 (1981).
- 18 Graybiel, A. M. & Ragsdale, C. W., Jr. Histochemically distinct compartments in the striatum of human, monkeys, and cat demonstrated by acetylthiocholinesterase staining. *Proceedings of the National Academy of Sciences of the United States of America* **75**, 5723-5726 (1978).
- 19 Hebert, J. M. & Fishell, G. The genetics of early telencephalon patterning: some assembly required. *Nature reviews. Neuroscience* (2008).
- 20 Houart, C. *et al.* Establishment of the telencephalon during gastrulation by local antagonism of Wnt signaling. *Neuron* **35**, 255-265 (2002).
- 21 Gutin, G. *et al.* FGF signalling generates ventral telencephalic cells independently of SHH. *Development* **133**, 2937-2946 (2006).
- 22 Shimamura, K. & Rubenstein, J. L. Inductive interactions direct early regionalization of the mouse forebrain. *Development* **124**, 2709-2718 (1997).
- 23 Storm, E. E. *et al.* Dose-dependent functions of Fgf8 in regulating telencephalic patterning centers. *Development* **133**, 1831-1844 (2006).
- 24 Shimamura, K., Martinez, S., Puelles, L. & Rubenstein, J. L. Patterns of gene expression in the neural plate and neural tube subdivide the embryonic forebrain into transverse and longitudinal domains. *Developmental Neuroscience* **19**, 88-96 (1997).
- 25 Martynoga, B., Morrison, H., Price, D. J. & Mason, J. O. Foxg1 is required for specification of ventral telencephalon and region-specific regulation of dorsal telencephalic precursor proliferation and apoptosis. *Dev Biol* **283**, 113-127, doi:10.1016/j.ydbio.2005.04.005 (2005).
- 26 Fuccillo, M., Rallu, M., McMahon, A. P. & Fishell, G. Temporal requirement for hedgehog signaling in ventral telencephalic patterning. *Development* **131**, 5031-5040 (2004).
- 27 Rallu, M. *et al.* Dorsoventral patterning is established in the telencephalon of mutants lacking both Gli3 and Hedgehog signaling. *Development* **129**, 4963-4974 (2002).
- 28 Gunhaga, L. *et al.* Specification of dorsal telencephalic character by sequential Wnt and FGF signaling. *Nat Neurosci* **6**, 701-707, doi:10.1038/nn1068 (2003).
- 29 Shimogori, T., Banuchi, V., Ng, H. Y., Strauss, J. B. & Grove, E. A. Embryonic signaling centers expressing BMP, WNT and FGF proteins interact to pattern the cerebral cortex. *Development* **131**, 5639-5647, doi:10.1242/dev.01428 (2004).



- 30 Corbin, J. G., Rutlin, M., Gaiano, N. & Fishell, G. Combinatorial function of  
the homeodomain proteins Nkx2.1 and Gsh2 in ventral telencephalic  
patterning. *Development* **130**, 4895-4906 (2003).
- 31 O'Leary, D. D., Chou, S. J. & Sahara, S. Area patterning of the  
mammalian cortex. *Neuron* **56**, 252-269,  
doi:10.1016/j.neuron.2007.10.010 (2007).
- 32 Hansen, D. V. *et al.* Non-epithelial stem cells and cortical interneuron  
production in the human ganglionic eminences. *Nature neuroscience* **16**,  
1576-1587, doi:10.1038/nn.3541 (2013).
- 33 Ma, T. *et al.* Subcortical origins of human and monkey neocortical  
interneurons. *Nature neuroscience* **16**, 1588-1597, doi:10.1038/nn.3536  
(2013).
- 34 Treiman, D. M. GABAergic mechanisms in epilepsy. *Epilepsia* **42 Suppl 3**,  
8-12 (2001).
- 35 Cobos, I. *et al.* Mice lacking Dlx1 show subtype-specific loss of  
interneurons, reduced inhibition and epilepsy. *Nat Neurosci* **8**, 1059-1068  
(2005).
- 36 Inan, M., Petros, T. J. & Anderson, S. A. Losing your inhibition: Linking  
cortical GABAergic interneurons to schizophrenia. *Neurobiol Dis* **53**, 36-  
48, doi:10.1016/j.nbd.2012.11.013 (2013).
- 37 Belforte, J. E. *et al.* Postnatal NMDA receptor ablation in corticolimbic  
interneurons confers schizophrenia-like phenotypes. *Nat Neurosci* **13**, 76-  
83, doi:10.1038/nn.2447 (2010).
- 38 Chao, H. T. *et al.* Dysfunction in GABA signalling mediates autism-like  
stereotypies and Rett syndrome phenotypes. *Nature* **468**, 263-269 (2010).
- 39 Anderson, S. A., Eisenstat, D. D., Shi, L. & Rubenstein, J. L. Interneuron  
migration from basal forebrain to neocortex: dependence on Dlx genes.  
*Science* **278**, 474-476 (1997b).
- 40 Wonders, C. P. & Anderson, S. A. The origin and specification of cortical  
interneurons. *Nature reviews. Neuroscience* **7**, 687-696,  
doi:10.1038/nrn1954 (2006).
- 41 Marin, O. Cellular and molecular mechanisms controlling the migration of  
neocortical interneurons. *The European journal of neuroscience* **38**, 2019-  
2029, doi:10.1111/ejn.12225 (2013).
- 42 Tanaka, D. H. & Nakajima, K. Migratory pathways of GABAergic  
interneurons when they enter the neocortex. *The European journal of  
neuroscience* **35**, 1655-1660, doi:10.1111/j.1460-9568.2012.08111.x  
(2012).
- 43 Wonders, C. & Anderson, S. A. Cortical interneurons and their origins.  
*Neuroscientist* **11**, 199-205 (2005).
- 44 Xu, Q., Tam, M. & Anderson, S. A. Fate mapping Nkx2.1-lineage cells in  
the mouse telencephalon. *J Comp Neurol* **506**, 16-29 (2008).

- 45 Butt, S. J. *et al.* The requirement of Nkx2-1 in the temporal specification of cortical interneuron subtypes. *Neuron* **59**, 722-732, doi:S0896-6273(08)00630-2 [pii]  
10.1016/j.neuron.2008.07.031 (2008).
- 46 Butt, S. J. *et al.* Transcriptional regulation of cortical interneuron development. *The Journal of neuroscience : the official journal of the Society for Neuroscience* **27**, 11847-11850 (2007).
- 47 Butt, S. J. *et al.* The temporal and spatial origins of cortical interneurons predict their physiological subtype. *Neuron* **48**, 591-604 (2005).
- 48 Miyoshi, G. *et al.* Genetic fate mapping reveals that the caudal ganglionic eminence produces a large and diverse population of superficial cortical interneurons. *The Journal of neuroscience : the official journal of the Society for Neuroscience* **30**, 1582-1594, doi:30/5/1582 [pii]  
10.1523/JNEUROSCI.4515-09.2010 (2010).
- 49 Xu, Q., Cobos, I., De La Cruz, E., Rubenstein, J. L. & Anderson, S. A. Origins of cortical interneuron subtypes. *The Journal of neuroscience : the official journal of the Society for Neuroscience* **24**, 2612-2622 (2004).
- 50 Hernandez-Miranda, L. R., Parnavelas, J. G. & Chiara, F. Molecules and mechanisms involved in the generation and migration of cortical interneurons. *ASN neuro* **2**, e00031, doi:10.1042/AN20090053 (2010).
- 51 Wichterle, H., Turnbull, D. H., Nery, S., Fishell, G. & Alvarez-Buylla, A. In utero fate mapping reveals distinct migratory pathways and fates of neurons born in the mammalian basal forebrain. *Development* **128**, 3759-3771 (2001).
- 52 Nery, S., Fishell, G. & Corbin, J. G. The caudal ganglionic eminence is a source of distinct cortical and subcortical cell populations. *Nat Neurosci* **5**, 1279-1287 (2002).
- 53 Faux, C., Rakic, S., Andrews, W. & Britto, J. M. Neurons on the move: migration and lamination of cortical interneurons. *Neuro-Signals* **20**, 168-189, doi:10.1159/000334489 (2012).
- 54 Tamamaki, N., Fujimori, K. E. & Takauji, R. Origin and route of tangentially migrating neurons in the developing neocortical intermediate zone. *The Journal of neuroscience : the official journal of the Society for Neuroscience* **17**, 8313-8323 (1997).
- 55 Parnavelas, J. G. *et al.* The contribution of the ganglionic eminence to the neuronal cell types of the cerebral cortex. *Novartis Found Symp* **228**, 129-139; discussion 139-147 (2000).
- 56 Marin, O., Yaron, A., Bagri, A., Tessier-Lavigne, M. & Rubenstein, J. L. Sorting of striatal and cortical interneurons regulated by semaphorin-neuropilin interactions. *Science* **293**, 872-875 (2001).
- 57 Lodato, S. *et al.* Excitatory projection neuron subtypes control the distribution of local inhibitory interneurons in the cerebral cortex. *Neuron* **69**, 763-779, doi:10.1016/j.neuron.2011.01.015 (2011).

- 58 Taniguchi, H. Genetic dissection of GABAergic neural circuits in mouse  
neocortex. *Front Cell Neurosci* **8**, 8, doi:10.3389/fncel.2014.00008 (2014).
- 59 DeFelipe, J. *et al.* New insights into the classification and nomenclature of  
cortical GABAergic interneurons. *Nature reviews. Neuroscience* **14**, 202-  
216, doi:10.1038/nrn3444 (2013).
- 60 Flames, N. & Marin, O. Developmental mechanisms underlying the  
generation of cortical interneuron diversity. *Neuron* **46**, 377-381 (2005).
- 61 Binaschi, A., Bregola, G. & Simonato, M. On the role of somatostatin in  
seizure control: clues from the hippocampus. *Reviews in the  
neurosciences* **14**, 285-301 (2003).
- 62 Levitt, P., Eagleson, K. L. & Powell, E. M. Regulation of neocortical  
interneuron development and the implications for neurodevelopmental  
disorders. *Trends Neurosci* **27**, 400-406 (2004).
- 63 Jiang, Z., Cowell, R. M. & Nakazawa, K. Convergence of genetic and  
environmental factors on parvalbumin-positive interneurons in  
schizophrenia. *Frontiers in behavioral neuroscience* **7**, 116,  
doi:10.3389/fnbeh.2013.00116 (2013).
- 64 Smith-Hicks, C. L. GABAergic dysfunction in pediatric neuro-  
developmental disorders. *Frontiers in cellular neuroscience* **7**, 269,  
doi:10.3389/fncel.2013.00269 (2013).
- 65 Monyer, H. & Markram, H. Interneuron Diversity series: Molecular and  
genetic tools to study GABAergic interneuron diversity and function.  
*Trends Neurosci* **27**, 90-97 (2004).
- 66 Petilla Interneuron Nomenclature, G. *et al.* Petilla terminology:  
nomenclature of features of GABAergic interneurons of the cerebral  
cortex. *Nature reviews. Neuroscience* **9**, 557-568, doi:10.1038/nrn2402  
(2008).
- 67 Taniguchi, H., Lu, J. & Huang, Z. J. The spatial and temporal origin of  
chandelier cells in mouse neocortex. *Science* **339**, 70-74,  
doi:10.1126/science.1227622 (2013).
- 68 Tamamaki, N. *et al.* Green fluorescent protein expression and  
colocalization with calretinin, parvalbumin, and somatostatin in the  
GAD67-GFP knock-in mouse. *The Journal of comparative neurology* **467**,  
60-79, doi:10.1002/cne.10905 (2003).
- 69 Xu, X., Roby, K. D. & Callaway, E. M. Immunochemical characterization of  
inhibitory mouse cortical neurons: three chemically distinct classes of  
inhibitory cells. *J Comp Neurol* **518**, 389-404 (2010).
- 70 Kawaguchi, Y. & Kubota, Y. GABAergic cell subtypes and their synaptic  
connections in rat frontal cortex. *Cereb Cortex* **7**, 476-486 (1997).
- 71 Karson, M. A., Tang, A. H., Milner, T. A. & Alger, B. E. Synaptic cross talk  
between perisomatic-targeting interneuron classes expressing  
cholecystokinin and parvalbumin in hippocampus. *The Journal of  
neuroscience : the official journal of the Society for Neuroscience* **29**,  
4140-4154, doi:10.1523/JNEUROSCI.5264-08.2009 (2009).

- 72 Gibson, J. R., Beierlein, M. & Connors, B. W. Two networks of electrically coupled inhibitory neurons in neocortex. *Nature* **402**, 75-79, doi:10.1038/47035 (1999).
- 73 Tamas, G., Buhl, E. H., Lorincz, A. & Somogyi, P. Proximally targeted GABAergic synapses and gap junctions synchronize cortical interneurons. *Nat Neurosci* **3**, 366-371 (2000).
- 74 Kim, T. *et al.* Cortically projecting basal forebrain parvalbumin neurons regulate cortical gamma band oscillations. *Proceedings of the National Academy of Sciences of the United States of America* **112**, 3535-3540, doi:10.1073/pnas.1413625112 (2015).
- 75 Nassar, M. *et al.* Diversity and overlap of parvalbumin and somatostatin expressing interneurons in mouse presubiculum. *Front Neural Circuits* **9**, 20, doi:10.3389/fncir.2015.00020 (2015).
- 76 Karube, F., Kubota, Y. & Kawaguchi, Y. Axon branching and synaptic bouton phenotypes in GABAergic nonpyramidal cell subtypes. *The Journal of neuroscience : the official journal of the Society for Neuroscience* **24**, 2853-2865, doi:10.1523/JNEUROSCI.4814-03.2004 (2004).
- 77 Ma, Y., Hu, H., Berrebi, A. S., Mathers, P. H. & Agmon, A. Distinct subtypes of somatostatin-containing neocortical interneurons revealed in transgenic mice. *The Journal of neuroscience : the official journal of the Society for Neuroscience* **26**, 5069-5082 (2006).
- 78 Kubota, Y. & Kawaguchi, Y. Three classes of GABAergic interneurons in neocortex and neostriatum. *The Japanese journal of physiology* **44 Suppl 2**, S145-148 (1994).
- 79 Gonchar, Y. & Burkhalter, A. Three distinct families of GABAergic neurons in rat visual cortex. *Cereb Cortex* **7**, 347-358 (1997).
- 80 Kubota, Y. & Kawaguchi, Y. Three classes of GABAergic interneurons in neocortex and neostriatum. *Jpn J Physiol* **44 Suppl 2**, S145-148 (1994).
- 81 Xu, X., Roby, K. D. & Callaway, E. M. Mouse cortical inhibitory neuron type that coexpresses somatostatin and calretinin. *J Comp Neurol* **499**, 144-160 (2006).
- 82 Lee, S., Hjerling-Leffler, J., Zaghera, E., Fishell, G. & Rudy, B. The largest group of superficial neocortical GABAergic interneurons expresses ionotropic serotonin receptors. *The Journal of neuroscience : the official journal of the Society for Neuroscience* **30**, 16796-16808, doi:10.1523/JNEUROSCI.1869-10.2010 (2010).
- 83 Rudy, B., Fishell, G., Lee, S. & Hjerling-Leffler, J. Three groups of interneurons account for nearly 100% of neocortical GABAergic neurons. *Developmental neurobiology* **71**, 45-61, doi:10.1002/dneu.20853 (2011).
- 84 Karagiannis, A. *et al.* Classification of NPY-expressing neocortical interneurons. *The Journal of neuroscience : the official journal of the Society for Neuroscience* **29**, 3642-3659, doi:10.1523/JNEUROSCI.0058-09.2009 (2009).

- 85 Kubota, Y. *et al.* Selective coexpression of multiple chemical markers defines discrete populations of neocortical GABAergic neurons. *Cerebral cortex* **21**, 1803-1817, doi:10.1093/cercor/bhq252 (2011).
- 86 Markram, H. *et al.* Interneurons of the neocortical inhibitory system. *Nature reviews. Neuroscience* **5**, 793-807 (2004).
- 87 Parra, P., Gulyas, A. I. & Miles, R. How many subtypes of inhibitory cells in the hippocampus? *Neuron* **20**, 983-993 (1998).
- 88 Kepecs, A. & Fishell, G. Interneuron cell types are fit to function. *Nature* **505**, 318-326, doi:10.1038/nature12983 (2014).
- 89 Kriegstein, A. R. Constructing circuits: neurogenesis and migration in the developing neocortex. *Epilepsia* **46 Suppl 7**, 15-21 (2005).
- 90 Hatanaka, Y., Hisanaga, S., Heizmann, C. W. & Murakami, F. Distinct migratory behavior of early- and late-born neurons derived from the cortical ventricular zone. *The Journal of comparative neurology* **479**, 1-14, doi:10.1002/cne.20256 (2004).
- 91 Porteus, M. H., Bulfone, A., Liu, J. K., Lo, L. C. & Rubenstein, J. L. R. DLX-2, MASH-1, and MAP-2 expression and bromodeoxyuridine incorporation define molecularly distinct cell populations in the embryonic mouse forebrain. *J. Neuroscience* **44**, 6370-6383 (1994).
- 92 Anderson, S. A. *et al.* Mutations of the homeobox genes Dlx-1 and Dlx-2 disrupt the striatal subventricular zone and differentiation of late born striatal neurons. *Neuron* **19**, 27-37 (1997a).
- 93 Dessaud, E., McMahon, A. P. & Briscoe, J. Pattern formation in the vertebrate neural tube: a sonic hedgehog morphogen-regulated transcriptional network. *Development* **135**, 2489-2503, doi:10.1016/j.dev.009324 (2008).
- 94 Wang, B., Waclaw, R. R., Allen, Z. J., 2nd, Guillemot, F. & Campbell, K. Ascl1 is a required downstream effector of Gsx gene function in the embryonic mouse telencephalon. *Neural development* **4**, 5, doi:10.1186/1749-8104-4-5 (2009).
- 95 Long, J. E., Cobos, I., Potter, G. B. & Rubenstein, J. L. Dlx1&2 and Mash1 transcription factors control MGE and CGE patterning and differentiation through parallel and overlapping pathways. *Cereb Cortex* **19 Suppl 1**, i96-106 (2009).
- 96 Casarosa, S., Fode, C. & Guillemot, F. Mash1 regulates neurogenesis in the ventral telencephalon. *Development* **126**, 525-534 (1999).
- 97 Horton, S., Meredith, A., Richardson, J. A. & Johnson, J. E. Correct coordination of neuronal differentiation events in ventral forebrain requires the bHLH factor MASH1. *Mol Cell Neurosci* **14**, 355-369 (1999).
- 98 Pleasure, S. J. *et al.* Cell migration from the ganglionic eminences is required for the development of hippocampal GABAergic interneurons. *Neuron* **28**, 727-740 (2000).

- 99 Petryniak, M. A., Potter, G. B., Rowitch, D. H. & Rubenstein, J. L. Dlx1 and Dlx2 control neuronal versus oligodendroglial cell fate acquisition in the developing forebrain. *Neuron* **55**, 417-433, doi:10.1016/j.neuron.2007.06.036 (2007).
- 100 Corbin, J. G., Gaiano, N., Machold, R. P., Langston, A. & Fishell, G. The Gsh2 homeodomain gene controls multiple aspects of telencephalic development. *Development* **127**, 5007-5020 (2000).
- 101 Waclaw, R. R., Wang, B. & Campbell, K. The homeobox gene Gsh2 is required for retinoid production in the embryonic mouse telencephalon. *Development* **131**, 4013-4020 (2004).
- 102 Toresson, H. & Campbell, K. A role for Gsh1 in the developing striatum and olfactory bulb of Gsh2 mutant mice. *Development* **128**, 4769-4780 (2001).
- 103 Pei, Z. *et al.* Homeobox genes Gsx1 and Gsx2 differentially regulate telencephalic progenitor maturation. *Proceedings of the National Academy of Sciences of the United States of America* **108**, 1675-1680, doi:10.1073/pnas.1008824108 (2011).
- 104 Inan, M., Welagen, J. & Anderson, S. A. Spatial and temporal bias in the mitotic origins of somatostatin- and parvalbumin-expressing interneuron subgroups and the chandelier subtype in the medial ganglionic eminence. *Cereb Cortex* **22**, 820-827, doi:10.1093/cercor/bhr148 (2012).
- 105 Sussel, L., Marin, O., Kimura, S. & Rubenstein, J. L. Loss of Nkx2.1 homeobox gene function results in a ventral to dorsal molecular respecification within the basal telencephalon: evidence for a transformation of the pallidum into the striatum. *Development* **126**, 3359-3370 (1999).
- 106 Sousa, V. H., Miyoshi, G., Hjerling-Leffler, J., Karayannis, T. & Fishell, G. Characterization of Nkx6-2-derived neocortical interneuron lineages. *Cereb Cortex* **19 Suppl 1**, i1-10, doi:bhp038 [pii] 10.1093/cercor/bhp038 (2009).
- 107 Fogarty, M. *et al.* Spatial genetic patterning of the embryonic neuroepithelium generates GABAergic interneuron diversity in the adult cortex. *The Journal of neuroscience : the official journal of the Society for Neuroscience* **27**, 10935-10946 (2007).
- 108 Wonders, C. P. *et al.* A spatial bias for the origins of interneuron subgroups within the medial ganglionic eminence. *Dev Biol* **314**, 127-136 (2008).
- 109 Elias, L. A., Potter, G. B. & Kriegstein, A. R. A time and a place for nkx2-1 in interneuron specification and migration. *Neuron* **59**, 679-682, doi:10.1016/j.neuron.2008.08.017 (2008).
- 110 Marin, O. *et al.* Directional guidance of interneuron migration to the cerebral cortex relies on subcortical Slit1/2-independent repulsion and cortical attraction. *Development* **130**, 1889-1901 (2003).

- 111 van den Berghe, V. *et al.* Directed migration of cortical interneurons depends on the cell-autonomous action of Sip1. *Neuron* **77**, 70-82, doi:10.1016/j.neuron.2012.11.009 (2013).
- 112 McKinsey, G. L. *et al.* Dlx1&2-dependent expression of Zfhx1b (Sip1, Zeb2) regulates the fate switch between cortical and striatal interneurons. *Neuron* **77**, 83-98, doi:10.1016/j.neuron.2012.11.035 (2013).
- 113 Du, T., Xu, Q., Ocbina, P. J. & Anderson, S. A. NKX2.1 specifies cortical interneuron fate by activating Lhx6. *Development* **135**, 1559-1567 (2008).
- 114 Fragkouli, A., van Wijk, N. V., Lopes, R., Kessarlis, N. & Pachnis, V. LIM homeodomain transcription factor-dependent specification of bipotential MGE progenitors into cholinergic and GABAergic striatal interneurons. *Development* **136**, 3841-3851, doi:10.1016/j.dev.038083 (2009).
- 115 Cho, H. H. *et al.* Isl1 directly controls a cholinergic neuronal identity in the developing forebrain and spinal cord by forming cell type-specific complexes. *PLoS Genet* **10**, e1004280, doi:10.1371/journal.pgen.1004280 (2014).
- 116 Lopes, R., Verhey van Wijk, N., Neves, G. & Pachnis, V. Transcription factor LIM homeobox 7 (Lhx7) maintains subtype identity of cholinergic interneurons in the mammalian striatum. *Proceedings of the National Academy of Sciences of the United States of America* **109**, 3119-3124, doi:10.1073/pnas.1109251109 (2012).
- 117 Jaglin, X. H., Hjerling-Leffler, J., Fishell, G. & Batista-Brito, R. The origin of neocortical nitric oxide synthase-expressing inhibitory neurons. *Frontiers in neural circuits* **6**, 44, doi:10.3389/fncir.2012.00044 (2012).
- 118 Close, J. *et al.* Satb1 is an activity-modulated transcription factor required for the terminal differentiation and connectivity of medial ganglionic eminence-derived cortical interneurons. *The Journal of neuroscience : the official journal of the Society for Neuroscience* **32**, 17690-17705, doi:10.1523/JNEUROSCI.3583-12.2012 (2012).
- 119 Batista-Brito, R. *et al.* The cell-intrinsic requirement of Sox6 for cortical interneuron development. *Neuron* **63**, 466-481, doi:10.1016/j.neuron.2009.08.005 (2009).
- 120 Azim, E., Jabaudon, D., Fame, R. M. & Macklis, J. D. SOX6 controls dorsal progenitor identity and interneuron diversity during neocortical development. *Nat Neurosci* **12**, 1238-1247, doi:10.1038/nn.2387 (2009).
- 121 Grigoriou, M., Tucker, A. S., Sharpe, P. T. & Pachnis, V. Expression and regulation of Lhx6 and Lhx7, a novel subfamily of LIM homeodomain encoding genes, suggests a role in mammalian head development. *Development* **125**, 2063-2074 (1998).

- 122 Zhao, Y. *et al.* Distinct molecular pathways for development of  
telencephalic interneuron subtypes revealed through analysis of Lhx6  
mutants. *J Comp Neurol* **510**, 79-99, doi:10.1002/cne.21772 (2008).
- 123 Lavdas, A. A., Grigoriou, M., Pachnis, V. & Parnavelas, J. G. The medial  
ganglionic eminence gives rise to a population of early neurons in the  
developing cerebral cortex. *The Journal of neuroscience : the official  
journal of the Society for Neuroscience* **19**, 7881-7888 (1999).
- 124 Liodis, P. *et al.* Lhx6 activity is required for the normal migration and  
specification of cortical interneuron subtypes. *The Journal of neuroscience  
: the official journal of the Society for Neuroscience* **27**, 3078-3089 (2007).
- 125 Xu, Q., Wonders, C. P. & Anderson, S. A. Sonic hedgehog maintains the  
identity of cortical interneuron progenitors in the ventral telencephalon.  
*Development* **132**, 4987-4998 (2005).
- 126 Gulacsi, A. & Anderson, S. A. Shh maintains Nkx2.1 in the MGE by a Gli3-  
independent mechanism. *Cereb Cortex* **16 Suppl 1**, i89-95 (2006).
- 127 Xu, Q. *et al.* Sonic hedgehog signaling confers ventral telencephalic  
progenitors with distinct cortical interneuron fates. *Neuron* **65**, 328-340  
(2010).
- 128 Shen, Q. *et al.* The timing of cortical neurogenesis is encoded within  
lineages of individual progenitor cells. *Nature neuroscience* **9**, 743-751,  
doi:10.1038/nn1694 (2006).
- 129 Glickstein, S. B., Monaghan, J. A., Koeller, H. B., Jones, T. K. & Ross, M.  
E. Cyclin D2 is critical for intermediate progenitor cell proliferation in the  
embryonic cortex. *The Journal of neuroscience : the official journal of the  
Society for Neuroscience* **29**, 9614-9624, doi:10.1523/JNEUROSCI.2284-  
09.2009 (2009).
- 130 Glickstein, S. B. *et al.* Selective cortical interneuron and GABA deficits in  
cyclin D2-null mice. *Development* **134**, 4083-4093 (2007).
- 131 Glickstein, S. B., Alexander, S. & Ross, M. E. Differences in cyclin D2 and  
D1 protein expression distinguish forebrain progenitor subsets. *Cereb  
Cortex* **17**, 632-642 (2007).
- 132 Koeller, H. B., Ross, M. E. & Glickstein, S. B. Cyclin D1 in excitatory  
neurons of the adult brain enhances kainate-induced neurotoxicity.  
*Neurobiology of disease* **31**, 230-241, doi:10.1016/j.nbd.2008.04.010  
(2008).
- 133 Petros, T. J., Bultje, R. S., Ross, M. E., Fishell, G. & Anderson, S. A.  
Apical vs. basal neurogenesis directs cortical interneuron subclass fate.  
*Cell Reports In Press* ( 2015).
- 134 Gal, J. S. *et al.* Molecular and morphological heterogeneity of neural  
precursors in the mouse neocortical proliferative zones. *The Journal of  
neuroscience : the official journal of the Society for Neuroscience* **26**,  
1045-1056, doi:10.1523/JNEUROSCI.4499-05.2006 (2006).
- 135 Stancik, E. K., Navarro-Quiroga, I., Sellke, R. & Haydar, T. F.  
Heterogeneity in ventricular zone neural precursors contributes to



- neuronal fate diversity in the postnatal neocortex. *The Journal of neuroscience : the official journal of the Society for Neuroscience* **30**, 7028-7036 (2010).
- 136 Tripodi, M., Filosa, A., Armentano, M. & Studer, M. The COUP-TF nuclear receptors regulate cell migration in the mammalian basal forebrain. *Development* **131**, 6119-6129 (2004).
- 137 Rubin, A. N. & Kessar, N. PROX1: a lineage tracer for cortical interneurons originating in the lateral/caudal ganglionic eminence and preoptic area. *PloS one* **8**, e77339, doi:10.1371/journal.pone.0077339 (2013).
- 138 Miyoshi, G. *et al.* Prox1 Regulates the Subtype-Specific Development of Caudal Ganglionic Eminence-Derived GABAergic Cortical Interneurons. *The Journal of neuroscience : the official journal of the Society for Neuroscience* **35**, 12869-12889, doi:10.1523/JNEUROSCI.1164-15.2015 (2015).
- 139 Lodato, S. *et al.* Loss of COUP-TFI alters the balance between caudal ganglionic eminence- and medial ganglionic eminence-derived cortical interneurons and results in resistance to epilepsy. *The Journal of neuroscience : the official journal of the Society for Neuroscience* **31**, 4650-4662, doi:10.1523/JNEUROSCI.6580-10.2011 (2011).
- 140 Flames, N. *et al.* Delineation of multiple subpallial progenitor domains by the combinatorial expression of transcriptional codes. *The Journal of neuroscience : the official journal of the Society for Neuroscience* **27**, 9682-9695 (2007).
- 141 Yun, K., Potter, S. & Rubenstein, J. L. Gsh2 and Pax6 play complementary roles in dorsoventral patterning of the mammalian telencephalon. *Development* **128**, 193-205 (2001).
- 142 Puelles, L. *et al.* Pallial and subpallial derivatives in the embryonic chick and mouse telencephalon, traced by the expression of the genes Dlx-2, Emx-1, Nkx-2.1, Pax-6, and Tbr-1. *J Comp Neurol* **424**, 409-438 (2000).
- 143 Merkle, F. T., Mirzadeh, Z. & Alvarez-Buylla, A. Mosaic organization of neural stem cells in the adult brain. *Science* **317**, 381-384, doi:10.1126/science.1144914 (2007).
- 144 Stenman, J., Toresson, H. & Campbell, K. Identification of two distinct progenitor populations in the lateral ganglionic eminence: implications for striatal and olfactory bulb neurogenesis. *The Journal of neuroscience : the official journal of the Society for Neuroscience* **23**, 167-174 (2003).
- 145 Waclaw, R. R. *et al.* The zinc finger transcription factor Sp8 regulates the generation and diversity of olfactory bulb interneurons. *Neuron* **49**, 503-516, doi:10.1016/j.neuron.2006.01.018 (2006).
- 146 Toresson, H., Potter, S. S. & Campbell, K. Genetic control of dorsal-ventral identity in the telencephalon: opposing roles for Pax6 and Gsh2. *Development* **127**, 4361-4371 (2000).

- 147 Kessel, M. & Gruss, P. Homeotic transformations of murine vertebrae and concomitant alteration of *Hox* codes induced by retinoic acid. *Cell* **67**, 89-104 (1991).
- 148 Maden, M. & Holder, N. Retinoic acid and development of the central nervous system. *BioEssays* **14**, 431-438 (1992).
- 149 LaMantia, A. S., Colbert, M. C. & Linney, E. Retinoic acid induction and regional differentiation prefigure olfactory pathway formation in the mammalian forebrain. *Neuron* **10**, 1035-1048 (1993).
- 150 Toresson, H., Mata de Urquiza, A., Fagerström, C., Perlmann, T. & Campbell, K. Retinoids are produced by glia in the lateral ganglionic eminence and regulate striatal neuron differentiation. *Development* **126**, 1317-1326 (1999).
- 151 Schneider, R. A., Hu, D., Rubenstein, J. L., Maden, M. & Helms, J. A. Local retinoid signaling coordinates forebrain and facial morphogenesis by maintaining FGF8 and SHH. *Development* **128**, 2755-2767 (2001).
- 152 Dupe, V. *et al.* A newborn lethal defect due to inactivation of retinaldehyde dehydrogenase type 3 is prevented by maternal retinoic acid treatment. *Proceedings of the National Academy of Sciences of the United States of America* **100**, 14036-14041, doi:10.1073/pnas.2336223100 (2003).
- 153 Chatzi, C., Brade, T. & Duester, G. Retinoic acid functions as a key GABAergic differentiation signal in the basal ganglia. *PLoS Biol* **9**, e1000609, doi:10.1371/journal.pbio.1000609 (2011).
- 154 Rataj-Baniowska, M. *et al.* Retinoic Acid Receptor beta Controls Development of Striatonigral Projection Neurons through FGF-Dependent and Meis1-Dependent Mechanisms. *The Journal of neuroscience : the official journal of the Society for Neuroscience* **35**, 14467-14475, doi:10.1523/JNEUROSCI.1278-15.2015 (2015).
- 155 Urban, N. *et al.* Nolz1 promotes striatal neurogenesis through the regulation of retinoic acid signaling. *Neural Dev* **5**, 21, doi:10.1186/1749-8104-5-21 (2010).
- 156 Ehrman, L. A. *et al.* The LIM homeobox gene *Isl1* is required for the correct development of the striatonigral pathway in the mouse. *Proceedings of the National Academy of Sciences of the United States of America* **110**, E4026-4035, doi:10.1073/pnas.1308275110 (2013).
- 157 Lu, K. M., Evans, S. M., Hirano, S. & Liu, F. C. Dual role for *Islet-1* in promoting striatonigral and repressing striatopallidal genetic programs to specify striatonigral cell identity. *Proceedings of the National Academy of Sciences of the United States of America* **111**, E168-177, doi:10.1073/pnas.1319138111 (2014).
- 158 Lobo, M. K., Karsten, S. L., Gray, M., Geschwind, D. H. & Yang, X. W. FACS-array profiling of striatal projection neuron subtypes in juvenile and adult mouse brains. *Nat Neurosci* **9**, 443-452, doi:10.1038/nn1654 (2006).

- 159 Garel, S., Marin, F., Grosschedl, R. & Charnay, P. Ebf1 controls early cell differentiation in the embryonic striatum. *Development* **126**, 5285-5294 (1999).
- 160 Lobo, M. K., Yeh, C. & Yang, X. W. Pivotal role of early B-cell factor 1 in development of striatonigral medium spiny neurons in the matrix compartment. *J Neurosci Res* **86**, 2134-2146, doi:10.1002/jnr.21666 (2008).
- 161 Zhang, Q. *et al.* The Zinc Finger Transcription Factor Sp9 Is Required for the Development of Striatopallidal Projection Neurons. *Cell Rep*, doi:10.1016/j.celrep.2016.06.090 (2016).
- 162 Arlotta, P., Molyneaux, B. J., Jabaudon, D., Yoshida, Y. & Macklis, J. D. Ctip2 controls the differentiation of medium spiny neurons and the establishment of the cellular architecture of the striatum. *The Journal of neuroscience : the official journal of the Society for Neuroscience* **28**, 622-632, doi:10.1523/JNEUROSCI.2986-07.2008 (2008).
- 163 Tamura, S., Morikawa, Y., Iwanishi, H., Hisaoka, T. & Senba, E. Foxp1 gene expression in projection neurons of the mouse striatum. *Neuroscience* **124**, 261-267, doi:10.1016/j.neuroscience.2003.11.036 (2004).
- 164 Bacon, C. *et al.* Brain-specific Foxp1 deletion impairs neuronal development and causes autistic-like behaviour. *Mol Psychiatry* **20**, 632-639, doi:10.1038/mp.2014.116 (2015).
- 165 Araujo, D. J. *et al.* FoxP1 orchestration of ASD-relevant signaling pathways in the striatum. *Genes Dev* **29**, 2081-2096, doi:10.1101/gad.267989.115 (2015).
- 166 Klausberger, T. & Somogyi, P. Neuronal diversity and temporal dynamics: the unity of hippocampal circuit operations. *Science* **321**, 53-57, doi:10.1126/science.1149381 (2008).
- 167 Marin, O. Interneuron dysfunction in psychiatric disorders. *Nature reviews. Neuroscience* **13**, 107-120, doi:10.1038/nrn3155 (2012).
- 168 Kitamura, K. *et al.* Mutation of ARX causes abnormal development of forebrain and testes in mice and X-linked lissencephaly with abnormal genitalia in humans. *Nature genetics* **32**, 359-369 (2002).
- 169 Galanopoulou, A. S. Mutations affecting GABAergic signaling in seizures and epilepsy. *Pflugers Archiv : European journal of physiology* **460**, 505-523, doi:10.1007/s00424-010-0816-2 (2010).
- 170 Eugene, E. *et al.* GABA(A) receptor gamma 2 subunit mutations linked to human epileptic syndromes differentially affect phasic and tonic inhibition. *The Journal of neuroscience : the official journal of the Society for Neuroscience* **27**, 14108-14116, doi:10.1523/JNEUROSCI.2618-07.2007 (2007).
- 171 Poduri, A. & Lowenstein, D. Epilepsy genetics--past, present, and future. *Current opinion in genetics & development* **21**, 325-332, doi:10.1016/j.gde.2011.01.005 (2011).

- 172 Marsh, E. D. & Golden, J. A. in *Jasper's Basic Mechanisms of the Epilepsies* (eds J. L. Noebels *et al.*) (2012).
- 173 Sherr, E. H. The ARX story (epilepsy, mental retardation, autism, and cerebral malformations): one gene leads to many phenotypes. *Curr Opin Pediatr* **15**, 567-571 (2003).
- 174 Colombo, E. *et al.* Inactivation of Arx, the murine ortholog of the X-linked lissencephaly with ambiguous genitalia gene, leads to severe disorganization of the ventral telencephalon with impaired neuronal migration and differentiation. *The Journal of neuroscience : the official journal of the Society for Neuroscience* **27**, 4786-4798 (2007).
- 175 Kato, M. & Dobyns, W. B. X-linked lissencephaly with abnormal genitalia as a tangential migration disorder causing intractable epilepsy: proposal for a new term, "interneuronopathy". *Journal of child neurology* **20**, 392-397 (2005).
- 176 Bonneau, D. *et al.* X-linked lissencephaly with absent corpus callosum and ambiguous genitalia (XLAG): clinical, magnetic resonance imaging, and neuropathological findings. *Ann Neurol* **51**, 340-349 (2002).
- 177 Okazaki, S. *et al.* Aristaless-related homeobox gene disruption leads to abnormal distribution of GABAergic interneurons in human neocortex: evidence based on a case of X-linked lissencephaly with abnormal genitalia (XLAG). *Acta Neuropathol* **116**, 453-462, doi:10.1007/s00401-008-0382-2 (2008).
- 178 Forman, M. S., Squier, W., Dobyns, W. B. & Golden, J. A. Genotypically defined lissencephalies show distinct pathologies. *J Neuropathol Exp Neurol* **64**, 847-857 (2005).
- 179 Colombo, E., Galli, R., Cossu, G., Gecz, J. & Broccoli, V. Mouse orthologue of ARX, a gene mutated in several X-linked forms of mental retardation and epilepsy, is a marker of adult neural stem cells and forebrain GABAergic neurons. *Dev Dyn* **231**, 631-639 (2004).
- 180 Friocourt, G. Identification of Arx targets unveils new candidates for controlling cortical interneuron migration and differentiation. *Frontiers in Cellular Neuroscience* **5**, doi:10.3389/fncel.2011.00028 (2011).
- 181 Vogt, D. *et al.* Lhx6 directly regulates Arx and CXCR7 to determine cortical interneuron fate and laminar position. *Neuron* **82**, 350-364, doi:10.1016/j.neuron.2014.02.030 (2014).
- 182 Escayg, A. & Goldin, A. L. Sodium channel SCN1A and epilepsy: mutations and mechanisms. *Epilepsia* **51**, 1650-1658, doi:10.1111/j.1528-1167.2010.02640.x (2010).
- 183 Yu, F. H. *et al.* Reduced sodium current in GABAergic interneurons in a mouse model of severe myoclonic epilepsy in infancy. *Nat Neurosci* **9**, 1142-1149, doi:10.1038/nn1754 (2006).
- 184 Ogiwara, I. *et al.* Nav1.1 localizes to axons of parvalbumin-positive inhibitory interneurons: a circuit basis for epileptic seizures in mice carrying an Scn1a gene mutation. *The Journal of neuroscience : the*

- official journal of the Society for Neuroscience* **27**, 5903-5914, doi:10.1523/JNEUROSCI.5270-06.2007 (2007).
- 185 Dutton, S. B. *et al.* Preferential inactivation of Scn1a in parvalbumin interneurons increases seizure susceptibility. *Neurobiology of disease* **49C**, 211-220, doi:10.1016/j.nbd.2012.08.012 (2012).
- 186 Sun, Y. *et al.* A deleterious Nav1.1 mutation selectively impairs telencephalic inhibitory neurons derived from Dravet Syndrome patients. *Elife* **5**, doi:10.7554/eLife.13073 (2016).
- 187 Catarino, C. B. *et al.* Dravet syndrome as epileptic encephalopathy: evidence from long-term course and neuropathology. *Brain : a journal of neurology* **134**, 2982-3010, doi:10.1093/brain/awr129 (2011).
- 188 Anderson, S. A. & Baraban, S. C. in *Jasper's Basic Mechanisms of the Epilepsies* (eds J. L. Noebels *et al.*) (2012).
- 189 Bjorklund, A. & Lindvall, O. Cell replacement therapies for central nervous system disorders. *Nat Neurosci* **3**, 537-544 (2000).
- 190 Tyson, J. A. & Anderson, S. A. GABAergic interneuron transplants to study development and treat disease. *Trends in neurosciences* **37**, 169-177, doi:10.1016/j.tins.2014.01.003 (2014).
- 191 Baraban, S. C. *et al.* Reduction of seizures by transplantation of cortical GABAergic interneuron precursors into Kv1.1 mutant mice. *Proceedings of the National Academy of Sciences of the United States of America* **106**, 15472-15477 (2009).
- 192 Zipancic, I., Calcagnotto, M. E., Piquer-Gil, M., Mello, L. E. & Alvarez-Dolado, M. Transplant of GABAergic precursors restores hippocampal inhibitory function in a mouse model of seizure susceptibility. *Cell Transplant* **19**, 549-564 (2010).
- 193 De la Cruz, E. *et al.* Interneuron progenitors attenuate the power of acute focal ictal discharges. *Neurotherapeutics* **8**, 763-773, doi:10.1007/s13311-011-0058-9 (2011).
- 194 Hunt, R. F., Girsakis, K. M., Rubenstein, J. L., Alvarez-Buylla, A. & Baraban, S. C. GABA progenitors grafted into the adult epileptic brain control seizures and abnormal behavior. *Nat Neurosci* **16**, 692-697, doi:10.1038/nn.3392 (2013).
- 195 Lewis, D. A., Hashimoto, T. & Volk, D. W. Cortical inhibitory neurons and schizophrenia. *Nature reviews. Neuroscience* **6**, 312-324 (2005).
- 196 Lewis, D. A. GABAergic local circuit neurons and prefrontal cortical dysfunction in schizophrenia. *Brain Res Brain Res Rev* **31**, 270-276 (2000).
- 197 Fung, S. J. *et al.* Expression of interneuron markers in the dorsolateral prefrontal cortex of the developing human and in schizophrenia. *The American journal of psychiatry* **167**, 1479-1488, doi:10.1176/appi.ajp.2010.09060784 (2010).
- 198 Elvevag, B. & Goldberg, T. E. Cognitive impairment in schizophrenia is the core of the disorder. *Critical reviews in neurobiology* **14**, 1-21 (2000).

- 199 Elvevag, B., Weinberger, D. R., Suter, J. C. & Goldberg, T. E. Continuous performance test and schizophrenia: a test of stimulus-response compatibility, working memory, response readiness, or none of the above? *The American journal of psychiatry* **157**, 772-780 (2000).
- 200 Woo, T. U., Whitehead, R. E., Melchitzky, D. S. & Lewis, D. A. A subclass of prefrontal gamma-aminobutyric acid axon terminals are selectively altered in schizophrenia. *Proceedings of the National Academy of Sciences of the United States of America* **95**, 5341-5346 (1998).
- 201 Benes, F. M. & Berretta, S. GABAergic interneurons: implications for understanding schizophrenia and bipolar disorder. *Neuropsychopharmacology* **25**, 1-27 (2001).
- 202 Li, D., Collier, D. A. & He, L. Meta-analysis shows strong positive association of the neuregulin 1 (NRG1) gene with schizophrenia. *Human molecular genetics* **15**, 1995-2002, doi:10.1093/hmg/ddl122 (2006).
- 203 Stefansson, H. *et al.* Association of neuregulin 1 with schizophrenia confirmed in a Scottish population. *American journal of human genetics* **72**, 83-87 (2003).
- 204 Hikida, T. *et al.* Dominant-negative DISC1 transgenic mice display schizophrenia-associated phenotypes detected by measures translatable to humans. *Proceedings of the National Academy of Sciences of the United States of America* **104**, 14501-14506, doi:10.1073/pnas.0704774104 (2007).
- 205 Wen, L. *et al.* Neuregulin 1 regulates pyramidal neuron activity via ErbB4 in parvalbumin-positive interneurons. *Proceedings of the National Academy of Sciences of the United States of America* **107**, 1211-1216 (2010).
- 206 Millar, J. K. *et al.* Disruption of two novel genes by a translocation co-segregating with schizophrenia. *Human molecular genetics* **9**, 1415-1423 (2000).
- 207 Del Pino, I. *et al.* Erbb4 deletion from fast-spiking interneurons causes schizophrenia-like phenotypes. *Neuron* **79**, 1152-1168, doi:10.1016/j.neuron.2013.07.010 (2013).
- 208 Hussman, J. P. Suppressed GABAergic inhibition as a common factor in suspected etiologies of autism. *J Autism Dev Disord* **31**, 247-248 (2001).
- 209 Jetty, P. V., Charney, D. S. & Goddard, A. W. Neurobiology of generalized anxiety disorder. *Psychiatr Clin North Am* **24**, 75-97 (2001).
- 210 Kalanithi, P. S. *et al.* Altered parvalbumin-positive neuron distribution in basal ganglia of individuals with Tourette syndrome. *Proceedings of the National Academy of Sciences of the United States of America* **102**, 13307-13312 (2005).
- 211 Chahrour, M. & Zoghbi, H. Y. The story of Rett syndrome: from clinic to neurobiology. *Neuron* **56**, 422-437, doi:10.1016/j.neuron.2007.10.001 (2007).

- 212 Samaco, R. C. *et al.* Loss of MeCP2 in aminergic neurons causes cell-autonomous defects in neurotransmitter synthesis and specific behavioral abnormalities. *Proceedings of the National Academy of Sciences of the United States of America* **106**, 21966-21971, doi:10.1073/pnas.0912257106 (2009).
- 213 Huang, Z. J., Di Cristo, G. & Ango, F. Development of GABA innervation in the cerebral and cerebellar cortices. *Nature reviews. Neuroscience* **8**, 673-686, doi:10.1038/nrn2188 (2007).
- 214 State, M. W. The genetics of child psychiatric disorders: focus on autism and Tourette syndrome. *Neuron* **68**, 254-269, doi:10.1016/j.neuron.2010.10.004 (2010).
- 215 State, M. W. Another piece of the autism puzzle. *Nature genetics* **42**, 478-479, doi:10.1038/ng0610-478 (2010).
- 216 Bourne, Y. & Marchot, P. The Neuroligins and Their Ligands: from Structure to Function at the Synapse. *Journal of molecular neuroscience : MN*, doi:10.1007/s12031-014-0234-6 (2014).
- 217 Xu, X. *et al.* Variations analysis of NLGN3 and NLGN4X gene in Chinese autism patients. *Molecular biology reports*, doi:10.1007/s11033-014-3284-5 (2014).
- 218 Lott, I. T. & Dierssen, M. Cognitive deficits and associated neurological complications in individuals with Down's syndrome. *Lancet neurology* **9**, 623-633, doi:10.1016/S1474-4422(10)70112-5 (2010).
- 219 Smith, G. K., Kesner, R. P. & Korenberg, J. R. Dentate gyrus mediates cognitive function in the Ts65Dn/DnJ mouse model of down syndrome. *Hippocampus* **24**, 354-362, doi:10.1002/hipo.22229 (2014).
- 220 Belichenko, P. V. *et al.* Excitatory-inhibitory relationship in the fascia dentata in the Ts65Dn mouse model of Down syndrome. *The Journal of comparative neurology* **512**, 453-466, doi:10.1002/cne.21895 (2009).
- 221 Fernandez, F. *et al.* Pharmacotherapy for cognitive impairment in a mouse model of Down syndrome. *Nature neuroscience* **10**, 411-413, doi:10.1038/nn1860 (2007).
- 222 Medina, L. & Reiner, A. Neurotransmitter organization and connectivity of the basal ganglia in vertebrates: implications for the evolution of basal ganglia. *Brain Behav Evol* **46**, 235-258 (1995).
- 223 Fuccillo, M. V. Striatal Circuits as a Common Node for Autism Pathophysiology. *Front Neurosci* **10**, 27, doi:10.3389/fnins.2016.00027 (2016).
- 224 Pappas, S. S., Leventhal, D. K., Albin, R. L. & Dauer, W. T. Mouse models of neurodevelopmental disease of the basal ganglia and associated circuits. *Curr Top Dev Biol* **109**, 97-169, doi:10.1016/B978-0-12-397920-9.00001-9 (2014).
- 225 Yael, D., Vinner, E. & Bar-Gad, I. Pathophysiology of tic disorders. *Mov Disord* **30**, 1171-1178, doi:10.1002/mds.26304 (2015).

- 226 Tremblay, L., Worbe, Y., Thobois, S., Sgambato-Faure, V. & Feger, J. Selective dysfunction of basal ganglia subterritories: From movement to behavioral disorders. *Mov Disord* **30**, 1155-1170, doi:10.1002/mds.26199 (2015).
- 227 Peterson, B. S. *et al.* Basal Ganglia volumes in patients with Gilles de la Tourette syndrome. *Arch Gen Psychiatry* **60**, 415-424, doi:10.1001/archpsyc.60.4.415 (2003).
- 228 Peterson, B. S. *et al.* A functional magnetic resonance imaging study of tic suppression in Tourette syndrome. *Arch Gen Psychiatry* **55**, 326-333 (1998).
- 229 Kataoka, Y. *et al.* Decreased number of parvalbumin and cholinergic interneurons in the striatum of individuals with Tourette syndrome. *J Comp Neurol* **518**, 277-291, doi:10.1002/cne.22206 (2010).
- 230 Xu, M. *et al.* Targeted ablation of cholinergic interneurons in the dorsolateral striatum produces behavioral manifestations of Tourette syndrome. *Proceedings of the National Academy of Sciences of the United States of America* **112**, 893-898, doi:10.1073/pnas.1419533112 (2015).
- 231 Zilhao, N. R., Smit, D. J., Boomsma, D. I. & Cath, D. C. Cross-Disorder Genetic Analysis of Tic Disorders, Obsessive-Compulsive, and Hoarding Symptoms. *Front Psychiatry* **7**, 120, doi:10.3389/fpsy.2016.00120 (2016).
- 232 Burguiere, E., Monteiro, P., Mallet, L., Feng, G. & Graybiel, A. M. Striatal circuits, habits, and implications for obsessive-compulsive disorder. *Current opinion in neurobiology* **30**, 59-65, doi:10.1016/j.conb.2014.08.008 (2015).
- 233 Saxena, S. & Rauch, S. L. Functional neuroimaging and the neuroanatomy of obsessive-compulsive disorder. *Psychiatr Clin North Am* **23**, 563-586 (2000).
- 234 Ting, J. T. & Feng, G. Neurobiology of obsessive-compulsive disorder: insights into neural circuitry dysfunction through mouse genetics. *Current opinion in neurobiology* **21**, 842-848, doi:10.1016/j.conb.2011.04.010 (2011).
- 235 Pujol, J. *et al.* Mapping structural brain alterations in obsessive-compulsive disorder. *Arch Gen Psychiatry* **61**, 720-730, doi:10.1001/archpsyc.61.7.720 (2004).
- 236 Atmaca, M., Yildirim, H., Ozdemir, H., Tezcan, E. & Poyraz, A. K. Volumetric MRI study of key brain regions implicated in obsessive-compulsive disorder. *Prog Neuropsychopharmacol Biol Psychiatry* **31**, 46-52, doi:10.1016/j.pnpbp.2006.06.008 (2007).
- 237 van den Heuvel, O. A. *et al.* The major symptom dimensions of obsessive-compulsive disorder are mediated by partially distinct neural systems. *Brain* **132**, 853-868, doi:10.1093/brain/awn267 (2009).



- 238 Whiteside, S. P., Port, J. D. & Abramowitz, J. S. A meta-analysis of functional neuroimaging in obsessive-compulsive disorder. *Psychiatry Res* **132**, 69-79, doi:10.1016/j.psychresns.2004.07.001 (2004).
- 239 Harrison, B. J. *et al.* Brain corticostriatal systems and the major clinical symptom dimensions of obsessive-compulsive disorder. *Biol Psychiatry* **73**, 321-328, doi:10.1016/j.biopsych.2012.10.006 (2013).
- 240 Carmin, C. N., Wiegartz, P. S., Yunus, U. & Gillock, K. L. Treatment of late-onset OCD following basal ganglia infarct. *Depress Anxiety* **15**, 87-90 (2002).
- 241 Welch, J. M. *et al.* Cortico-striatal synaptic defects and OCD-like behaviours in Sapap3-mutant mice. *Nature* **448**, 894-900, doi:10.1038/nature06104 (2007).
- 242 Burguiere, E., Monteiro, P., Feng, G. & Graybiel, A. M. Optogenetic stimulation of lateral orbitofronto-striatal pathway suppresses compulsive behaviors. *Science* **340**, 1243-1246, doi:10.1126/science.1232380 (2013).
- 243 Ahmari, S. E. *et al.* Repeated cortico-striatal stimulation generates persistent OCD-like behavior. *Science* **340**, 1234-1239, doi:10.1126/science.1234733 (2013).
- 244 Shmelkov, S. V. *et al.* Slitrk5 deficiency impairs corticostriatal circuitry and leads to obsessive-compulsive-like behaviors in mice. *Nat Med* **16**, 598-602, 591p following 602, doi:10.1038/nm.2125 (2010).
- 245 Simpson, E. H., Kellendonk, C. & Kandel, E. A possible role for the striatum in the pathogenesis of the cognitive symptoms of schizophrenia. *Neuron* **65**, 585-596, doi:10.1016/j.neuron.2010.02.014 (2010).
- 246 Weinstein, J. J. *et al.* Pathway-Specific Dopamine Abnormalities in Schizophrenia. *Biol Psychiatry*, doi:10.1016/j.biopsych.2016.03.2104 (2016).
- 247 Howes, O. D. & Kapur, S. The dopamine hypothesis of schizophrenia: version III--the final common pathway. *Schizophr Bull* **35**, 549-562, doi:10.1093/schbul/sbp006 (2009).
- 248 Davis, K. L., Kahn, R. S., Ko, G. & Davidson, M. Dopamine in schizophrenia: a review and reconceptualization. *Am J Psychiatry* **148**, 1474-1486, doi:10.1176/ajp.148.11.1474 (1991).
- 249 Frankle, W. G. Neuroreceptor imaging studies in schizophrenia. *Harv Rev Psychiatry* **15**, 212-232, doi:10.1080/10673220701679812 (2007).
- 250 Abi-Dargham, A. *et al.* Increased baseline occupancy of D2 receptors by dopamine in schizophrenia. *Proceedings of the National Academy of Sciences of the United States of America* **97**, 8104-8109 (2000).
- 251 Schizophrenia Working Group of the Psychiatric Genomics, C. Biological insights from 108 schizophrenia-associated genetic loci. *Nature* **511**, 421-427, doi:10.1038/nature13595 (2014).
- 252 Kellendonk, C. Modeling excess striatal D2 receptors in mice. *Prog Brain Res* **179**, 59-65, doi:10.1016/S0079-6123(09)17907-4 (2009).

- 253 Pycock, C. J., Carter, C. J. & Kerwin, R. W. Effect of 6-hydroxydopamine lesions of the medial prefrontal cortex on neurotransmitter systems in subcortical sites in the rat. *J Neurochem* **34**, 91-99 (1980).
- 254 Roberts, A. C. *et al.* 6-Hydroxydopamine lesions of the prefrontal cortex in monkeys enhance performance on an analog of the Wisconsin Card Sort Test: possible interactions with subcortical dopamine. *The Journal of neuroscience : the official journal of the Society for Neuroscience* **14**, 2531-2544 (1994).
- 255 Li, Y. C., Kellendonk, C., Simpson, E. H., Kandel, E. R. & Gao, W. J. D2 receptor overexpression in the striatum leads to a deficit in inhibitory transmission and dopamine sensitivity in mouse prefrontal cortex. *Proceedings of the National Academy of Sciences of the United States of America* **108**, 12107-12112, doi:10.1073/pnas.1109718108 (2011).
- 256 Ward, R. D. *et al.* Impaired timing precision produced by striatal D2 receptor overexpression is mediated by cognitive and motivational deficits. *Behav Neurosci* **123**, 720-730, doi:10.1037/a0016503 (2009).
- 257 Drew, M. R. *et al.* Transient overexpression of striatal D2 receptors impairs operant motivation and interval timing. *The Journal of neuroscience : the official journal of the Society for Neuroscience* **27**, 7731-7739, doi:10.1523/JNEUROSCI.1736-07.2007 (2007).
- 258 Cazorla, M., Shegda, M., Ramesh, B., Harrison, N. L. & Kellendonk, C. Striatal D2 receptors regulate dendritic morphology of medium spiny neurons via Kir2 channels. *The Journal of neuroscience : the official journal of the Society for Neuroscience* **32**, 2398-2409, doi:10.1523/JNEUROSCI.6056-11.2012 (2012).
- 259 Sibille, E., Morris, H. M., Kota, R. S. & Lewis, D. A. GABA-related transcripts in the dorsolateral prefrontal cortex in mood disorders. *Int J Neuropsychopharmacol* **14**, 721-734 (2011).
- 260 Lewis, D. A., Curley, A. A., Glausier, J. R. & Volk, D. W. Cortical parvalbumin interneurons and cognitive dysfunction in schizophrenia. *Trends Neurosci* **35**, 57-67, doi:10.1016/j.tins.2011.10.004 (2012).
- 261 Lewis, D. A., Fish, K. N., Arion, D. & Gonzalez-Burgos, G. Perisomatic inhibition and cortical circuit dysfunction in schizophrenia. *Current opinion in neurobiology* **21**, 866-872, doi:10.1016/j.conb.2011.05.013 (2011).
- 262 Stefanits, H., Wesseling, C. & Kovacs, G. G. Loss of Calbindin immunoreactivity in the dentate gyrus distinguishes Alzheimer's disease from other neurodegenerative dementias. *Neuroscience letters*, doi:10.1016/j.neulet.2014.02.026 (2014).
- 263 Tyson, J. A. & Anderson, S. A. The protracted maturation of human ESC-derived interneurons. *Cell Cycle* **12**, 3129-3130, doi:10.4161/cc.26351 (2013).
- 264 Maroof, A. M. *et al.* Directed differentiation and functional maturation of cortical interneurons from human embryonic stem cells. *Cell Stem Cell* **12**, 559-572, doi:10.1016/j.stem.2013.04.008 (2013).

- 265 Nicholas, C. R. *et al.* Functional maturation of hPSC-derived forebrain interneurons requires an extended timeline and mimics human neural development. *Cell Stem Cell* **12**, 573-586, doi:10.1016/j.stem.2013.04.005 (2013).
- 266 Germain, N. D., Banda, E. C., Becker, S., Naegele, J. R. & Grabel, L. B. Derivation and isolation of NKX2.1-positive basal forebrain progenitors from human embryonic stem cells. *Stem cells and development* **22**, 1477-1489, doi:10.1089/scd.2012.0264 (2013).
- 267 Liu, Y. *et al.* Medial ganglionic eminence-like cells derived from human embryonic stem cells correct learning and memory deficits. *Nature biotechnology* **31**, 440-447, doi:10.1038/nbt.2565 (2013).
- 268 Maroof, A. M., Brown, K., Shi, S. H., Studer, L. & Anderson, S. A. Prospective isolation of cortical interneuron precursors from mouse embryonic stem cells. *The Journal of neuroscience : the official journal of the Society for Neuroscience* **30**, 4667-4675 (2010).
- 269 Tyson, J. A. *et al.* Duration of culture and sonic hedgehog signaling differentially specify PV versus SST cortical interneuron fates from embryonic stem cells. *Development* **142**, 1267-1278, doi:10.1242/dev.111526 (2015).
- 270 Danjo, T. *et al.* Subregional specification of embryonic stem cell-derived ventral telencephalic tissues by timed and combinatorial treatment with extrinsic signals. *The Journal of neuroscience : the official journal of the Society for Neuroscience* **31**, 1919-1933 (2011).
- 271 Watanabe, K. *et al.* Directed differentiation of telencephalic precursors from embryonic stem cells. *Nat Neurosci* **8**, 288-296 (2005).
- 272 Petros, T. J., Maurer, C. W. & Anderson, S. A. Enhanced derivation of mouse ESC-derived cortical interneurons by expression of Nkx2.1. *Stem Cell Res* **11**, 647-656, doi:10.1016/j.scr.2013.02.009 (2013).
- 273 Au, E. *et al.* A modular gain-of-function approach to generate cortical interneuron subtypes from ES cells. *Neuron* **80**, 1145-1158, doi:10.1016/j.neuron.2013.09.022 (2013).
- 274 Doetschman, T. C., Eistetter, H., Katz, M., Schmidt, W. & Kemler, R. The in vitro development of blastocyst-derived embryonic stem cell lines: formation of visceral yolk sac, blood islands and myocardium. *J Embryol Exp Morphol* **87**, 27-45 (1985).
- 275 Gaspard, N. & Vanderhaeghen, P. Laminar fate specification in the cerebral cortex. *F1000 Biol Rep* **3**, 6, doi:10.3410/B3-6 (2011).
- 276 Ohkubo, Y., Chiang, C. & Rubenstein, J. L. Coordinate regulation and synergistic actions of BMP4, SHH and FGF8 in the rostral prosencephalon regulate morphogenesis of the telencephalic and optic vesicles. *Neuroscience* **111**, 1-17 (2002).
- 277 Glinka, A. *et al.* Dickkopf-1 is a member of a new family of secreted proteins and functions in head induction. *Nature* **391**, 357-362, doi:10.1038/34848 (1998).

- 278 Huang, S. M. *et al.* Tankyrase inhibition stabilizes axin and antagonizes Wnt signalling. *Nature* **461**, 614-620, doi:10.1038/nature08356 (2009).
- 279 Southwell, D. G. *et al.* Interneurons from embryonic development to cell-based therapy. *Science* **344**, 1240622, doi:10.1126/science.1240622 (2014).
- 280 Tyson, J. A., Goldberg, E. M., Maroof, A. M., Petros, T. P. & Anderson, S. A. Duration of culture and Sonic Hedgehog signaling differentially specify PV versus SST cortical interneuron fates from embryonic stem cells. *Development* **142**, 1267-1278 (2015).
- 281 Harmacek, L. *et al.* A unique missense allele of BAF155, a core BAF chromatin remodeling complex protein, causes neural tube closure defects in mice. *Developmental neurobiology*, doi:10.1002/dneu.22142 (2013).
- 282 Tsui, D. *et al.* CBP regulates the differentiation of interneurons from ventral forebrain neural precursors during murine development. *Dev Biol* **385**, 230-241, doi:10.1016/j.ydbio.2013.11.005 (2014).
- 283 Wang, J. *et al.* CBP histone acetyltransferase activity regulates embryonic neural differentiation in the normal and Rubinstein-Taybi syndrome brain. *Developmental cell* **18**, 114-125, doi:10.1016/j.devcel.2009.10.023 (2010).
- 284 Vorhagen, S. & Niessen, C. M. Mammalian aPKC/Par polarity complex mediated regulation of epithelial division orientation and cell fate. *Exp Cell Res* **328**, 296-302, doi:10.1016/j.yexcr.2014.08.008 (2014).
- 285 Klezovitch, O., Fernandez, T. E., Tapscott, S. J. & Vasioukhin, V. Loss of cell polarity causes severe brain dysplasia in Lgl1 knockout mice. *Genes Dev* **18**, 559-571, doi:10.1101/gad.1178004  
18/5/559 [pii] (2004).
- 286 Petros, T. J., Bultje, R. S., Ross, M. E., Fishell, G. & Anderson, S. A. Apical versus Basal Neurogenesis Directs Cortical Interneuron Subclass Fate. *Cell Rep* **13**, 1090-1095, doi:10.1016/j.celrep.2015.09.079 (2015).
- 287 Wang, J. *et al.* Metformin activates an atypical PKC-CBP pathway to promote neurogenesis and enhance spatial memory formation. *Cell Stem Cell* **11**, 23-35, doi:10.1016/j.stem.2012.03.016 (2012).
- 288 Fatt, M. *et al.* Metformin Acts on Two Different Molecular Pathways to Enhance Adult Neural Precursor Proliferation/Self-Renewal and Differentiation. *Stem Cell Reports* **5**, 988-995, doi:10.1016/j.stemcr.2015.10.014 (2015).
- 289 Mah, I. K., Soloff, R., Hedrick, S. M. & Mariani, F. V. Atypical PKC-iota Controls Stem Cell Expansion via Regulation of the Notch Pathway. *Stem Cell Reports* **5**, 866-880, doi:10.1016/j.stemcr.2015.09.021 (2015).
- 290 Atwood, S. X., Li, M., Lee, A., Tang, J. Y. & Oro, A. E. GLI activation by atypical protein kinase C iota/lambda regulates the growth of basal cell carcinomas. *Nature* **494**, 484-488, doi:10.1038/nature11889 (2013).
- 291 Tucker, E. S. *et al.* Molecular specification and patterning of progenitor cells in the lateral and medial ganglionic eminences. *The Journal of*

- neuroscience : the official journal of the Society for Neuroscience* **28**, 9504-9518, doi:10.1523/JNEUROSCI.2341-08.2008 (2008).
- 292 Makarova, K. S., Aravind, L. & Koonin, E. V. SWIM, a novel Zn-chelating domain present in bacteria, archaea and eukaryotes. *Trends in biochemical sciences* **27**, 384-386 (2002).
- 293 Atlas, A. B. *Allen Institute for Brain Science*, <<http://www.alleninstitute.org>> (2012).
- 294 Mahrour, N. *et al.* Characterization of Cullin-box sequences that direct recruitment of Cul2-Rbx1 and Cul5-Rbx2 modules to Elongin BC-based ubiquitin ligases. *J Biol Chem* **283**, 8005-8013, doi:10.1074/jbc.M706987200 (2008).
- 295 Smith, J. D. *et al.* Exome sequencing identifies a recurrent de novo ZSWIM6 mutation associated with acromelic frontonasal dysostosis. *Am J Hum Genet* **95**, 235-240, doi:10.1016/j.ajhg.2014.07.008 (2014).
- 296 Gao, Z. *et al.* An AUTS2-Polycomb complex activates gene expression in the CNS. *Nature* **516**, 349-354, doi:10.1038/nature13921 (2014).
- 297 Gil, J. & O'Loghlen, A. PRC1 complex diversity: where is it taking us? *Trends Cell Biol* **24**, 632-641, doi:10.1016/j.tcb.2014.06.005 (2014).
- 298 Schwartz, Y. B. & Pirrotta, V. Ruled by ubiquitylation: a new order for polycomb recruitment. *Cell Rep* **8**, 321-325, doi:10.1016/j.celrep.2014.07.001 (2014).
- 299 Son, E. Y. & Crabtree, G. R. The role of BAF (mSWI/SNF) complexes in mammalian neural development. *Am J Med Genet C Semin Med Genet* **166C**, 333-349, doi:10.1002/ajmg.c.31416 (2014).
- 300 Dietrich, N. *et al.* REST-mediated recruitment of polycomb repressor complexes in mammalian cells. *PLoS Genet* **8**, e1002494, doi:10.1371/journal.pgen.1002494 (2012).
- 301 Gao, Z. *et al.* PCGF homologs, CBX proteins, and RYBP define functionally distinct PRC1 family complexes. *Mol Cell* **45**, 344-356, doi:10.1016/j.molcel.2012.01.002 (2012).
- 302 Laugesen, A. & Helin, K. Chromatin repressive complexes in stem cells, development, and cancer. *Cell Stem Cell* **14**, 735-751, doi:10.1016/j.stem.2014.05.006 (2014).
- 303 McDonel, P., Costello, I. & Hendrich, B. Keeping things quiet: roles of NuRD and Sin3 co-repressor complexes during mammalian development. *Int J Biochem Cell Biol* **41**, 108-116, doi:10.1016/j.biocel.2008.07.022 (2009).
- 304 Yoo, A. S. & Crabtree, G. R. ATP-dependent chromatin remodeling in neural development. *Current opinion in neurobiology* **19**, 120-126, doi:10.1016/j.conb.2009.04.006 (2009).
- 305 Koga, M. *et al.* Involvement of SMARCA2/BRM in the SWI/SNF chromatin-remodeling complex in schizophrenia. *Human molecular genetics* **18**, 2483-2494, doi:10.1093/hmg/ddp166 (2009).

- 306 Tuoc, T. C., Narayanan, R. & Stoykova, A. BAF chromatin remodeling complex: cortical size regulation and beyond. *Cell Cycle* **12**, 2953-2959, doi:10.4161/cc.25999 (2013).
- 307 Staahl, B. T. & Crabtree, G. R. Creating a neural specific chromatin landscape by npBAF and nBAF complexes. *Current opinion in neurobiology* **23**, 903-913, doi:10.1016/j.conb.2013.09.003 (2013).
- 308 Ronan, J. L., Wu, W. & Crabtree, G. R. From neural development to cognition: unexpected roles for chromatin. *Nat Rev Genet* **14**, 347-359, doi:10.1038/nrg3413 (2013).
- 309 McCarthy, S. E. *et al.* De novo mutations in schizophrenia implicate chromatin remodeling and support a genetic overlap with autism and intellectual disability. *Mol Psychiatry* **19**, 652-658, doi:10.1038/mp.2014.29 (2014).
- 310 Iossifov, I. *et al.* The contribution of de novo coding mutations to autism spectrum disorder. *Nature* **515**, 216-221, doi:10.1038/nature13908 (2014).
- 311 Gallagher, D. *et al.* Ankrd11 is a chromatin regulator involved in autism that is essential for neural development. *Developmental cell* **32**, 31-42, doi:10.1016/j.devcel.2014.11.031 (2015).
- 312 Helsmoortel, C. *et al.* A SWI/SNF-related autism syndrome caused by de novo mutations in ADNP. *Nature genetics* **46**, 380-384, doi:10.1038/ng.2899 (2014).
- 313 Lopez, A. J. & Wood, M. A. Role of nucleosome remodeling in neurodevelopmental and intellectual disability disorders. *Front Behav Neurosci* **9**, 100, doi:10.3389/fnbeh.2015.00100 (2015).
- 314 Twigg, S. R. *et al.* Acromelic frontonasal dysostosis and ZSWIM6 mutation: phenotypic spectrum and mosaicism. *Clin Genet*, doi:10.1111/cge.12721 (2015).
- 315 Wieczorek, D. *et al.* A comprehensive molecular study on Coffin-Siris and Nicolaides-Baraitser syndromes identifies a broad molecular and clinical spectrum converging on altered chromatin remodeling. *Human molecular genetics* **22**, 5121-5135, doi:10.1093/hmg/ddt366 (2013).
- 316 Schrier, S. A. *et al.* The Coffin-Siris syndrome: a proposed diagnostic approach and assessment of 15 overlapping cases. *Am J Med Genet A* **158A**, 1865-1876, doi:10.1002/ajmg.a.35415 (2012).
- 317 Mukhopadhyay, A., McGuire, T., Peng, C. Y. & Kessler, J. A. Differential effects of BMP signaling on parvalbumin and somatostatin interneuron differentiation. *Development* **136**, 2633-2642, doi:10.1242/dev.034439 (2009).
- 318 Marin, O. Human cortical interneurons take their time. *Cell Stem Cell* **12**, 497-499, doi:10.1016/j.stem.2013.04.017 (2013).
- 319 Gonzales, K. K. & Smith, Y. Cholinergic interneurons in the dorsal and ventral striatum: anatomical and functional considerations in normal and diseased conditions. *Ann N Y Acad Sci* **1349**, 1-45, doi:10.1111/nyas.12762 (2015).

- 320 Hatayama, M. *et al.* Zic2 hypomorphic mutant mice as a schizophrenia model and ZIC2 mutations identified in schizophrenia patients. *Sci Rep* **1**, 16, doi:10.1038/srep00016 (2011).
- 321 Teipel, S. J. *et al.* The cholinergic system in mild cognitive impairment and Alzheimer's disease: An in vivo MRI and DTI study. *Hum Brain Mapp* (2010).
- 322 Hyde, T. M. & Crook, J. M. Cholinergic systems and schizophrenia: primary pathology or epiphenomena? *J Chem Neuroanat* **22**, 53-63 (2001).
- 323 McCarroll, S. A. & Hyman, S. E. Progress in the genetics of polygenic brain disorders: significant new challenges for neurobiology. *Neuron* **80**, 578-587, doi:10.1016/j.neuron.2013.10.046 (2013).
- 324 Ripke, S. *et al.* Genome-wide association analysis identifies 13 new risk loci for schizophrenia. *Nature genetics* **45**, 1150-1159, doi:10.1038/ng.2742 (2013).
- 325 Visel, A., Thaller, C. & Eichele, G. GenePaint.org: an atlas of gene expression patterns in the mouse embryo. *Nucleic Acids Res* **32**, D552-556, doi:10.1093/nar/gkh029 (2004).
- 326 Blackshaw, S. *et al.* Molecular pathways controlling development of thalamus and hypothalamus: from neural specification to circuit formation. *The Journal of neuroscience : the official journal of the Society for Neuroscience* **30**, 14925-14930, doi:10.1523/JNEUROSCI.4499-10.2010 (2010).
- 327 Shepherd, G. M. Corticostriatal connectivity and its role in disease. *Nature reviews. Neuroscience* **14**, 278-291, doi:10.1038/nrn3469 (2013).
- 328 Hansen, D. V. *et al.* Non-epithelial stem cells and cortical interneuron production in the human ganglionic eminences. *Nat Neurosci*, doi:10.1038/nn.3541 (2013).
- 329 Ma, T. *et al.* Subcortical origins of human and monkey neocortical interneurons. *Nat Neurosci*, doi:10.1038/nn.3536 (2013).
- 330 Ackermann, A. M., Wang, Z., Schug, J., Naji, A. & Kaestner, K. H. Integration of ATAC-seq and RNA-seq identifies human alpha cell and beta cell signature genes. *Mol Metab* **5**, 233-244, doi:10.1016/j.molmet.2016.01.002 (2016).
- 331 Lesch, B. J. & Page, D. C. Poised chromatin in the mammalian germ line. *Development* **141**, 3619-3626, doi:10.1242/dev.113027 (2014).
- 332 Geling, A., Steiner, H., Willem, M., Bally-Cuif, L. & Haass, C. A gamma-secretase inhibitor blocks Notch signaling in vivo and causes a severe neurogenic phenotype in zebrafish. *EMBO Rep* **3**, 688-694, doi:10.1093/embo-reports/kvf124 (2002).
- 333 Dovey, H. F. *et al.* Functional gamma-secretase inhibitors reduce beta-amyloid peptide levels in brain. *J Neurochem* **76**, 173-181 (2001).

- 334 Fujiwara, T. *et al.* Mutations of sodium channel alpha subunit type 1 (SCN1A) in intractable childhood epilepsies with frequent generalized tonic-clonic seizures. *Brain* **126**, 531-546 (2003).
- 335 Roth, B. L. DREADDs for Neuroscientists. *Neuron* **89**, 683-694, doi:10.1016/j.neuron.2016.01.040 (2016).
- 336 Armbruster, B. N., Li, X., Pausch, M. H., Herlitze, S. & Roth, B. L. Evolving the lock to fit the key to create a family of G protein-coupled receptors potently activated by an inert ligand. *Proceedings of the National Academy of Sciences of the United States of America* **104**, 5163-5168, doi:10.1073/pnas.0700293104 (2007).
- 337 Klapoetke, N. C. *et al.* Independent optical excitation of distinct neural populations. *Nat Methods* **11**, 338-346, doi:10.1038/nmeth.2836 (2014).
- 338 Rothwell, P. E. *et al.* Autism-associated neuroligin-3 mutations commonly impair striatal circuits to boost repetitive behaviors. *Cell* **158**, 198-212, doi:10.1016/j.cell.2014.04.045 (2014).
- 339 Barch, D. M. & Dowd, E. C. Goal representations and motivational drive in schizophrenia: the role of prefrontal-striatal interactions. *Schizophr Bull* **36**, 919-934, doi:10.1093/schbul/sbq068 (2010).
- 340 Morris, R. W., Quail, S., Griffiths, K. R., Green, M. J. & Balleine, B. W. Corticostriatal control of goal-directed action is impaired in schizophrenia. *Biol Psychiatry* **77**, 187-195, doi:10.1016/j.biopsych.2014.06.005 (2015).
- 341 Noakes, Z., Fjodorova, M. & Li, M. Deriving striatal projection neurons from human pluripotent stem cells with Activin A. *Neural Regen Res* **10**, 1914-1916, doi:10.4103/1673-5374.169621 (2015).
- 342 Victor, M. B. *et al.* Generation of human striatal neurons by microRNA-dependent direct conversion of fibroblasts. *Neuron* **84**, 311-323, doi:10.1016/j.neuron.2014.10.016 (2014).
- 343 Antoine, M. W., Hubner, C. A., Arezzo, J. C. & Hebert, J. M. A causative link between inner ear defects and long-term striatal dysfunction. *Science* **341**, 1120-1123, doi:10.1126/science.1240405 (2013).
- 344 Mwilambwe-Tshilobo, L., Davis, A. J., Aizenberg, M. & Geffen, M. N. Selective Impairment in Frequency Discrimination in a Mouse Model of Tinnitus. *PloS one* **10**, e0137749, doi:10.1371/journal.pone.0137749 (2015).
- 345 McKerchar, T. L., Zarcone, T. J. & Fowler, S. C. Use of a force-plate actometer for detecting and quantifying vertical leaping induced by amphetamine in BALB/cJ mice, but not in C57BL/6J, DBA/2J, 129X1/SvJ, C3H/HeJ, and CD-1 mice. *J Neurosci Methods* **153**, 48-54, doi:10.1016/j.jneumeth.2005.10.002 (2006).
- 346 Fowler, S. C. *et al.* A force-plate actometer for quantitating rodent behaviors: illustrative data on locomotion, rotation, spatial patterning, stereotypies, and tremor. *J Neurosci Methods* **107**, 107-124 (2001).